
GIS based analysis of suitable areas of forest growth in the Chong Kemin National Park, Kyrgyzstan

Master thesis of
Andreas Rechenmacher, BSc.

for obtaining the academic degree of Master of Sciences
(MSc.)



Supervisor: Harald Vacik , Ao. Univ. Prof. Dipl.-Ing. Dr. MAS (GIS)
Co-supervisor: Markus Immitzer, Bakk.techn. Dipl.-Ing. MSc.

Submitted in July 2016 to the
Institute of Silviculture
Department of Forest- and Soil Sciences
BOKU - University of Natural Resources and Life Sciences

Affidavit

I hereby declare that I am the sole author of this work; no assistance other than that permitted has been used and all quotes and concepts taken from unpublished sources, published literature or the internet in wording or in basic content have been identified by footnotes or with precise source citations.

August, 2016

Andreas Rechenmacher

Acknowledgement

In Bishkek I was supported by Mr. Abdybek J. Asanaliev, Mr. Nurgaziev Mairambek and Mr. Almazbek Orozumbekov, all from the Centre of Innovation Technology in Agriculture, Faculty of Innovation Technology, Kyrgyz National Agrarian University. The students Seidali and Kuba helped arranging wherever it was possible.

I would like to express my appreciation to my supervisor Harald Vacik and my Co-supervisor Markus Immitzer. Thanks to their steady disposability and helpfulness, it was a real pleasure to write this thesis.

I would like to thank my friends, especially Wolfgang, Francesca and Wolfgang for their patience and the invaluable time together.

Finally yet importantly, my endless gratitude goes to my family. My parents and brothers made this important experience of my life possible.

August, 2016

Andreas Rechenmacher

Abbreviations

DEM = Digital Elevation Model

DFHGI = Department of Forest, Hunting and Ground Inventory

DOY = Day of the year

DTM = Digital Terrain Model

FAO = Food and Agriculture Organization of the United Nations

GDD = Growing degree days

GIS = Geographic information system

m.a.s.l. = Meter above sea level

m ü.NN = Meter über Normalnull (Meter above sea level)

N = North

ND = No data available

NE = Northeast

NP = National Park

NW = Northwest

PET = Potential Evapotranspiration

SAEPF = Kyrgyz State Agency for Environmental Protection and Forestry

SFF = State Forest Fund

SRTM = Shuttle Radar Topography Mission

WGS84 = World Geodetic System 84 (a geodetic reference system developed in 1984)

Abstract

GIS based analysis of suitable areas of forest growth in the Chong Kemin National Park, Kyrgyzstan

Forests protect against natural hazards and are a sustainable source of energy and construction material. The long-term objective of the Kyrgyz Republic is to increase the forest cover from around 4.5% to 6% until 2030. The selection of suitable areas for afforestation is difficult in an environment characterized by an arid, mostly continental climate. The objectives of this thesis are to define the potential treeline and suitable forest areas of forest growth in the Chong Kemin National Park, Kyrgyzstan.

ArcGis spatial analyst tools are used to analyze a map of the current forest distribution in the Chong Kemin NP, a very high resolution satellite image with a spatial resolution of 0.5 m, a digital terrain model with a spatial resolution of 30 m and a set of interpolated climate data comprising monthly mean values for precipitation, temperature and global radiation. Forest maps were digitalized to outline forest areas and the species distribution in the study area of 17,850 ha. Several climatic and morphologic parameters were determined from the input data and the climate-dataset was further refined with Kriging interpolation to a resolution of around 30 m.

The actual treeline was found at an elevation of about 2,900 m.a.s.l. While Shrenk's spruce is the dominant tree species, the five forest types comprising Shrenk's spruce (*Picea shrenkiana*), birch (*Betula tianschanica*), juniper (*Juniperus sp.*), bushes and plantations are distinguished with different spatial distribution pattern. The different forest types showed to grow under very distinct climatic conditions. A logistic regression model was developed to calculate the probability of forest growth in the context of the above-mentioned climate and morphology parameters. The topographic characteristics slope, aspect and elevation, together with solar radiation as a climate variable are found to be the most suitable parameters to define the probability of forest growth (~80 % model accuracy). A map of the estimated forest area was produced and compared with the actual forest area to identify differences to the current forest distribution. The model proposes around 18 % of the study area suitable for forest growth, were no forests stock currently. Discrepancies can rather be caused by human impacts or by morphological and climatic peculiarities.

Abstract (deutsch)

GIS gestützte Analyse von geeigneten Flächen für Waldwachstum im Chong Kemin Nationalpark, Kirgizstan

Wald schützt nicht nur gegen Naturgefahren, er gilt auch als eine nachhaltige Quelle für Holz zur stofflichen- und energetischen Nutzung. Die Kirgisische Republik hat sich daher zum Ziel gesetzt den Waldanteil des Landes von derzeit rund 4.5 % auf 6 % im Jahre 2030 zu erhöhen. Geeignete Flächen für Aufforstungen zu finden ist in einem arid und kontinental geprägten Land daher schwierig. Diese Arbeit hat sich zum Ziel gemacht genau diese Flächen für den Chong Kemin Nationalpark zu ermitteln.

Mit dem Spatial Analyst Werkzeug von ArcGis wurden eine Karte mit aktuellem Waldvorkommen, ein hochaufgelöstes Satellitenbild (Auflösung 0,5 m), ein digitales Höhenmodell (Auflösung 30 m) und ein interpolierter Klimadatensatz analysiert. Der Klimadatensatz enthielt Langzeit-Monatsmittelwerte für Niederschlag, Temperatur und Globalstrahlung.

Waldkarten wurden digitalisiert um die aktuelle Waldverteilung sowie die Baumartenverteilung innerhalb des 17.850 ha großen Studiengebiets zu erfassen. Aus den Eingangsdaten wurden verschiedene klimatologische und morphologische Parameter ermittelt. Der Klimadatensatz wurde mit Hilfe von Kriging-Interpolationen auf eine Auflösung von 30 m verfeinert.

Die aktuelle Waldgrenze liegt auf einer Meereshöhe von ca. 2.900 m ü. NN. Die Waldflächen wurden in fünf Waldtypen eingeteilt: neben Wäldern mit Schrenks Fichte (*Picea schrenkiana*) als Hauptbaumart, wurden auch Birke (*Betula tianschanica*), Wacholder (*Juniperus sp.*), Sträucher und Aufforstungen unterschieden. Die Waldtypen zeigten unterschiedliche räumliche Wachstumsverteilungen und kommen unter verschiedenen klimatischen Bedingungen vor. Mit Hilfe eines logistischen Regressionsmodells wurde mit den genannten klimatologischen und morphologischen Faktoren die Wahrscheinlichkeit für das Auftreten von Wald berechnet. Die topografischen Parameter Hangneigung, Exposition und Meereshöhe stellten sich neben der klimatischen Variable Globalstrahlung als signifikante Eingangsvariablen für das Modell (Modellgenauigkeit ~80 %) heraus.

Eine Karte mit den potentiell ermittelten Waldflächen wurde mit der tatsächlichen vorhandenen Waldfläche verglichen. Das Modell schätzte rund 8 % mehr Fläche des Studiengebietes als geeignet für Waldwachstum ein, wo derzeit jedoch kein Wald stockt. Abweichungen zwischen Modell und Wirklichkeit können auf anthropogenen Einflüssen oder auf morphologischen- und klimatischen Besonderheiten beruhen.

Table of contents

1	Introduction & goals.....	1
1.1	Research questions	1
2	State of the art	2
2.1	Altitudinal vegetation zones	2
2.2	Limiting and facilitating factors of tree & forest growth	4
2.2.1	Growing degree days (GDD)	4
2.2.2	The vegetation period	5
2.2.3	Radiation	8
2.2.4	The role of water supply during the vegetation period	11
2.2.5	The Potential Evapotranspiration (PET)	11
3	Methods and material.....	12
3.1	Description of the Chong Kemin National Park & the study area	12
3.1.1	Morphology, Soil & Flora.....	14
3.1.2	Climate.....	17
3.2	Data.....	18
3.2.1	Forest map.....	18
3.2.2	Digital Elevation Model (DEM)	19
3.2.3	Climate dataset from Böhner (2006).....	20
3.3	Analysis	21
3.3.1	Defining forested and non-forested area.....	21
3.3.2	Defining the Vegetation period	21
3.3.3	Logistic regression model	22
3.3.4	Estimating solar radiation with the ArcGis Solar analyst tool.....	25
3.3.5	Calculation of the Potential Evapotranspiration	25
4	Results	28
4.1	Morphological parameters & Forest occurrence.....	28
4.1.1	Elevation	28
4.1.2	Aspect & Slope.....	29
4.1.3	Forest occurrence.....	31
4.2	Climatological parameters & Forest occurrence	36

4.2.1	Temperature.....	36
4.2.2	Precipitation	38
4.2.3	PET (Potential Evapotranspiration)	39
4.2.4	Radiation	41
4.2.5	Forest occurrence.....	42
4.3	Logistic Regression model.....	46
5	Discussion	53
6	References.....	57
6.1	List of tables	61
6.2	Tables of figures.....	61
7	Appendix.....	63

1 Introduction & goals

One of the main tasks of Kyrgyz forest authorities is to prevent and fight soil erosion, landslides and avalanches (Fet 2007; Undeland 2012; Zeidler et al. 2016). Additionally, forests are considered an important source for both wood-products (fire- and construction timber) and non-woody forest products (mushrooms, herbs, fruits) (Lal et al. 2007). The aim of Kyrgyz forest authorities is therefore to increase forest area from actual ~5.0% (2009) to 6.0% of total country area in 2025. This is an increment of approx. 200,000 ha (Dzunusova 2008; Orozumbekov et al. 2009). The single forest farms (Leshoz), are responsible for the implementation on site (Orozumbekov et al. 2009; DFHGI 2015).

Due to different human- and non-human induced reasons, the Kyrgyz forest area is reduced in respect to its natural distribution (Cantarello et al. 2014; Klinge et al. 2015; Zeidler et al. 2016). In Soviet ages, forest area diminished to about half of the actual area. In this decades, timber harvest was on average 3.7 times higher than the current increment (Undeland 2012). After clearings, former forest land was (and is still) used as grazing land leading to negative consequences such as erosion and degradation of soils (FAO 2014). Many areas all over the National territory are currently subjected to erosion processes (DFHGI 2015). These phenomena are intensified by prolonged summer- and autumn rains and rapid spring thaw (FAO & UNESCO 1978; Lal et al. 2007).

To accelerate the desired reforestation, Kyrgyz authorities also use afforestation as an aid. Around 9,000 ha of new forest were planted only from 1993 to 2008. Most of the new forest areas are however derived by natural regeneration followed by a land use change (no more grazing) (Undeland 2012). Not all of the planted tree seedlings establish. Losses are sometimes high (Orozumbekov et al. 2009). It is therefore crucial to know under which climatic and morphological criteria forest is able to grow successfully in order to save time and economical effort.

This study aims to have a closer look under which conditions forest grows in the Chong Kemin National Park in the Northeaster part of Kyrgyzstan. A statistic model should be developed which is able to identify areas where forest growth is theoretically possible when all the climatological and morphological parameters are favorable. These calculated areas will be compared with the actual forest distribution and possible discrepancies will be discussed and tried to explain.

1.1 Research questions

- Where is the actual tree line and the current distribution and pattern of forests in the study area?
- Under which conditions do the different forest types spruce, plantation, birch, juniper and bushes grow?
- Are there discrepancies between predicted forest areas by the model and the actual forest area?
- What can be the reasons for these discrepancies?

2 State of the art

2.1 Altitudinal vegetation zones

Alexander von Humboldt was one of the pioneers of biogeography. At the beginning of the 19th century on his scientific travels around the globe while studying hundreds of different sites he had the need to somehow classify the different vegetation types he observed. One of the probably most important things was the classification of ecosystems and altitudinal vegetation zones (Körner, 2012). He stated the high elevation treeline to be the best bio-climatic reference. Using climate rather than altitude allows therefore the latitudinal comparison of biota.

The classification of the study area in altitudinal vegetation zones is therefore needed to have a reference guide when dealing with comparable sites elsewhere. To categorize the different altitudinal zones in a worldwide comparable system, an appropriate classification scheme has to be chosen in order to reach standardization and systemization of mountain altitudinal belts. According to Miede et al. (2004), the today common nomination of the altitudinal zones is strongly based on the humid alpine conditions of Central Europe with its forested zones and glaciers. This kind of classification is generally used also in (sub)-tropical mountainous areas, even on the Southern hemisphere as long as there is forest occurring.

There are a number of exceptions: in Mediterranean mountain systems for example the classification starts at sea level with the thermomediterranean, followed by mesomediterranean, the supramediterranean and the oromediterranean (to be compared to the montane zone). Higher in altitude the subalpine, alpine and nival zones follow as they are in the classical zone classification.

In drier environments (arid zones), forests are not occurring at all which also means a distinction between montane (forest is occurring) and alpine (no more forest occurring) is not possible. Furthermore, the seasonal snow cover to define the nival zone is often missing as well (Miede et al., 2004). In the tropic mountainous environment (between 18°N and 10°S) the expressions colline and alpine are used in a different manner. This classification is used to distinguish between the thermal seasons with a dormant period in winter and the hygical periods (diurnal climate, dry- and wet periods). The wet and dry period in this cases is called winter. The dry period with daily temperature fluctuations is called summer (Schickhoff et al. 2015).

Altitudinal belts can also be based on other biotic and abiotic factors. According to Zhang et al. (2004) there are basically two types of altitudinal belts when talking about regional classification: the ones which are based on vegetation regions and the ones based on spectrum structure or climate types (with usually a 2 or 3 level hierarchy). For the Tien Shan region they found more than one system that are applied: systems of altitudinal belts based on soil zones (without any elevational influence), systems of altitudinal belts based on vegetation zones, systems of altitudinal belts based on ecogeographic types, systems of altitudinal belts based on structure types and systems of altitudinal belts based on digital spectrum. Another approach is to define a "zone" by the main dominant tree species as used by (Colak & Rotherham 2007) for the Turkish high mountains.

As already mentioned, the today commonly used definition of altitudinal vegetation zones is historically strongly related to the humid alpine environment (see Figure 1). In the contemporary literature therefore we find many zonation approaches which are based on the findings of Heinz Ellenberg, a prominent German scientist of the 20th century.

Almost all over the Northern hemisphere, subalpine forests are characterized by forests consisting of the species *Abies*, *Picea* and other moisture-loving conifers (Miehe et al. 2004; Schickhoff et al. 2015).

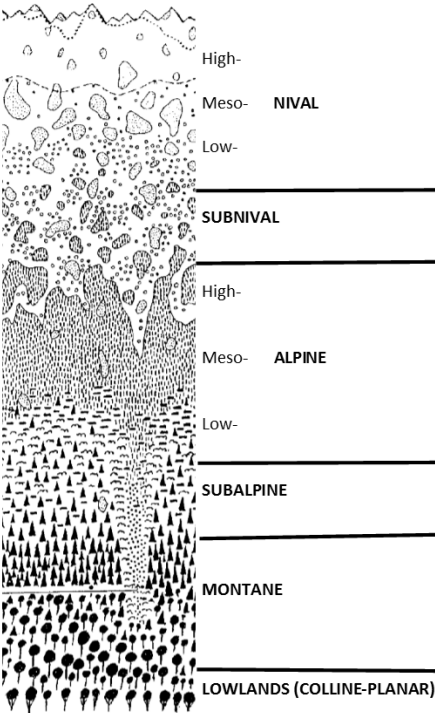


Figure 1: Altitudinal zonation, Ellenberg (1996)

2.2 Limiting and facilitating factors of tree & forest growth

2.2.1 Growing degree days (GDD)

The concept of thermal time or heat units was introduced in the 18th century by a french scientist named René Antoine Ferchault de Réaumur and developed through the centuries to the GDD. They are expressed in heat units of a certain area within a defined time period (e.g. positive GDD to define vegetation period of a given area). It is a frequently used equation to describe time pattern of different biological processes. The aim is to define the heat energy a plant gets over a defined period. In agricultural sciences it became a standard tool to predict and describe phenological behavior of crops (McMaster & Wilhelm 1997). They describe the mathematical procedure as: “integrate the area under the diurnal temperature curve, sum the daily heat energy over an interval of time, and then relate the accumulation of heat energy to progress in development or growth processes”, (Equation 1).

$$\text{GDD} = \sum \left(\frac{T_{\max} - T_{\min}}{2} - T_b \right) \quad (1)$$

where T_{\max} and T_{\min} is the daily maximum and minimum temperature, T_b ($=T_{\text{Base}}$) is the base temperature, that defines the temperature below which a certain process does not happen (this can be plant growth, germination, flowering, ripening, etc.).

Calculating thermal sums directly at tree lines is a practice that was used not very often. For the Warm temperate zone (28–42°N, 36°S), (Körner 2012) found thermal-sum values of around 1,000 ($>0^\circ\text{C}$) and 400 when ($>5^\circ\text{C}$).

In Central Asia most of the areas do not exceed 4,000 degree days per year (Figure 2) whereas in the tropics values above 8,000 are very common (Lal et al. 2007).

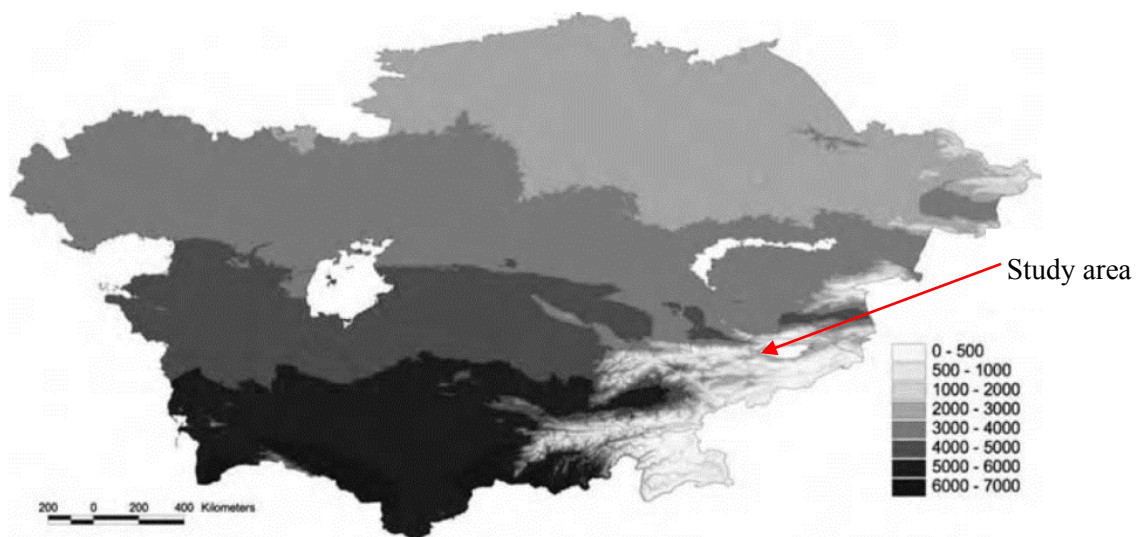


Figure 2: Accumulated yearly GDD above 0°C in Central Asia, (Lal et al. 2007)

The point in time a woody plant restarts with growth or other phenological changes after the dormant period can be assessed with a linear regression (Equation 2) after (Murray et al. 1989):

$$HU_{req} = \sum_{t_0}^{t_{LF}} (T_t - T_{th}) \quad \text{if } T_t > T_{th} \quad (2)$$

where HU_{req} is the heat unit requirement for leaf flushing, t_{LF} is the day of leaf flushing, t_0 is the starting date for heat accumulation, T_t is the mean daily air temperature, T_{th} is the threshold temperature for heat accumulation. According to different literature findings e.g. (Kramer 1994a; Fu et al. 2015), at daily mean temperature values higher than 5°C the accumulation of heat in most cases starts. Other authors like De Beurs and Henebry (2004), in their studies regarding land use changes, used -273.3°K (0°C) as T_{Base} .

For this study unfortunately, GGD cannot be calculated due to the lack of daily temperature values. The findings of Orozumbekov et al. (2009) however, can be helpful to define the vegetation period. For the Kyrgyz mountains they found positive annual temperature values for the different altitudinal/vegetation zonation: from 3,600 to 4,900°C for the valley-sub mountain zone, about 2,700 - 4,000°C for the mountain zone, between 600 and 2,600°C for the high-mountain zone and 600 to 800°C for the nival areas (see 2.1).

2.2.2 The vegetation period

There are different approaches to define the vegetation period:

- «The growing period, as a climatic concept, is the time of the year when neither temperature nor moisture limit biomass production» (Lal et al. 2007).
- «The growing season is defined as the period between the first and last passing of a weekly mean of air temperature of 0°C» (Körner 2012).
- «The vegetation period can be defined as:...all days with a daily mean temperature >0.9 °C, and a mean of 6.4 °C across all these days (Paulsen & Körner 2014).
- «Results suggest that mean air temperature and growing degree days (GDDs) above 5 °C during late winter and spring...are the most important controls on the beginning and end dates of the growing season» (Chen & Pan 2002)

A long vegetation period is not necessarily an indicator of strong tree /plant growth. A part from water and nutrients availability, temperature regime during the growing period influence the growth performance of trees. A steadily low temperature will restrict trees to have high increment rates. Also trees are, due to their height, stronger coupled to the atmospheric conditions than low growing plants (Harsch & Bader 2011; Körner 1999). The leaf unfolding of trees in spring is strongly correlated with temperature and reflects therefore the thermal regime of an area. It has to be mentioned that also higher temperatures in late winter are shifting the leaf-unfolding point to an earlier date (Chmielewski & Rotzer 2001; Chen & Pan 2002).

The length of the vegetation period is likely to increase with changing global climatic conditions. High altitude temperatures are rising particularly fast when compared with lowland pattern. This

conjuncture does not necessarily lead to an upwards shift of tree lines (Heikkinen et al. 2002; Cleland et al. 2007; Pretzsch et al. 2014). In some cases, the opposite is true. Higher temperatures can in some cases lead to increasing snowfall and therefore later snowmelt. This leads than to a shorter vegetation period (Way & Oren 2010).

The overall and very generalized mean temperature for the cool temperate zone's tree lines (45-47° N on Northern hemisphere) during the vegetation period was described by Körner (2012) as around 7°C. The duration is approx. 4.5 months, which means 135 days. For the warm temperate zone (28–42°N, 36° S) he found the mean temperatures during the vegetation period season to be from 5.8-7.8°C and the length of the period to be around 140 to 150 days.

By Chmielewski & Rotzer (2001) the length of the vegetation period in European study sites was found to increase between 0.6 and 6.3 days per decade during 1969 and 1998. Similar results were obtained by Pretzsch et al. (2014): the vegetation period of the last 110 years was prolonged on average for 22 days with a stronger increase in the last 5 decades. This also led to an increased annual volume increment at stand level. An extension of the vegetation period by 10.8 days was reported by Menzel & Fabian (1999) since 1960 on European scale. In Table 1 examples of vegetation periods of various areas are listed according to their duration.

Table 1: Start and End of vegetation period from selected regions, for the period from 1969-1998, DOY = day of the year, ND = no data available , own table, source of data: Chmielewski and Rotzer (2001); Körner (2012)*

Area	Beginning (DOY)	Beginning Date	End (DOY)	End Date	Length (Days)
North Scandinavia	143	22 April	282	08 October	139
Treelines in the warm temperate zones*	ND	ND	ND	ND	140-150
Treeline (2750-2929 m.a.s.l. in Tien Shan Mountains Kyrgyzstan*	115	25 April	270	27 October	155
North Atlantic Mountain Region	127	06 May	299	25 October	172
Bav.-Bohemian Highlands	119	28 April	296	22 October	177
EU (Mean)	113	22 April	301	27 October	188
Baltic Sea Region	120	29 April	309	04 November	189
Dinaric Mountain Region/Dalmatia	109	18 April	300	26 October	191
North Alpine Foreland	110	19 April	303	29 October	193
Southern Central European Highlands	108	17 April	305	31 October	197
North Sea/Central European Lowlands	104	13 April	302	28 October	198
Northern Central European Highlands	106	15 April	305	31 October	199
British Isles/Channel Coast	101	10 April	301	27 October	200
Great Hungarian Lowlands	101	10 April	303	29 October	202
Equatorial tropics*	ND	ND	ND	ND	365

In addition, moisture can be an important factor to define the length of the vegetation period. In most cases however, it is a combination of both, moisture and temperature. Lal et al. (2007) found a mean temperature of the vegetation period for Central Asia to be 206 days (st.dev. = ± 51) whereas only 6% of the region have to cope with a period length being less than 150 days. This is true mostly for high altitude areas (Figure 3). For the moisture-limited vegetation period a mean value was found being 178 days (st.dev. = ± 69). The lowest values can be found in the deserts/semi deserts, in the steppes and in intra-montane depressions. If these two values now get combined, the temperature- and moisture-limited vegetation period can be calculated.

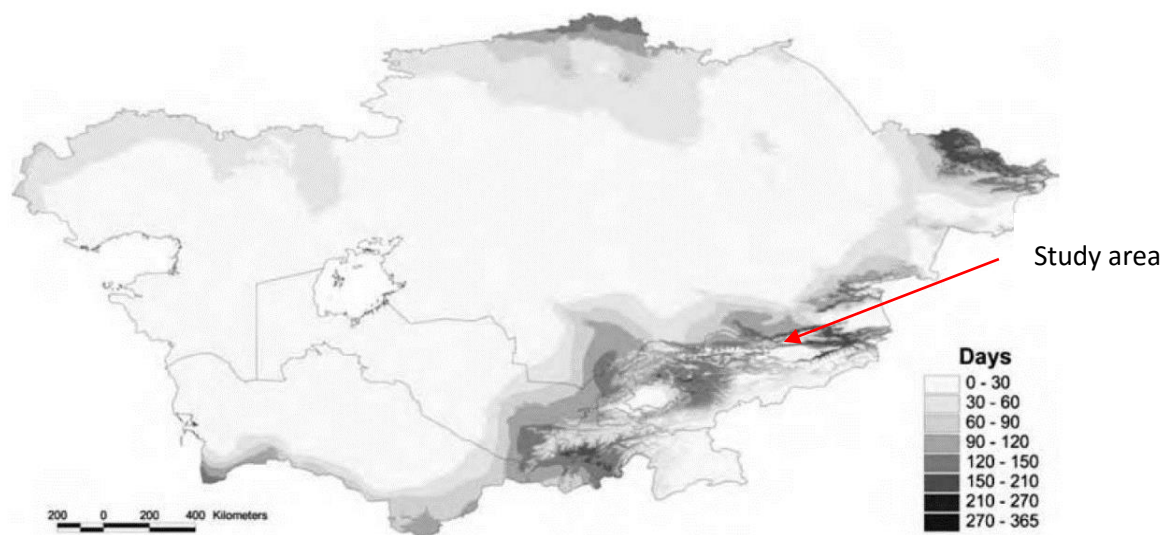


Figure 3: Length of the vegetation period in Central Asia, limited both by temperature and moisture (Lal et al. 2007)

Season length depends also on slope direction. On north facing slopes, snow cover lasts longer and vegetation period (the temperature and light limited one) is shorter. On the same hand, due to a different moisture regime, there will be more plant available water (Paulsen and Körner 2001). Other factors influencing the duration of a growing season can be soil characteristics or even genes. That's why, when these environmental factors change, plants can serve as a useful biological indicator because they react on these changes (Menzel & Fabian 1999).

The length of the vegetation period seems not to be correlated with tree line elevation (Körner 1999). On the other hand, duration of vegetation season is strongly correlated with latitude. The temperature during the vegetation period however is decisive on the elevational position of the climatic tree line (Paulsen and Körner, 2001). The temperature regime within the vegetation period is a good indicator for determining the conifer tree line worldwide. The fact that a similar vegetation-period-temperature-pattern can be found at tree line elevation is true especially for the forests of the Northern hemisphere (Harsch & Bader 2011).

Which role does the temperature fluctuation between night and day play? In experimental tests (Hoch & Körner 2009) proved that diurnal oscillation in temperatures (with the same identical thermal sum) did not influence the growth of conifer seedlings. As long as the thermal sum was the same, the higher day-temperatures were able to compensate for the low night temperatures.

Table 2: Defining vegetation period: temperature values to compare different scientific findings, (Klinge, Böhner, and Erasmi 2015*; Körner 2012,Paulsen and Körner 2014***)**

	Minimum average temperature during the vegetation period
Upper treeline of <i>Picea shrenkiana</i> *	5
Upper forest line in Kyrgyzstan**	6.5
Tree growth limit in general***	0.9 - 6.4

The leaf fall in spring and the end of the vegetation period do not show such a clear relationship to the air temperature as the beginning of the vegetation period does. It was found that prolonging factors are:

- Higher mean air temperatures in late winter months and spring
- Lower precipitation values in autumn (Chmielewski & Rotzer 2001; Chen & Pan 2002).

Another important influencing factor of stopping woody plants to grow is the shortening of the photoperiod. Finally, the plant is ready for the essential low temperature period in winter (chilling). To get into the so called dormancy, temperatures have to absolutely drop a certain level (-4 to 5°C for temperate and boreal tree species) (Man & Lu 2010).

2.2.3 Radiation

Insolation, the radiation which hits the earth, is the driving force for all physical and biological systems on earth's surface (Fu & Rich 1999). Insolation maps are widely used in agriculture and more and more also in forestry to gain more knowledge about the available energy in a certain area (Fu & Rich 2002). The insolation on the earth surface is mostly shortwave radiation (Will 2011). Every incoming sunbeam had passed the world's atmosphere. Depending on different parameters, this sunbeam reaches the surface of our planet with a wide range of impact intensity. Depending on the latitude, altitude and atmospheric conditions, the sunbeam's way through the atmosphere can be a longer or shorter one and a direct or a deflected/diffuse one. With increasing latitude the distance from outer atmosphere to the earth surface increases. The sunray has to pass through a 'thicker' atmosphere meaning pass more suspended solids and gas particles which can scatter the sunbeam and so reduce its energy (diffuse radiation) (Sultan et al. 2014).

A part from the latitude, also slope and aspect of ridges play an important role when it comes to radiation intensity. High variation in insolation values measured in topographic complex areas has been measured. This is due the direct and indirect radiation which are reflected off by the surrounding terrain (Figure 4), (Fu & Rich 2002).

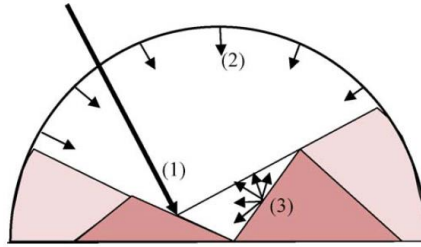


Figure 4: The three energy sources on a slope: (1) direct radiation from the sun, (2) diffuse sky radiation, where a portion of the overlying hemisphere may be obstructed, (3) diffuse and direct radiation reflected off by nearby terrain. Source: Gastli (2010)

The total insolation, according to Will (2011) on earth therefore is:

$$R_{\downarrow} = R_{dir} + R_{dif} + R_{ref} \quad (3)$$

Where R_{\downarrow} = the total amount of insolation reaching a defined point on earth, R_{dir} = direct radiation, R_{dif} = diffuse radiation and R_{ref} = diffuse and direct radiation reflected by topographic elements. Figure 5 shows the insolation values for an area similar to the study site (similar latitude and altitudes). The example was chosen to illustrate how the proportion of the single insolation types changes over the year.

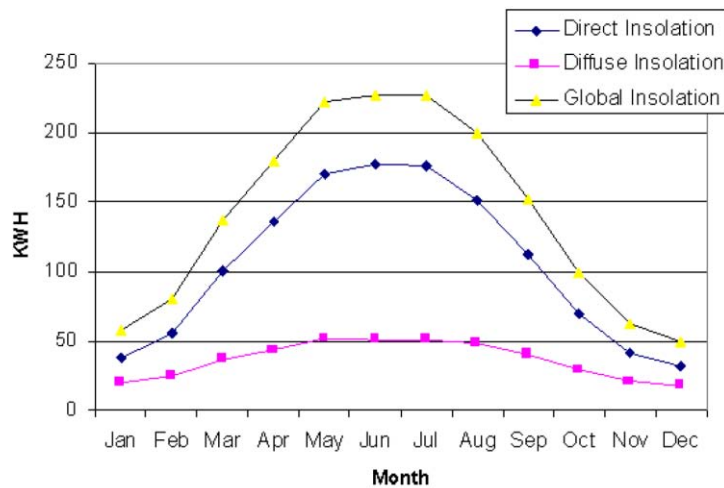


Figure 5: Proportion of direct, diffuse and global insolation during the year, example study site in the Rocky mountains, Colorado, 2,532 to 4,340 m.a.s.l., (Fu & Rich 1999)

According to Saha (2008) the factors which influence the amount of incoming light are:

1. "The value of the solar constant
2. The transparency of the atmosphere (transmittivity)
3. The latitude of the location
4. The seasonal and diurnal variation".

The insolation in Watt per unit area outside the tropics is highest in summer months and much lower in winter months (Figure 6). The level of insolation can vary strongly also on small scale. Slope, exposition, the heterogeneity of landscape and obstruction by topographic elements create insolation

patterns which are often more complex than expected. Computing insolation maps based on a DEM is much more accurate than a global theoretical assumption based on interpolation and extrapolation because it is able to consider all the topographic- and landscape factors (Fu & Rich 2002).

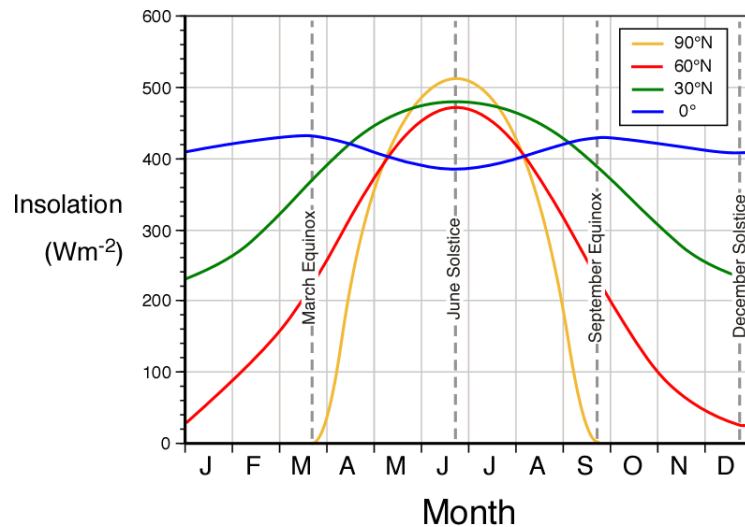


Figure 6: Monthly values of potential insolation [W/m^2] at different latitudes, (Pidwirny & Jones 2009)

Not only the distance from outer atmosphere to earth-surface is determining sunlight intensity. The angle of incidence is an even more important factor. The changes in the position of earth’s rotation axis leads to a shift of the sunbeam’s angle of incidence of 47° every year. This leads to a bigger area of impact of the single sunbeam, reducing therefore the radiation per unit of surface area. The intensity of radiation on earth surface is therefore: $SINUS$ (angle of sunlight incidence).

As mentioned above the incoming radiation scattered by molecules or suspended solids in the atmosphere, is called diffuse sky radiation. Only a small percentage of the total radiation striking the outer atmosphere ($\sim 1367 W/m^2$) reaches the earth’s surface as the diffuse light proportion. Cloud cover, dust and haze are influencing factors. The higher the proportion of these factors is, the bigger the rate of diffuse light. At clear-sky days in a dry environment this rate is negligible whereas at cloudy or foggy days with water vapor saturated air the diffuse light proportion can be almost 100% (Sultan et al. 2014). Transmittivity or transmissivity (“the condition of the atmosphere”) is a value from 0 to 1 compound by more than one variables: the amount and the thickness of eventual clouds (the most decisive factor), the absorption of light by water vapor, other gasses or smoke and scattering (Matsuda et al. 2006).

2.2.4 The role of water supply during the vegetation period

Precipitation patterns, especially the ones during summer months, are important factors which can determine forest growth and the characteristics of treelines (Heikkinen et al. 2002; Weemstra et al. 2013).

Tree species react in a different manner on lack of groundwater and high PET (Potential Evapotranspiration) values. Weemstra et al. (2013) found difference on how temperate species respond to water stress (reducing water body table) and drought (high temperatures/no water supply). There was a similar feedback for all species to drought but considerable differences when the water table was lowered. Here, shade tolerant species showed almost no negative reaction whereas non-shade-tolerant species showed a strong decrease in increment and tree ring width.

2.2.5 The Potential Evapotranspiration (PET)

A simple explanation of the term can be found in Pidwirny & Jones (2009): “Potential evapotranspiration is a measure of the ability of the atmosphere to remove water from the surface through the processes of evaporation and transpiration assuming no control on water supply”.

When dealing with plant growth on a certain site it is important to know the amount of Potential Evapotranspiration. Temperature and precipitation alone may not be sufficient to understand the climatic conditions. Whether a certain site can be considered a dry site or a moist site is almost impossible knowing only precipitation values. It is essential to know if the loss back to the atmosphere (evaporation) and the consumption of plant communities (transpiration) are lower or bigger than the water supply (Thornthwaite 1948).

Forest Evapotranspiration can have a balancing effect positively the local climate. Consequently there are mitigation effects on surface runoff, runoff peaks, sediment transport in rivers and temperature (Komatsu et al. 2012).

There are first of all two different approaches how to calculate Evapotranspiration. The simple and the more complex models (Komatsu et al. 2012). Whereas the simple models require none but a few meteorological input data of coarse time- and spatial resolution, complex models need different meteorological parameters at a much higher time resolution and information about the characteristics of the forest.

The American scientist Charles Warren Thornthwaite developed a straightforward method to calculate the Potential Evaporation and plantal transpiration of water vapor back to the atmosphere; «the reverse of precipitation» (Thornthwaite 1948).

3 Methods and material

In November 2015, a scientific stay of three weeks in Kyrgyzstan (Bishkek and Chong Kemin National Park) was made to gather forest-relevant information from local authorities. The preceded communication with members from the Kyrgyz National Agrarian University (KNAU) was supposed to establish helpful contacts at the National Department of Forest, Hunting and Ground Inventory. Especially Mr. Abdybek J. Asanaliev, Mr. Nurgaziev Mairambek and Mr. Almazbek Orozumbekov, all from the Centre of Innovation Technology in Agriculture, Faculty of Innovation Technology, did assist and support the task to gather scientific information from the Department.

A two-day field survey was made to take pictures and to get an overview of the study area at stand level. The transition of forested to non-forested areas gained a special attention, as did the upper and lower forest line being both main subject of this thesis. The upper forest edge at around 2,900 m.a.s.l. is reachable by foot or by horse only. No forest road exists in the NP area. The field survey was useful to understand the peculiarities of this ecosystem and to see the common features with the European/alpine ecotones, which sometimes where surprisingly identical.

3.1 Description of the Chong Kemin National Park & the study area

The study area is situated in Northern Kyrgyzstan. Figure 7 gives an overlook about the forest occurrence inside the National park and shows the growth pattern inside the study area. It is clearly observable that forest is not growing in a uniform and steady way. Often, there are very sharp and well defined forest edges and grassland in between. The detailed image shows *Picea shrenkiana* forest patterns inside the study area, at around 2,700 m.a.s.l.

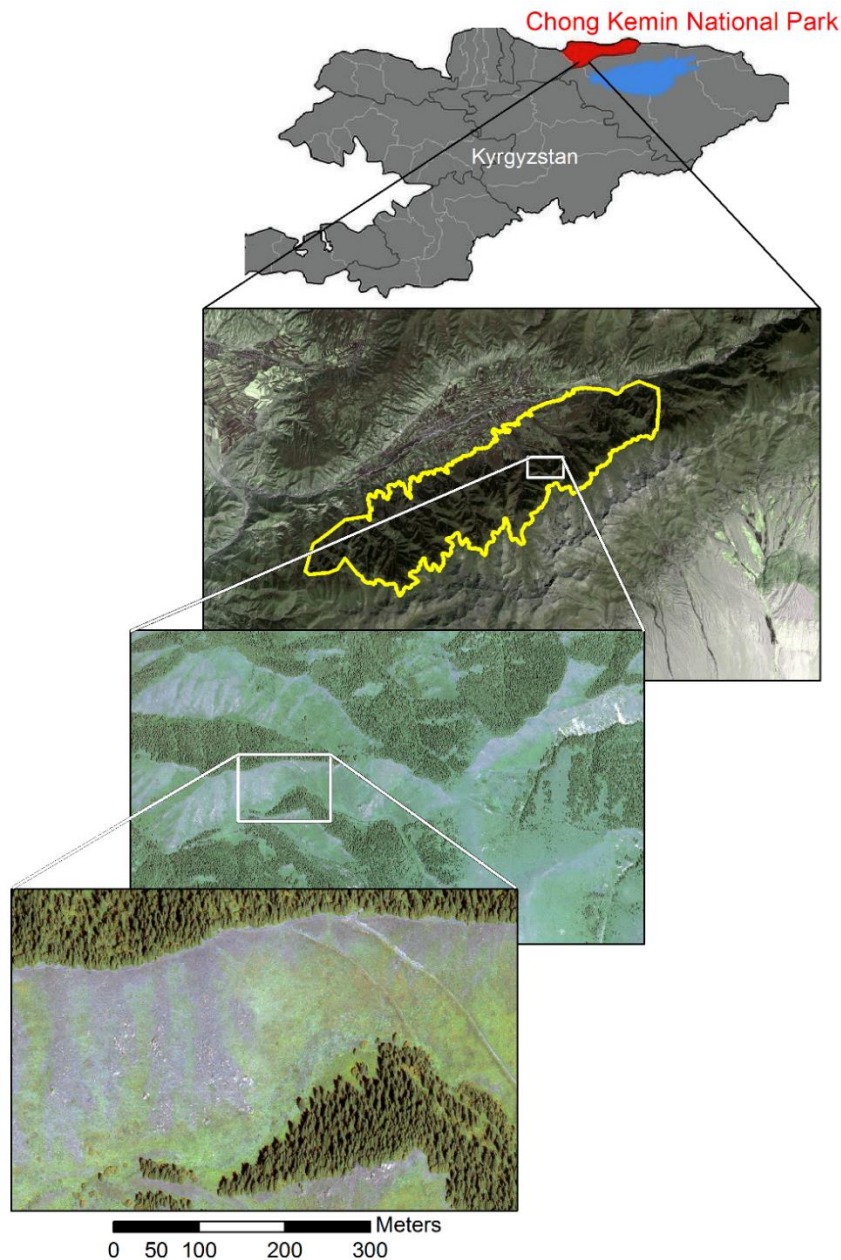


Figure 7: Overview and detail of the study area (yellow edged outline), own figure.

There is no presence of noteworthy rock faces or scree. The entire area is situated at the foothills of a mountain ridge with a maximum elevation of approx. 3,900 m.a.s.l. This means forest/treeline separates 1,000 m elevation from the rocky summits. The area between treeline and peaks is characterized by a typical alpine and finally nival traits.

The National territory of Kyrgyzstan is situated at a latitude between 39° and 43° North which, transferred to Europe means the same latitude as Southern Italy, Spain or Portugal. Due to the geographical given conditions, the study site and similar European areas are not comparable (3.1.1). Applying the Mediterranean altitudinal zonation system would make no sense. A broader more generic system is much more suitable to the Central Asiatic reality.

The standard altitudinal zonation for the climatic and natural situation at the Kyrgyz National territory is according to Orozumbekov et al. (2009):

- **Lowlands** (valley-sub mountain zone, <1,200 m.a.s.l.)
 - **Mountain** (1,200 – 2,200 m.a.s.l.)
 - **High mountain** (~2,200 – 3,000 m.a.s.l.)
 - **Nival** (higher than 3,000 m.a.s.l.)
- (modified from Ellenberg 1996, Miehe et al. 2004, Orozumbekov et al. 2009, (see 3.1.1)).

3.1.1 Morphology, Soil & Flora

The Chong Kemin NP is characterized by steppe vegetation, forests and alpine meadows. Each of these vegetation type is represented by various groups of plants, influenced by climatic conditions, terrain, exposure and steepness of slopes. In addition to these basic types of vegetation there are groups like cushion plants, riparian - aquatic and wetland plants (DFHGI 2015).

The bottom belt of mountains and the valley bottom, which is only small area of the park, is covered by steppe vegetation. Due to different farming activities, original vegetation is seldom here (Undeland 2012). Because of the low precipitation and high temperature peaks in summer many woody plants are not to grow. The State Agency for Environmental Protection and Forestry classified there areas into steppe and meadow. Whereas Dry steppe is mostly represented by fescue herbs (*Festuca* sp.), which occupy the southern slopes, i.e. places with insufficient moisture and frequent outcrops of bedrock. Vegetation height is not higher than 25-35 cm and the dominant soil type is Brown Desert-Steppe Soil. A low humus content and a high gravel content are typically for this kind of soil (FAO & UNESCO 1978).

Steppe: the main representatives of this plant communities are Fescue, *Poa pratensis*, *Ziziphora*, *Artemisia*, *Phleum*, feather grasses, *Zmeegolovnika*, *Galium verum*, thyme and others. This type is used as a spring-autumn pastures for all kinds of cattle, but mainly sheep (DFHGI 2015).

Meadow steppes are mostly located on the northern slopes on Chernozem soils (FAO & UNESCO 1978). In contrast to the steppe, the hydrologic situation is more favorable. Therefore, there is a larger variety of grasses and mesophytic shrubs.

Additionally to the plants growing on steppe, on meadow steppe it can be found: *Geranium* sp., *Artemisia* sp., *Avena* sp., *Gentian* sp. and other forage grasses. They can have fleshy foliage and large, colorful flowers blooming all at the same time. It is an area of rich fodder production and ideal as summer pasture (FAO & UNESCO 1978). The non-woody vegetation reach heights of up to 70 cm. The bushes which grow sparsely here, are *Rosa* sp., *Spiraea* sp., *Lonicera* sp.

Ascending, on North-facing slopes, the forest belt is located (see Figure 8). The main species is Shrenk's spruce, *Picea schrenkiana* Fisch. et May. It is a semi-shade-tolerant species (Cantarello et al. 2014). According to Klinge et al. (2015), Schrenk's spruce needs 250 mm/year of precipitation as a minimum to grow (not taking in account all the other site-relevant parameter). A positive correlation has been found between summer precipitation and growth for the Schrenk's spruce (Magnuszewski et al. 2015). Especially the period from April to September of the precedent year significantly influenced tree ring increment. Even if it is growing in rather arid environments such as part the Kyrgyz mountains, spruce is a hygrophilous tree species. This means it relies on the precipitation of this year's vegetation period to build up organic substance on the next season (Magnuszewski et al. 2015).



Figure 8: *Picea shrenkiana* forests growing on North-facing slopes, alpine meadow or steppe on all other slopes, Chong Kemin NP, approx. 2,600 m.a.s.l., November 2015, own picture.

Other tree-forming species in the Chong Kemin NP are *Pinus* sp. (planted), birch (*Betula tianschanica*), poplar species and willow. Chernozem and relativ thin-layered Brown earths are the prevailing soil types under forest cover (Orozumbekov et al. 2009). Figure 9 shows the altitudinal distribution of the different plant communities and species of selected Central Asian areas. The Kyrgyz ridge (northern slopes) represents quite well the study area inside the Chong Kemin National park. The shrub vegetation in the lower parts of the Chong Kemin valley are followed by a layer of coniferous forest which is, together with Juniper, forming the treeline at around 2,900 m.a.s.l. Above the treeline, the tall grass meadows at elevations between 2,900 and 3,500 m.a.s.l. are followed by low/short grass meadows which can reach up to 4,000 m.a.s.l.

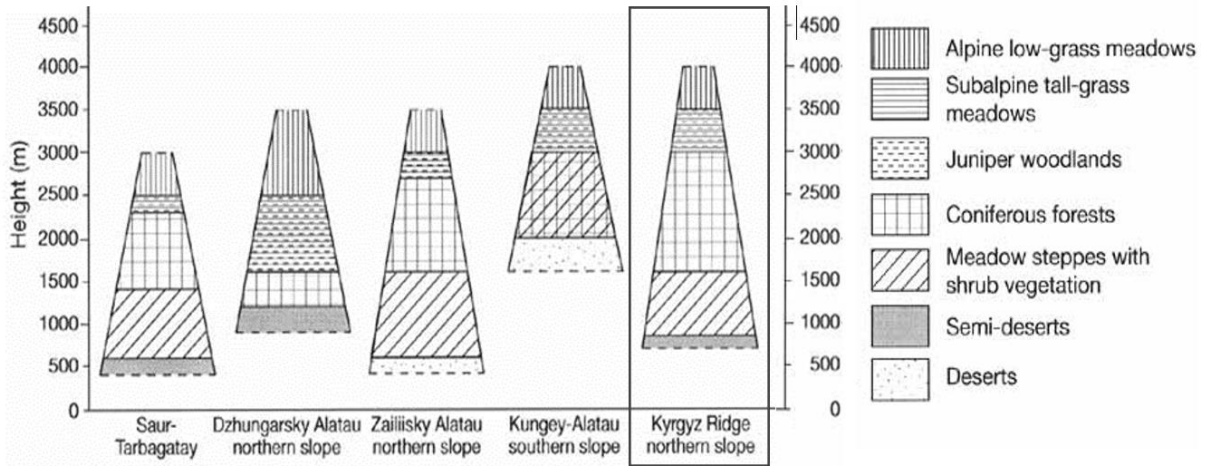


Figure 9: Sequence of vegetation types, examples of the Tien-Shan mountain chain, Kyrgyz ridge marked with the box, (from Agakhanyants 1981, 1986)

Treeline is sometimes formed by clustered groups of single trees and sometimes by a gradual transition from closed forest to single (progressively smaller) trees. This is the so-called *Diffuse treeline* (Figure 10). Not always, it is an easy task to distinguish between forest- and treeline. In many environments a treeline-forming *Krummholz*-zone can be found (Harsch & Bader 2011) with stumped and multi-stem trees. This form of treeline is missing in the study area. Only single-stem trees (in most cases *Picea shrenkiana*) are present (Figure 11).

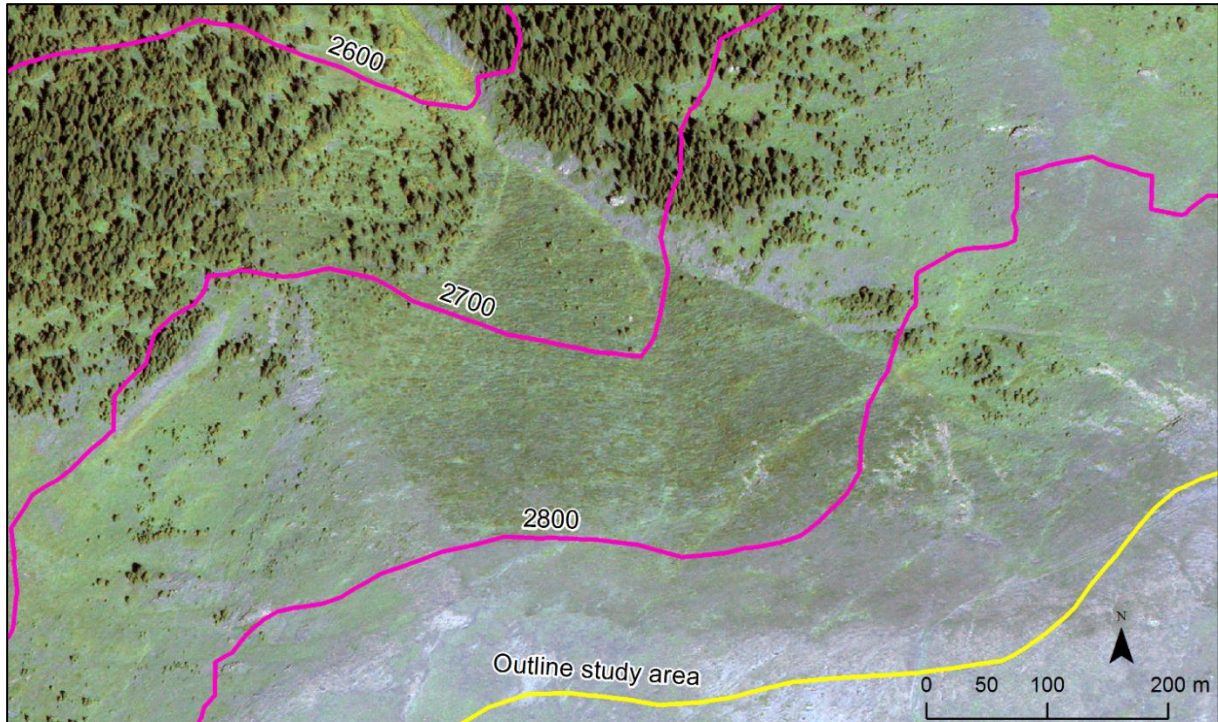


Figure 10: Forest- and treeline behavior at the upper forest border, contour lines (pink) with altitude values [m.a.s.l.], *Picea shrenkiana* forest, own figure.



Figure 11: Treeline-ecotone at the study area: alpine meadow mostly on South-facing slopes; *Picea shrenkiana* trees in foreground; treeline on North-facing ridge in the background; picture taken at approx. 2,800 m.a.s.l.; November 2015, own picture.

3.1.2 Climate

Generally, a sharply continental climate prevails in the Chong Kemin National Park area. There is however a great variety, depending on the altitude and the exposure and steepness of slopes. The higher the elevation, the lower the temperature, the higher the relative and absolute humidity, the higher rainfall, the longer and thicker snow cover, the earlier starts freezing and the later it ends, the shorter the duration of the frost-free period (DFHGI 2015). In the lower parts of the Park, the typical steppe climate prevails. Winters are cold (-20°C are possible) and summers dry. Winter precipitation, mostly in the form of snow (average date of first frost in autumn is September 20 and for late frost 20 May) faces Potential Evapotranspiration values of zero (FAO & UNESCO 1978).

Talking about the entire National Park, the average date of occurrence for the first snow is 27 October. The last snow in spring however on average occurs on 14 April. The average date of first frost in autumn is September 20 and for late frost 20 May. Prevailing wind directions are North-, North-West and North-East at an average speed of 1.8 m/sec (DFHGI, 2015).

An increase of precipitation during the past decades was found for Kyrgyz and Tajik Mountains (Lioubimtseva & Henebry 2009).

3.2 Data

3.2.1 Forest map

The base map of forest types was obtained from the Department of Forest, Hunting and Ground Inventory in digital form (pdf-format), available only in Russian language and later translated (Figure 12). This map was of high importance for the entire work. It is the fundament on which the classification and delineation of forest areas was based. The forest types were subdivided by the Kyrgyz authorities into classes according to the canopy closure:

- 10-50%
- 50-80%
- > 80%

The coloration of the single classes looks like: the higher the canopy cover of the forest, the darker the coloration of the map. For my study (as in Gehrig-Fasel et al. 2007), the amount of canopy closure was not considered. Only forested and non-forested areas were distinguished.

The forest map had to be georeferenced first and projected into a projected coordinate system than in ArcGis. For the entire study, the Geographic Coordinate System: WGS_1984 was applied. All the Gis-based analysis and creating of maps was performed in the Projected Coordinate System WGS_1984_UTM_zone_43N.

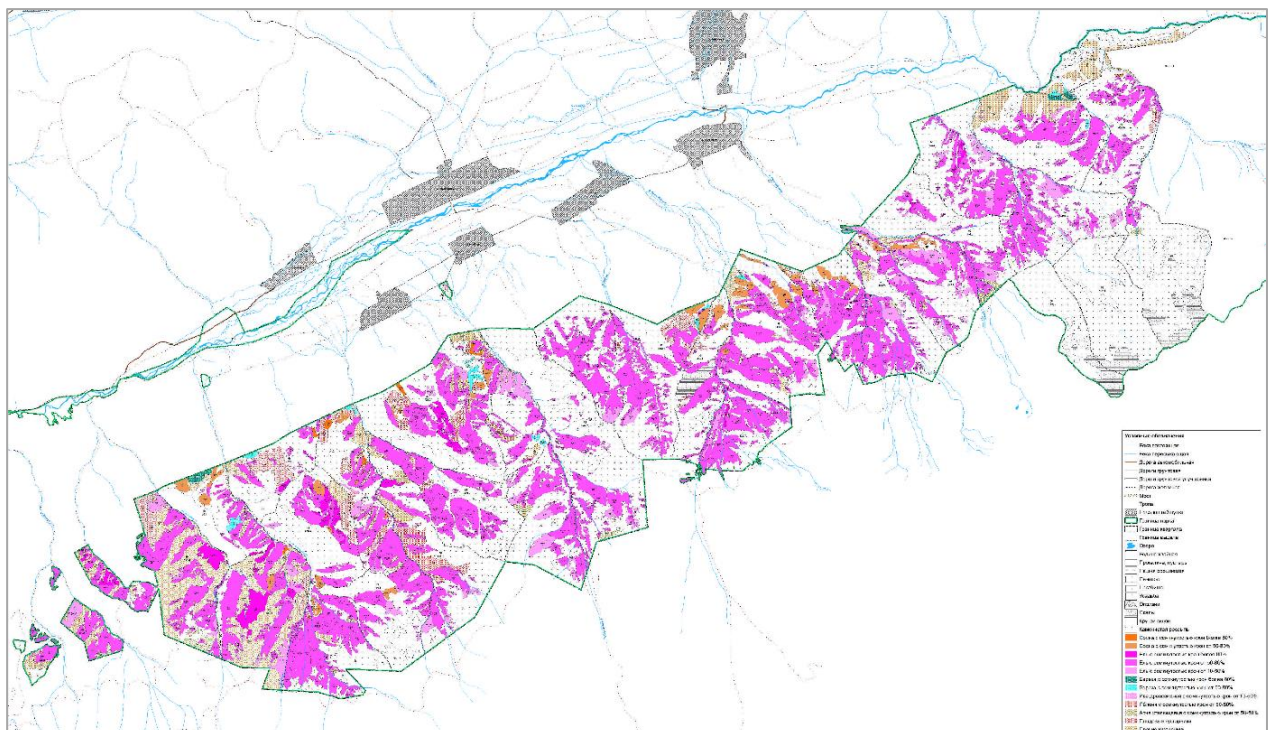


Figure 12: Original Forest map obtained by the Department of Forest, Hunting and Ground Inventory in November 2015. The legend (in Russian language) shows forest and shrub types, rivers, streets, settlement areas and morphological peculiarities such as eroded or rocky areas. (the map is visible in better resolution in Appendix)

Additionally to the forest map, a very-high-resolution (VHR) image was acquired from the satellite-image provider Digital Globe (UK). The 26 km² image is an Ortho Ready Standard-item with a bit depth

of 16 and a resolution of approx. 0.5 m. Taken in August 2012 with an almost zero cloud cover percentage, it was appropriate to digitalize, together with the forest map, the forest types present in the study area (Figure 13).

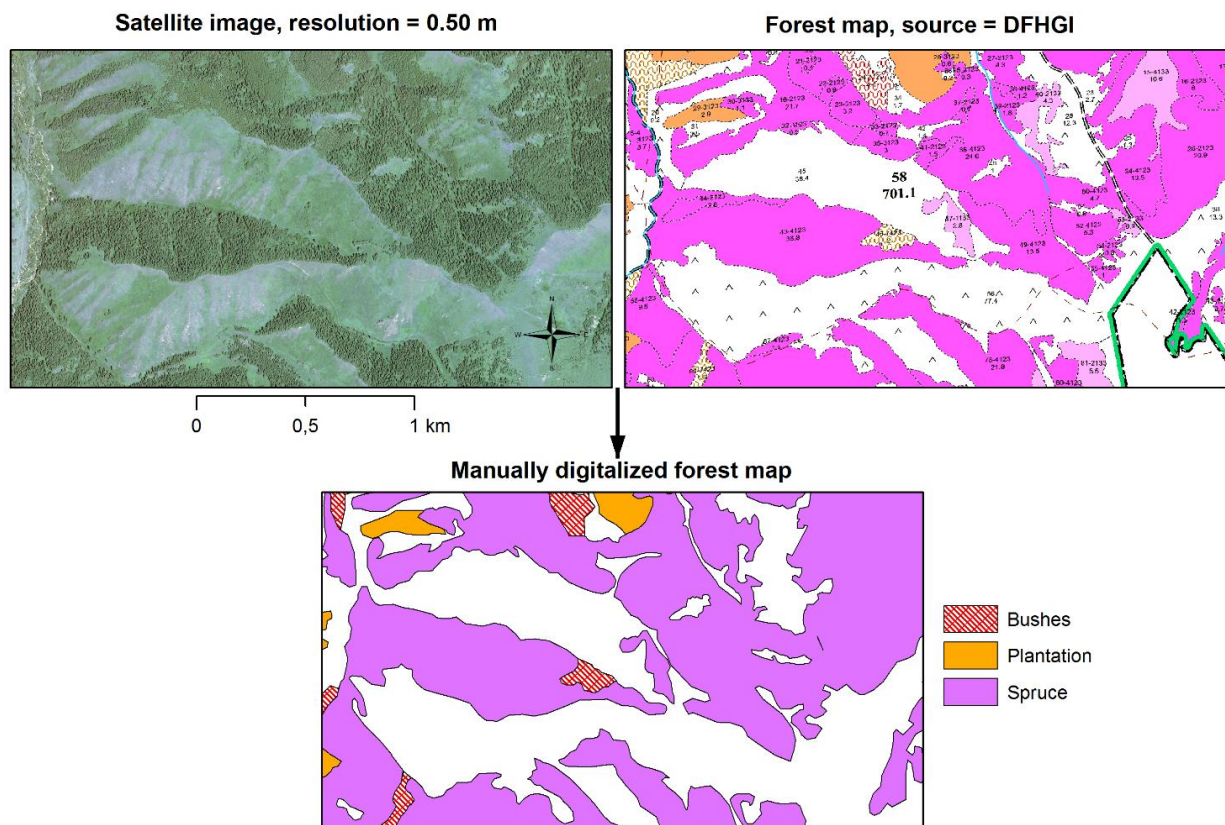


Figure 13: Digitalization process of the forest areas with the help of a high resolution satellite image (upper left) and the forest map obtained by Kyrgyz authorities (upper right), own figure.

3.2.2 Digital Elevation Model (DEM)

A digital elevation model or digital terrain model (DTM) is used as basis for the calculation of radiation values. For this study, an ASTER Global digital elevation model is used. ASTER stands for “Advanced Space borne Thermal Emission and Reflection Radiometer” which is an imaging device on board of a NASA satellite launched in 1999 and still working (NASA & METI 2016).

ASTER GDEM data are available free of charge on the homepage of the Land Processes Distributed Active Archive Center (LP DAAC). This center is part of the U.S. Geological Survey (USGS) which again belongs to the U.S. Department of the Interior.

Although data are chargeable at no costs, strict citation rules and distribution restrictions are implemented for the ASTER GDEM v2 data. This is not true for all the other ASTER data and products available online. Since the digital elevation models of this work are exclusively obtained as ASTER GDEM v2 – data, this restrictions and rules are valid.

From the LP DAAC homepage (<http://gdex.cr.usgs.gov/gdex/>) it is possible to define the desired area by entering longitudinal and latitudinal coordinates or to use a country/state browser. Additionally a polygon or rectangular area on the world map can be drawn by hand (NASA & METI 2016). ASTER uses near infrared cameras since 2001 to produce digital elevation models having vertical accuracies

between 10 and 25 meters (root mean squared error). The data output are GeoTIFF (Geographic Tagged Image File Format) files (see Table 3). They are embedded in the WGS84 coordinate system and lay on a grid with a resolution of 1 arc second (which is about 30m at latitude 0°). As geopotential model, the EGM96 (developed in the U.S.) is used.

Table 3: ASTER GDEM v2 Data Set Characteristics (NASA & METI 2016)

Tile Size	3601 x 3601 (1 degree by 1 degree)
Pixel Size	1 arc-second
Geographic coordinates	Geographic latitude and longitude
DEM output format	GeoTIFF, signed 16 bits in units of vertical meters
Geoid reference	WGS84/EGM96
Special DN values	-9999 for void pixels, and 0 for sea water body
Tile volume	25 MB uncompressed, 4–5 MB compressed
Coverage	North 83 degrees to south 83 degrees, 22,702 tiles

For this study, 6 tiles were needed to cover the Kyrgyz national territory. The South to North extension was from the 39th to the 44th parallel. The West to North extension from 69°E to 81°E meaning that each has an area of around 93,000 km². In ArcGis a Raster Mosaic was created to merge the raster files to a single one to work with. Conclusively the DEM was projected in the Transverse Mercator projection WGS_1984_UTM_Zone_43N as the rest of the dataset.

A Digital Elevation Model with an appropriate resolution is a basic requirement to obtain a reliable solar radiation map (Fu & Rich 2002). Therefore, a DEM with cell size 27.3 x 27.3 m was applied. This resolution is higher than the one used by (Klinge et al. 2015) which was 90 x 90 m but applied on a much larger scale (several hundreds of square kilometers).

3.2.3 Climate dataset from Böhner (2006)

An important climate data set data was kindly provided by Prof. Dr. Jürgen Böhner, Institute of Geography, University of Hamburg, Germany in January 2016. Originally, these data were generated by Böhner (2006), covering all Central Asia but only the part covering Kyrgyzstan and smaller parts outside were considered here. In total, the area covers around 560,000 km².

The spatial resolution is of 1.0 arc seconds that means around 2,300 m in longitudinal and 1,700 m in latitudinal direction. In total 150,851 single points were used as climate database. Each of these points represent an area of approx. 390 ha contains:

- Exact point center coordinates
- Elevation [m.a.s.l.]
- Global radiation [Joule/cm²/day]
- Monthly Temperature means [°C]
- Precipitation [mm] for January, July and annual mean

Where radiation-, temperature- and precipitation values represent monthly means from 1961 to 1990.

According to (Klinge et al. 2015) data were generated with empirical models by statistical downscaling from coarse resolution atmospheric fields from GCMs (General Circulation Models). Temperature and precipitation records from around 400 meteorological stations (scattered in whole Central and High Asia) were used as the empirical data base on which data elaboration method was developed (Böhner 2006). The output is a monthly time series with long-term means with a time span reaching from 1961 to 1990. Additionally, evapotranspiration data from 64 Chinese meteorological stations were available. At the end, a check and a homogenization of time series were accomplished. An detailed description of the dataset and the modeling approach are given in (Böhner 2006; Böhner & Antonic 2009).

3.3 Analysis

3.3.1 Defining forested and non-forested area

When talking about forest, various definitions can be found. Many countries have their own legal definition. Trees which are at least 3 m high (Paulsen & Körner 2001; Szerencsits 2012), a canopy closure of 20 % (Paulsen & Körner 2001) or a canopy closure of 50 % (Szerencsits 2012) are just a few of them. No matter if matching or not in one or more of these systems, forested areas have one important feature in common: they protect against natural hazards caused by gravitation. These can be landslide, snow avalanches, rockfall, debris flow, debris avalanches and erosion, just to name the most important ones (Zeidler et al. 2016).

3.3.2 Defining the Vegetation period

To define the radiation input values, the length of the vegetation period has to be predefined. To model forest lines and forest distribution patterns in Central Asia (Klinge et al. 2015) defined the main vegetation period to last from «March to November» without specifying further. Other authors found similar timeframes (see 2.2.2).

The aim was to find the time span with a mean daily temperature more than 0°C for the study area. The mean temperature values vary strongly inside the study area. The elevational difference from the bottom line (1,700 m.a.s.l. up to the upper boundary line (elevation 2,900 m.a.s.l.) is 1,200 m. It comprises the montane and sub-alpine level (see 2.1). The temperature difference between upper and lower forest border is about 7°C in April and around 9°C in September. The annual mean values vary around 8°C from the bottom to the top. To calculate the vegetation-period-length, the start point was set to April 15 where a daily mean air temperature of around 0°C can be expected at the upper boundary line (see Appendix III). The remaining part of the study area has a higher mean temperature but should mostly fall into the 0-5°C interval proposed by literature.

Talking about the entire National Park, the average date of occurrence for the first snow is 27 October. The last snow in spring however on average occurs on April 14. The average date of first frost in autumn is September 20 and for late frost May 20 (DFHGI 2015).

The end of the vegetation period is expected to be at the point in time when mean temperatures fall below 0-5°C again. This is happening at the end of September (see Appendix IV). Considering that the

figures show monthly means and the October-mean is around -10°C at the upper boundary line, it is assumed that the 0°C isoline reaches this elevation at the end of September. The vegetation period lasts therefore 169 days or 5.6 months. This matches with the length of vegetation period found by (Körner 2012) for the tree limit in the Kyrgyz Tien Shan mountains: 155 days. To compare different vegetation-period-lengths see Table 1.

3.3.3 Logistic regression model

For the analysis of the influence of multiple independent variables on a categorical dependent variable the logistic regression is a suitable method (Zeidler et al. 2016). Forest types represent the independent variables and climatological and morphological parameter are the dependent variables. Probabilities of assignment can be determined (maximum likelihood assignment) as well as influences on their probabilities when the value of an observed (independent) variable is changing (Backhaus et al. 2007). The independent variable can be both categorical and metric scaled. In this case, it is categorical and is split into a dichotome (binary) variable: forest / no-forest. To “train” the model, forest pixels were randomly sampled as well as non-forested pixels in the same quantity.

Both data-types (independent and dependent variables) were generated with ArcGis. Raster datasets were created and further processed with R statistics. Logistic regression modelling as well as generating plots and graphs was done with Rstudio as well (R Development Core Team 2010).

As coefficient of determination, Nagelkerke’s R^2 was calculated. It describes how good the model can explain the dataset. R^2 greater 0.2 can be considered as acceptable, values greater than 0.4 can be considered as good and values higher than 0.5 as very good (Backhaus et al. 2007).

A correlation matrix of all the morphological and climatological parameters which could explain forest growth, was made in R (Appendix I). Four of these independent variables showed no correlation ($<\pm 0.5$) with the other variables: slope, aspect, April temperature and radiation. The fact that they do not correlate with other parameters makes them suitable for being used to explain forest growth or no-forest growth. The April temperature was not considered but instead the variable elevation was used.

To work on the relative small-scaled study area (17,849.1 ha), data interpolation was used to obtain a higher resolution (for the workflow in ArcGis see Figure 15). To work with spatial high resolution climate data in Geographic Information systems (GIS), Böhner (2005) proposed geostatistical Kriging as an appropriate method. The ArcGis Geostatistical Analyst toolset contains different Interpolation tools. The ‘Empirical Bayesian Kriging’ tool was used to bring the resolution of the different climatological parameters from around $2,300 \times 2,300$ m to the lowest resolution used in this work, which is $27.28 \text{ m} \times 27.28 \text{ m}$ (Figure 14). For this purpose, a rectangle of approx. 30×50 km was created around the study area in order to make the interpolation work properly.

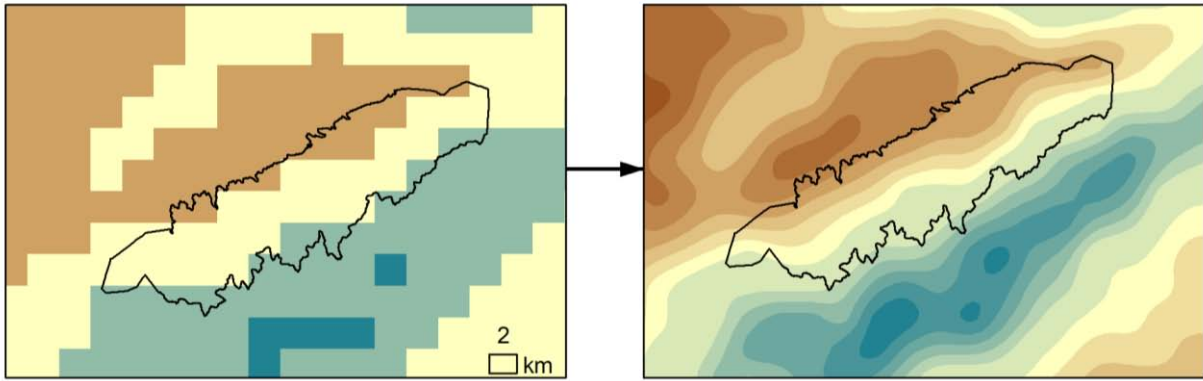


Figure 14: Comparison of data resolution before (left) and after (right) geostatistical Kriging, yearly temperature means, own figure.

Kriging interpolation “accounts for the error in estimating the underlying semivariogram through repeated simulations”. It is a straightforward and robust method when it is to interpolate empirical data in a spatial context. Especially for statistical downscaling of low resolution climate data and to connect local point climate observations with bigger, trans-regional climate phenomena (ESRI 2016; Böhner 2004). The difference between the Empirical Bayesian Kriging (EBK) method (developed by Konstantin Krivurochko, Esri) and the classical Kriging methods is that EBK accounts for errors introduced by the estimation of the semivariogram model. “This is done by estimating and then using, many semivariogram models rather than a single semivariogram”. By interpolating data, not only the optical appearance is smoother, also it is helpful to downscale data to get a more accurate output. The input data in the tool are point data (vector data). The output geometry type is raster data. The analysis was accomplished with tool-default settings of ArcGis.

Most of the results extracted from the climate dataset obtained by Jürgen Böhner where derived with GIS analysis. The Model Builder Tool was used to ease these procedures that are very similar but at the same time quite comprehensive (9 different tools to extract and interpolate climate data from Böhner (2006)). The advantage of the Model Builder Tool is the way to run a variety of models one after another with the only parameter to change being the input parameters (Figure 15).

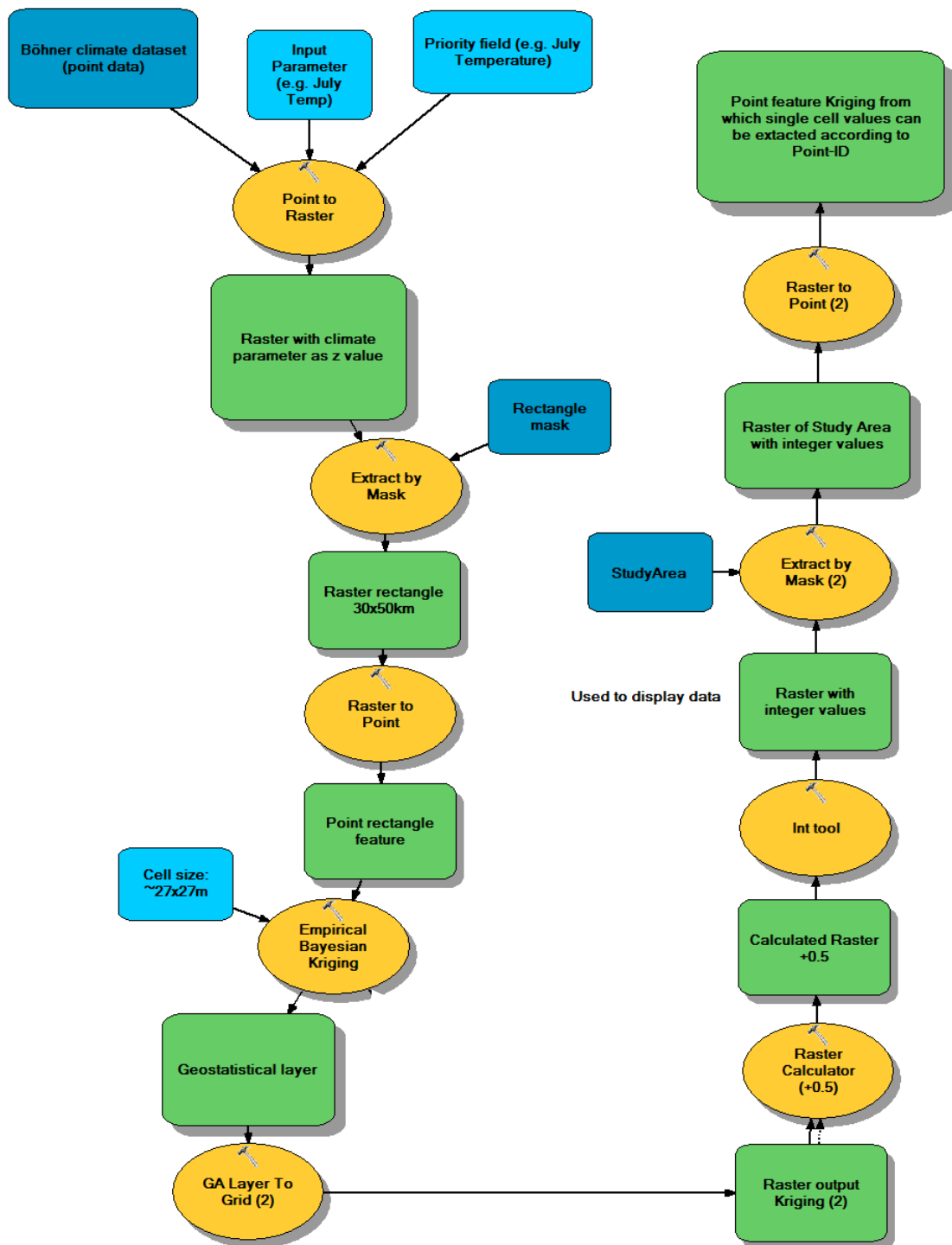


Figure 15: Workflow to extract climate data from Böhner (2006), ArcGis Model builder, own figure.

3.3.4 Estimating solar radiation with the ArcGis Solar analyst tool

This tool was created by Fu & Rich (1999) for the American software producer Esri (Environmental Systems Research Institute). It is best suited for temporal patterns compared with spatially patterns. In most cases an insufficient amount of information is available to compare time periods (e.g. subsequent vegetation periods) (Fu & Rich 1999).

The amount of incoming solar radiation is depending on sky transmissivity, rainfall and clouds, latitude, elevation, topography (see 2.2.3). For the study area the 'Diffuse proportion' setting in the Solar analyst tool was set to 0.35 because during the vegetation period, especially in the summer month, sunny weather conditions over several months can be expected (see 3.1.1). According to (Fu & Rich 1999) the Diffuse proportion value 0.3 is implemented for clear sky conditions and values between 0.6 and 0.7 for very cloudy skies. Considering that the beginning and the end of the vegetation period (which lasts from April 15 until 30 September, =275 days), can include also several rainy weeks.

The Chong Kemin National Park is situated around the 43th parallel. The extension of the study area precisely goes from 42.6th to the 42.7th Northern parallel. The Solar analyst tool takes the latitude in account automatically.

Table 4: Example of solar incidence and percent of the total radiation intensity of the city of Tokmok (42.8°N), about 50km West of the study area

	Jan	Feb	Mar	Apr	May	Jun	Jul	Aug	Sep	Oct	Nov	Dec
Angle of sunlight incidence	31°	39°	47°	55°	63°	70°	63°	55°	47°	39°	31°	24°
True radiation	52%	63%	73%	82%	89%	94%	89%	82%	73%	63%	52%	41%

For the transmissivity (see 2.2.3) setting, the default value of 0.5 (default value for a generally clear sky condition) is kept. It indicates the fraction of radiation that is able to pass through the atmosphere. This is an average of all wavelengths and values range from 0 (no transmission) to 1 (full transmission). As proposed by (Fu & Rich 2002) the average sky condition settings can be implemented in case of lacking daily cloud data.

Radiation is an important factor when it comes to tree growth in arid climatic conditions (Klinge et al. 2015). To calculate radiation at the study area, the Böhner (2006)-dataset was not used due to its low resolution and especially due to the complex topography of the surface (Matsuda et al. 2006) which can influence tree growth.

3.3.5 Calculation of the Potential Evapotranspiration (PET)

The dry period during summer months is certainly not favoring tree growth (Weemstra et al. 2013). The lower border of the study site, due to its poor rain values and high PET values, can almost be considered dryland (Table 6) according to (FAO 2004). Precipitation/PET values between 0.5 and 0.65

indicate the so called 'Dry subhumid'-type. At the lower edge of the study area, values around 0.67 occur. The higher elevations have lower Precipitation/PET values, falling therefore definitely out of the FAO-dryland classification.

There is a big variety of methods to estimate PET. Approaches to calculate PET are: estimating the water budget, the mass transfer, radiation, temperature based approaches and combined approaches (Xu & Singh 2002).

For this study the temperature based Thornthwaite's method (Thornthwaite 1948) was used to calculate Potential Evapotranspiration (Equation 5). Temperature (mean monthly values) and latitude of the study area are the only input values every temperature based model requires (Xu & Singh 2002).

Because of its simplicity and reliability it was applied by many scientists worldwide for this specific purpose (Kumar and Rakhecha 1987). The method is based on an annual temperature efficiency index J defined as the sum of 12 monthly values of heat index I. Each index I is a function of the mean monthly temperature T (in °C) as follows:

$$I = \left(\frac{T}{5}\right)^{1.514} \quad (4)$$

Potential evapotranspiration is then calculated by the following formula:

$$PET(Latitude) = 1.6 \left(\frac{10T}{J}\right)^c \quad (5)$$

Where PET(0) is the potential evapotranspiration per month in cm at 0° latitude and c is an exponent to be evaluated as formula 6:

$$c = 0.000000675J^3 - 0.0000771J^2 + 0.01792J + 0.49239 \quad (6)$$

$$J = \sum_{i=1}^{12} I(i) \quad (7)$$

At latitudes other than 0°, potential evapotranspiration is calculated by:

$$PET(L) = K PET(0) \quad (8)$$

Where K (Table 5) is a constant for each month of the year, varying as a function of latitude.

Table 5: Constant K in Thornthwaite method, K is a constant to correct PET for latitudes other than 0°

Latitude	Jan	Feb	Mar	Apr	May	Jun	Jul	Aug	Sep	Oct	Nov	Dec
60°N	0.54	0.67	0.97	1.19	1.33	1.56	1.55	1.33	1.07	0.84	0.58	0.48
50°N	0.71	0.84	0.98	1.14	1.28	1.36	1.33	1.21	1.06	0.90	0.76	0.68
40°N	0.80	0.89	0.99	1.10	1.20	1.25	1.23	1.15	1.04	0.93	0.83	0.78
30°N	0.87	0.93	1.00	1.07	1.14	1.17	1.16	1.11	1.03	0.96	0.89	0.85
20°N	0.92	0.96	1.00	1.05	1.09	1.11	1.10	1.07	1.02	0.98	0.93	0.91
10°N	0.97	0.98	1.00	1.03	1.05	1.06	1.05	1.04	1.02	0.99	0.97	0.96
0°	1.00	1.00	1.00	1.00	1.00	1.00	1.00	1.00	1.00	1.00	1.00	1.00
10°S	1.05	1.04	1.02	0.99	0.97	0.96	0.97	0.98	1.00	1.03	1.05	1.06
20°S	1.10	1.07	1.02	0.98	0.93	0.91	0.92	0.96	1.00	1.05	1.09	1.11
30°S	1.16	1.11	1.03	0.96	0.89	0.85	0.87	0.93	1.00	1.07	1.14	1.17
40°S	1.23	1.15	1.04	0.93	0.83	0.78	0.80	0.89	0.99	1.10	1.20	1.25
50°S	1.33	1.19	1.05	0.89	0.75	0.68	0.70	0.82	0.97	1.13	1.27	1.36

For a quick check of Potential Evapotranspiration values, there is a point-based online calculator available. It was developed by the Visualab team (Visualab 2016), a group of scientists working for the San Diego State University in California. The interface is straight forward (Figure 16), simple to use and to understand. The input data are the monthly means and the latitude in degree. The output are monthly PET values at a given point. The tool was used to validate the values obtained by Jürgen Böhner at some selected points.

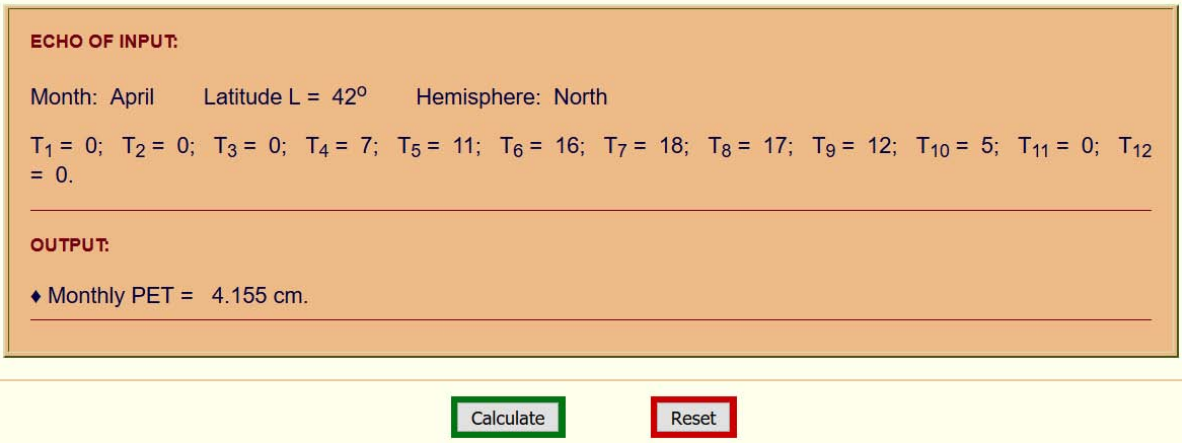


Figure 16: Interface of online PET-Thornthwaite-method-calculator, (Visualab 2016)

4 Results

4.1 Morphological parameters & Forest occurrence

4.1.1 Elevation

According to the altitudinal classification of Orozumbekov et al. (2009)(see 3.1), more than 40% of Kyrgyzstan are considered Nival zone. High mountain zone and Mountain zone contribute with more than 20% each to the Kyrgyz National territory. Only a small percentage (9.4%) makes part of the lowlands meaning with elevation values lower than 1,200 m.a.s.l. (Figure 17).

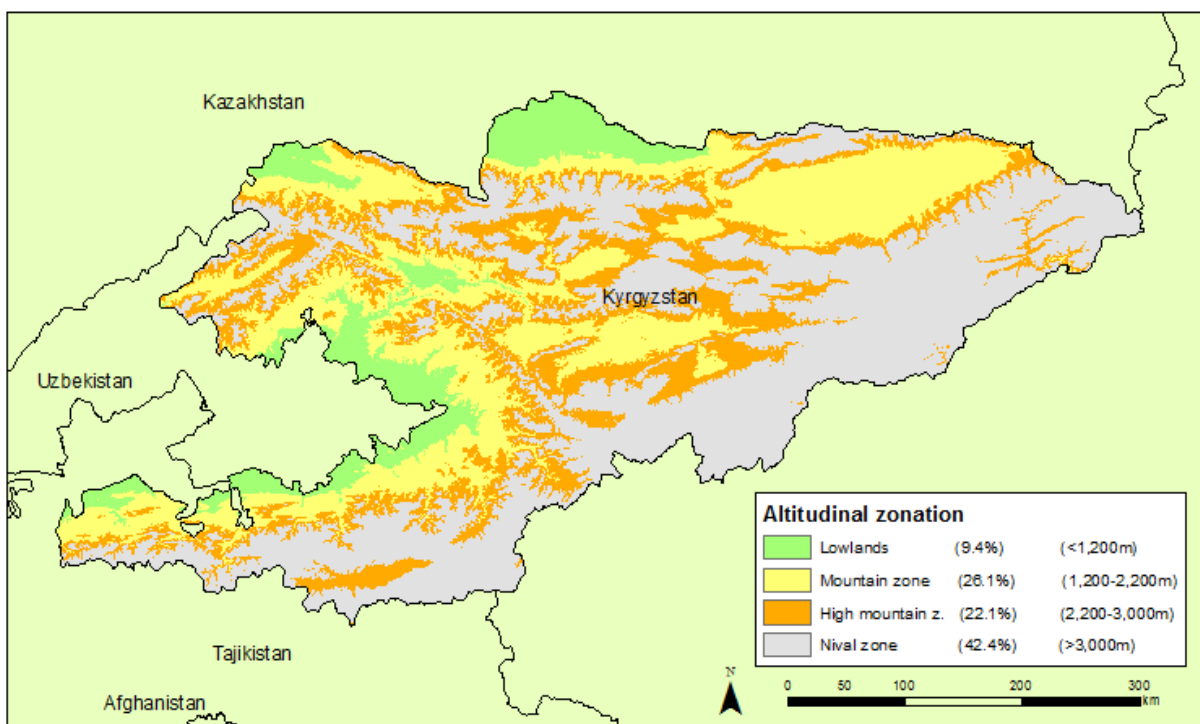


Figure 17: Altitudinal zonation of Kyrgyz National territory, proportion [%] of the total country area, meters above sea level [m], own figure.

Inside the study area two altitudinal zonations can be found (Figure 18): the Mountain zone at the lower areas and the High mountain zone at elevations > 2,200 m.a.s.l. It is constatable that forest areas are occurring mostly inside the High mountain zone.

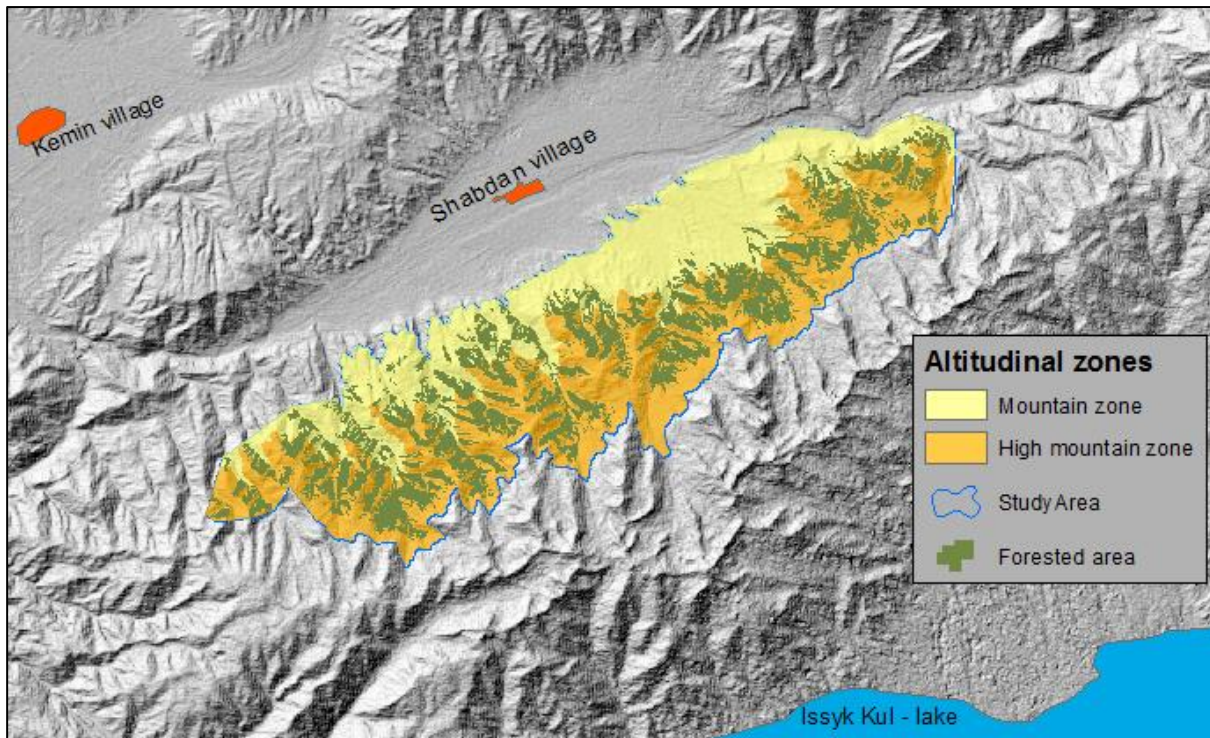


Figure 18: Altitudinal zonation and forest occurrence of the study area according to Orozumbekov et al. (2009), own figure.

4.1.2 Aspect & Slope

Most of the slopes at the study site are North-facing slopes (43%). This is because of the North-oriented position of the study area. The proportion of East-facing, South-facing and West-facing slopes is 16%, 6% and 35% respectively (Figure 19). The study area is situated in the semi-arid mountain zone where forest growth is highly dependent on aspect (exposition) (Fet 2007).

The slope values of the study area have a range from 0°- 46°. In the lower parts, there are some spots with low slope gradients. In the Northeastern and Southwestern parts especially, higher slope values (with a maximum of 46°) occur (figure 20). Only 3% of the total area have slope values below 10°, around 20% of the area have slope values between 10-20°, 32% have values between 20-30°, 31% have slope values between 30-40° and 14% of the total area are steeper than 40°.

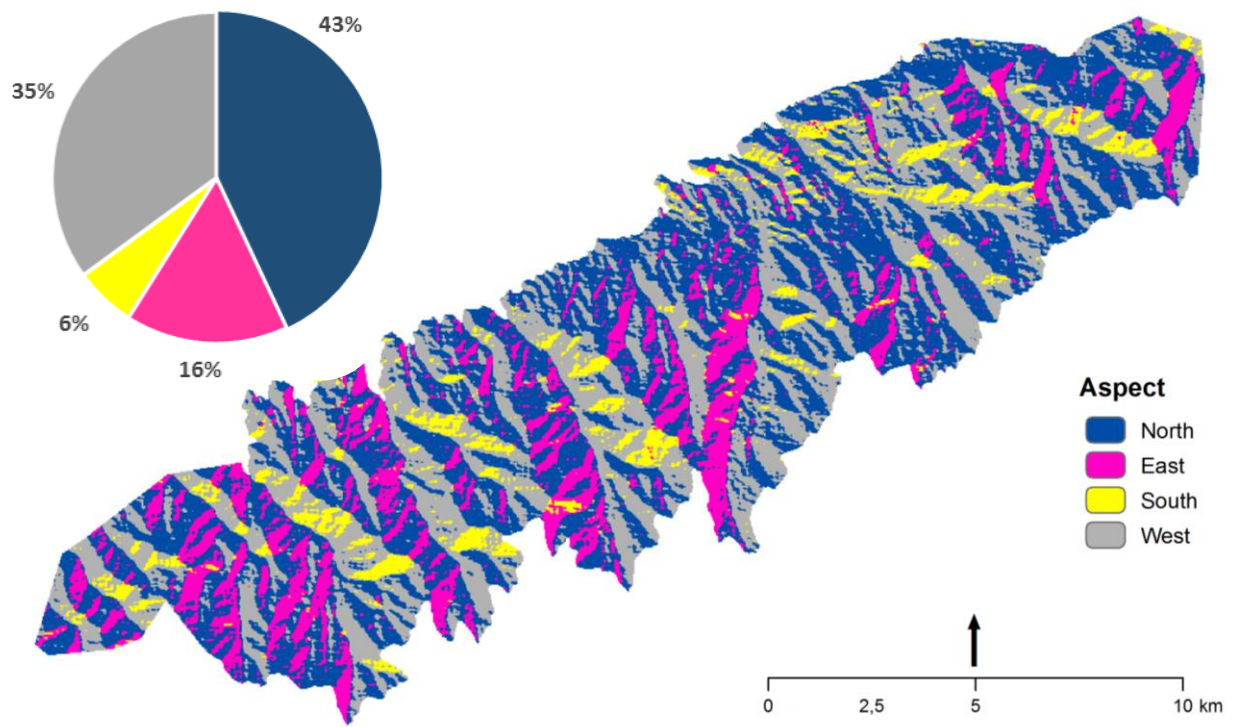


Figure 19: Aspect classes (cardinal direction) of the study area. N=315-0° and 0-45°, E=45-135°, S=135-225°, W=225-315°, own figure.

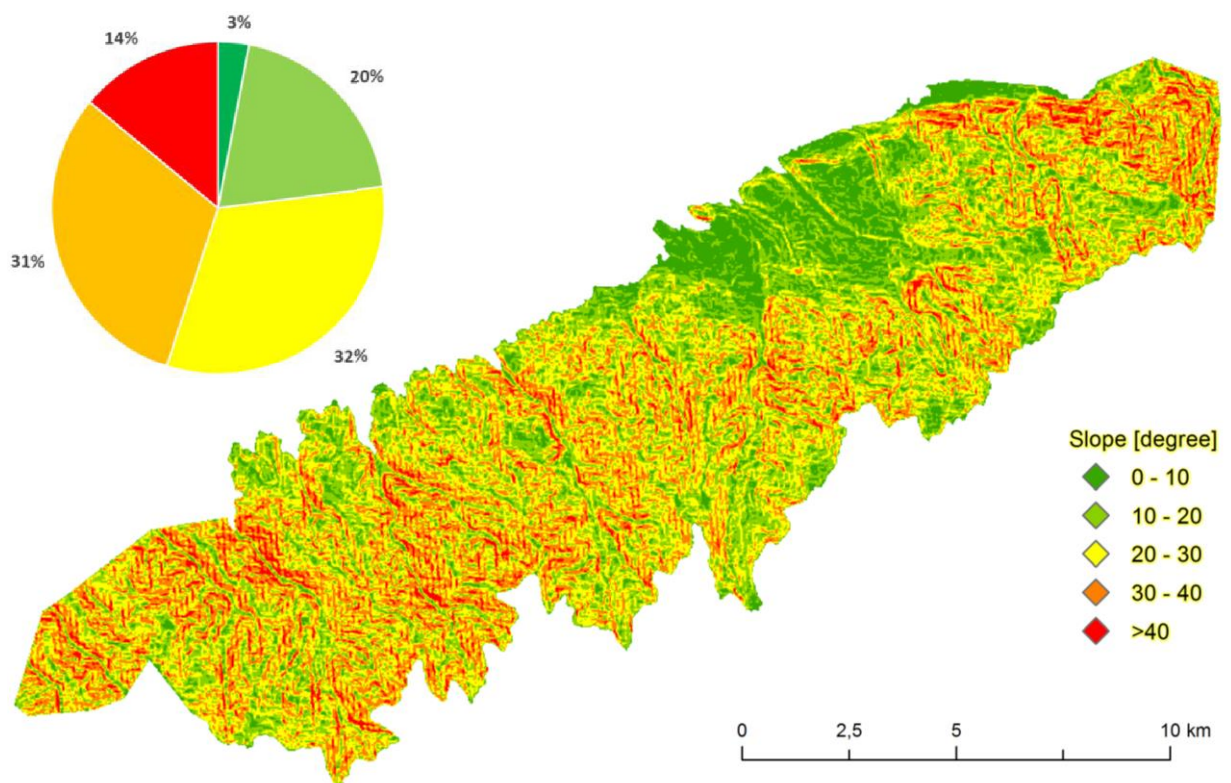


figure 20: Map of slope values at the study area and the share of the slope classes (top left), own figure.

4.1.3 Forest occurrence

The total forested area inside the study area (or area covered with established woody plant species) is about 6,618 ha, where 46 ha are covered with birch forest, 61 ha with juniper trees, 198 ha are planted forest (mostly *Pinus* sp.), 1,313 ha are covered with different bushes and around 5,000 ha with spruce forest (Figure 21).

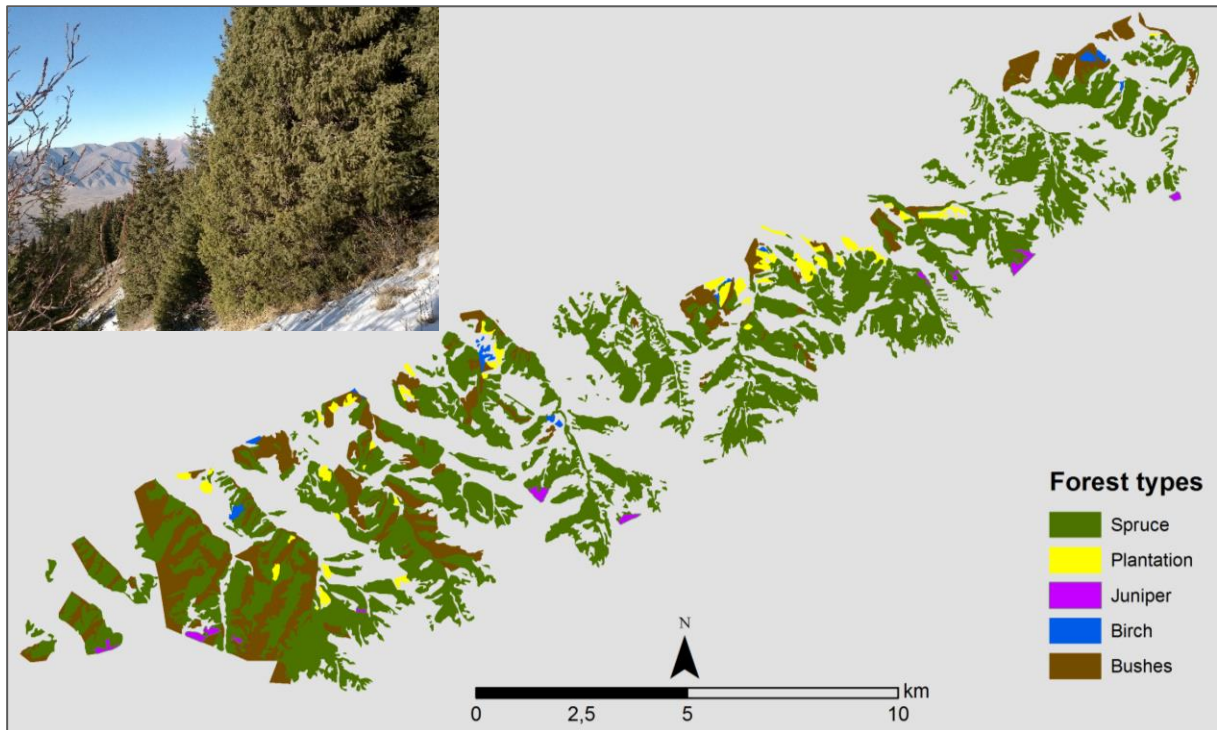


Figure 21: Spruce forest edge image and forest types distribution in the study area, own figure.

The altitudinal range of the study area is from 1,600 to 3,000 m.a.s.l. whereas the share lower than 1,700 m.a.s.l. and higher than 2,900 m.a.s.l. is negligible. Forest occurs from ~1,700 to ~2,900 m.a.s.l. with an even distributed pattern (Figure 22, left). At lower elevations, there are large parts with no forest cover (see also Figure 18). Forest is not growing on every slope-cardinal direction (aspect). On southern slopes, no forest occurs. The closer it comes towards South, the less forest grows. A few hectares of bushes is the only exception of woody plants growing on south-facing slopes (see Figure 23, right). The plotted inclination (slope) values of the study area show a slightly right skewed distribution. Different from the total slope distribution, forest occurrence shows an even distributed curve but with the same range. Forest is therefore growing on every slope gradient.

When analyzing the following histograms, it is important to always consider the possible different scaling of the Y-axis. This can lead to confusion when interpreting the graphs and has to be kept always in mind.

Juniper forest is growing exclusively at elevations above 2,300 m.a.s.l. (Figure 22, right). It's distribution trend is towards higher elevations with a peak between 2,700 and 2,800 m.a.s.l. It is therefore also occurring at treeline elevations and forming treeline (2,900 m.a.s.l.). Juniper growth seems to be influenced very little by aspect. Only on direct-South-facing slopes it does not grow. There

is, however a slight preference to grow on Northwest-North-Northeast (NW-N-NE) facing slopes. The inclination values (slope) of Juniper growth follow the overall slope values and do not show preferences.

Spruce forest grows from ~1,700 to ~2,900 m.a.s.l. with a slightly left skewed distribution curve (Figure 23). Concerning the aspect, spruce is completely absent on Southeast-, South- and Southwest-facing slopes. Slope seems not to influence the growth of spruce forest. It is occurring on all the different inclinations.

Bushes have the same elevational amplitude as spruce, growing therefore from ~1,700 to ~2,900 m.a.s.l., almost following the trend of the total elevation distribution but with a light peak at lower elevations (Figure 23, right). Their growth behavior regarding the aspect is different from the one of the other forest types. They do not avoid South-facing slopes whereas on North-facing and adjacent slopes, their distribution seems to be limited. Slope seems not to influence the growth of bushes in the study area. It is occurring on all the different inclinations.

Birch forest occurs mostly at lower elevations between 1,700 and 2,300 m.a.s.l. (see Figure 24, left). There shall not be forgotten to consider the small amount of birch forest areas (about 46 ha out of 6,618 ha of total forest area). Birch forest is completely avoiding Southeast- and South-facing slopes but growing sparsely on Southeast-facing slopes. The inclination (slope) distribution shows a slight trend towards flatter areas.

Planted forest areas occur mostly at elevations between 1,800 and 2,400 m.a.s.l. and only on a few spots up to 2,700 m.a.s.l. (Figure 24, right). No occurrence is statable on Southeast-, South- and Southwest- facing slopes. The distribution of planted forest regarding slope values shows an even distribution.

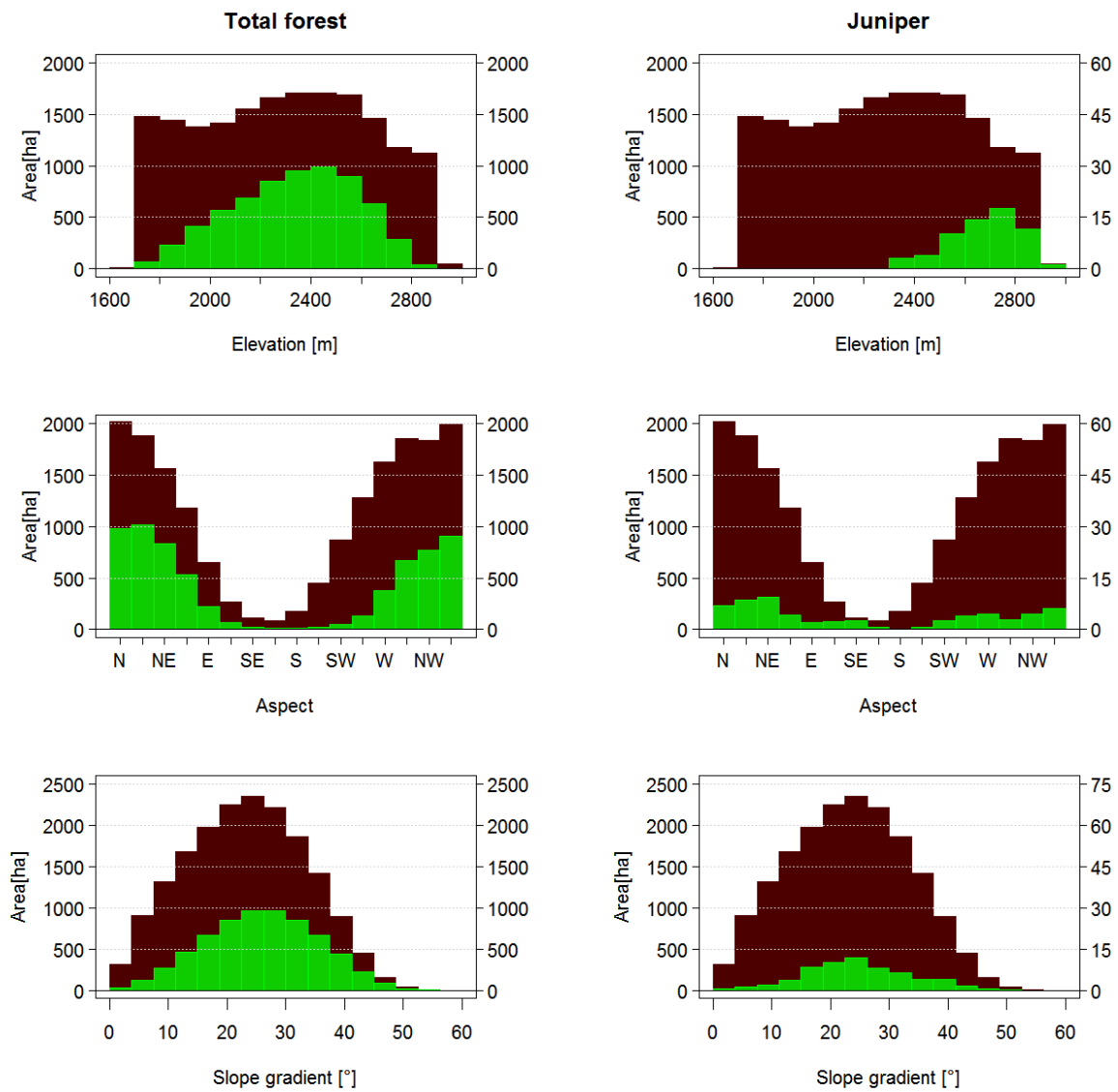


Figure 22: Frequency distribution of morphological parameters of the study area (brown columns, left Y-axis) and different forest types (green columns, left Y-axis). Mind the possible diverging Y-axis scaling.

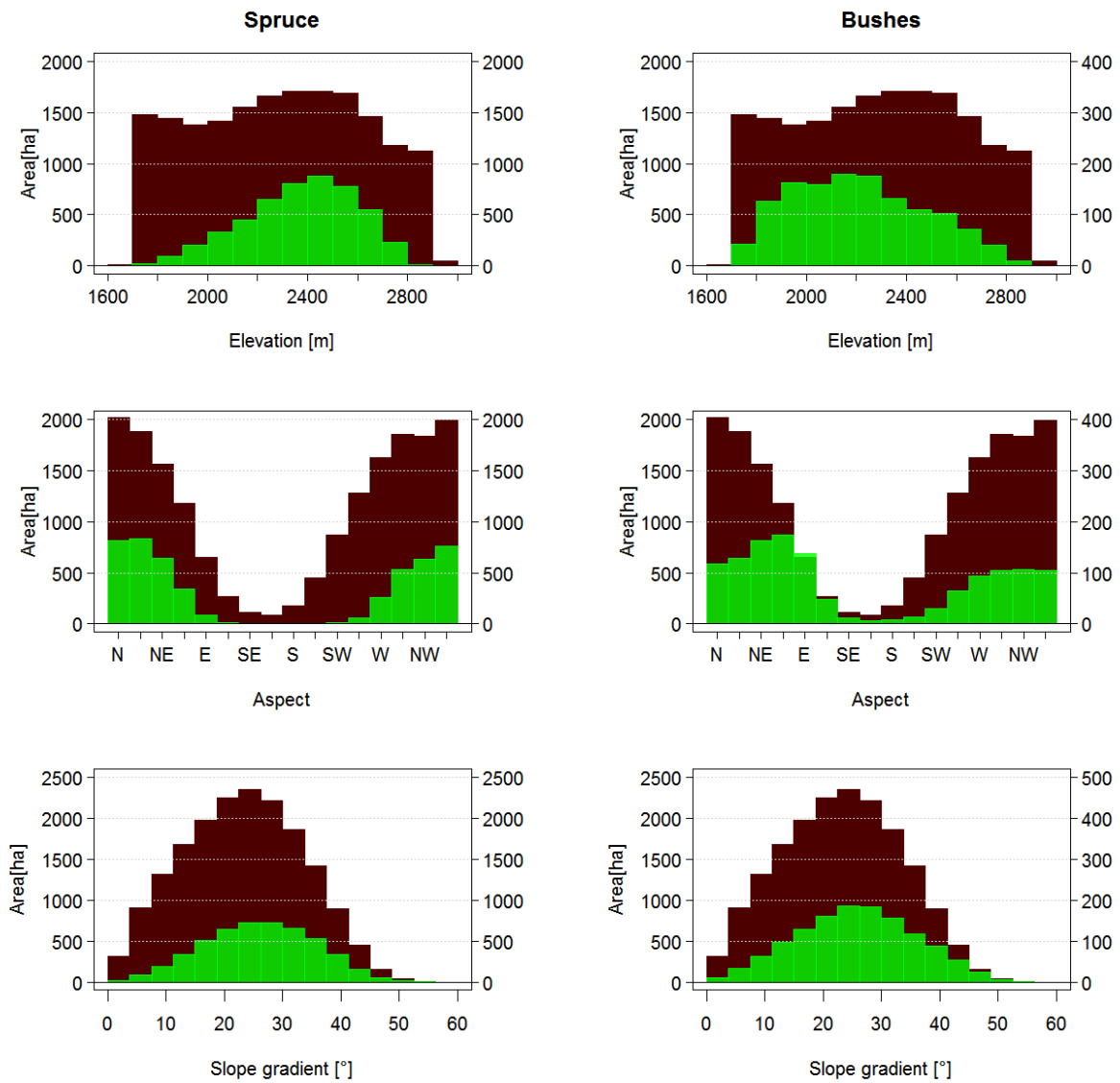


Figure 23: Frequency distribution of morphological parameters of the study area (brown columns, left Y-axis) and different forest types (green columns, left Y-axis). Mind the possible diverging Y-axis scaling.

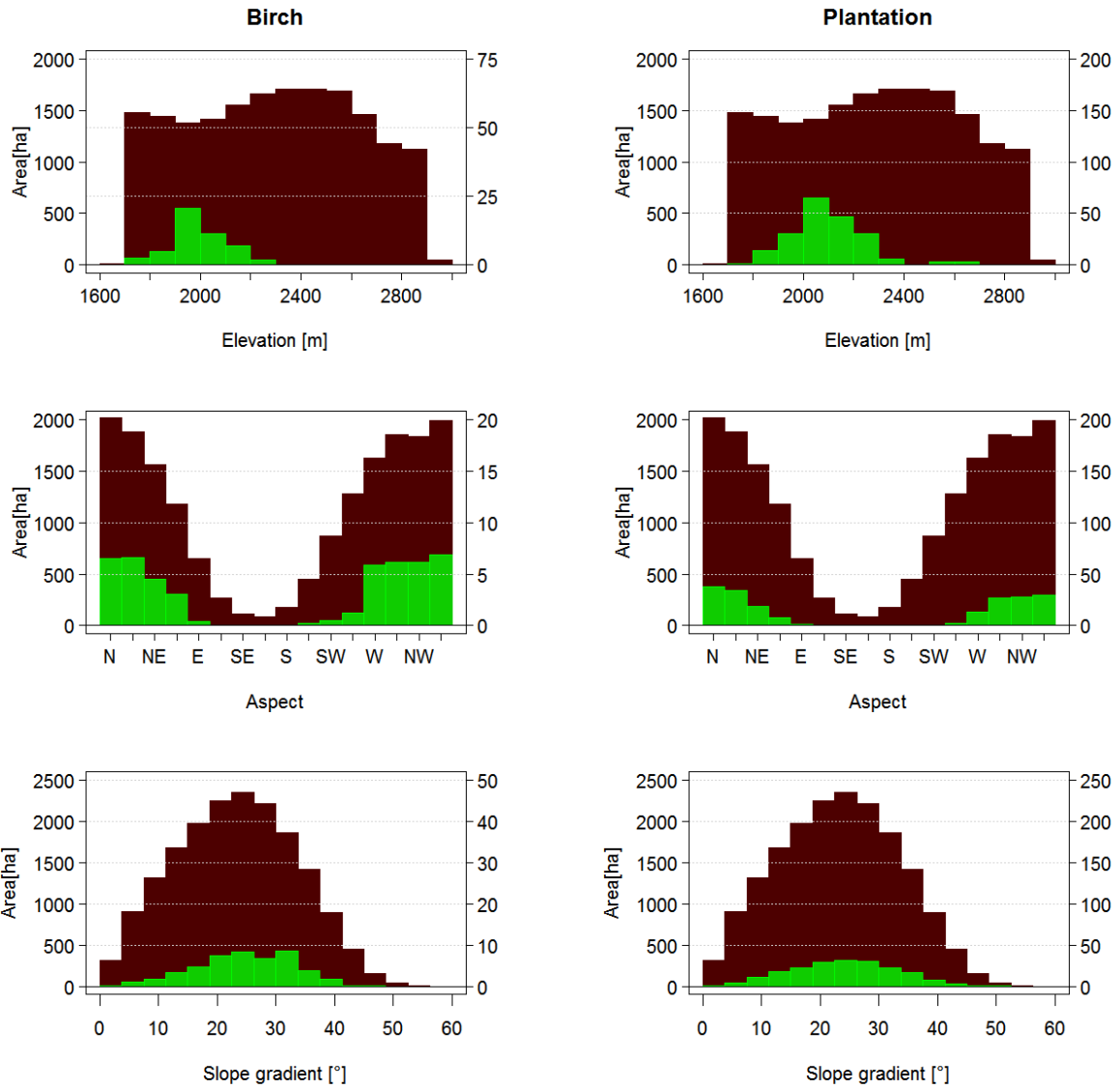


Figure 24: Frequency distribution of morphological parameters of the study area (brown columns, left Y-axis) and different forest types (green columns, left Y-axis). Mind the possible diverging Y-axis scaling.

4.2 Climatological parameters & Forest occurrence

4.2.1 Temperature

The study area can be subdivided in two different altitudinal zones (see 2.1). The Mountain zone (1,200 – 2,200 m.a.s.l.) and High mountain zone (~2,200 – 3,000 m.a.s.l.). There is a distinct vertical zoning regarding climate pattern. Whereas at the valley bottom at the lower edge of the study area the mean annual temperature is around 4 °C, it is distinctly below zero at the upper border (Figure 25).

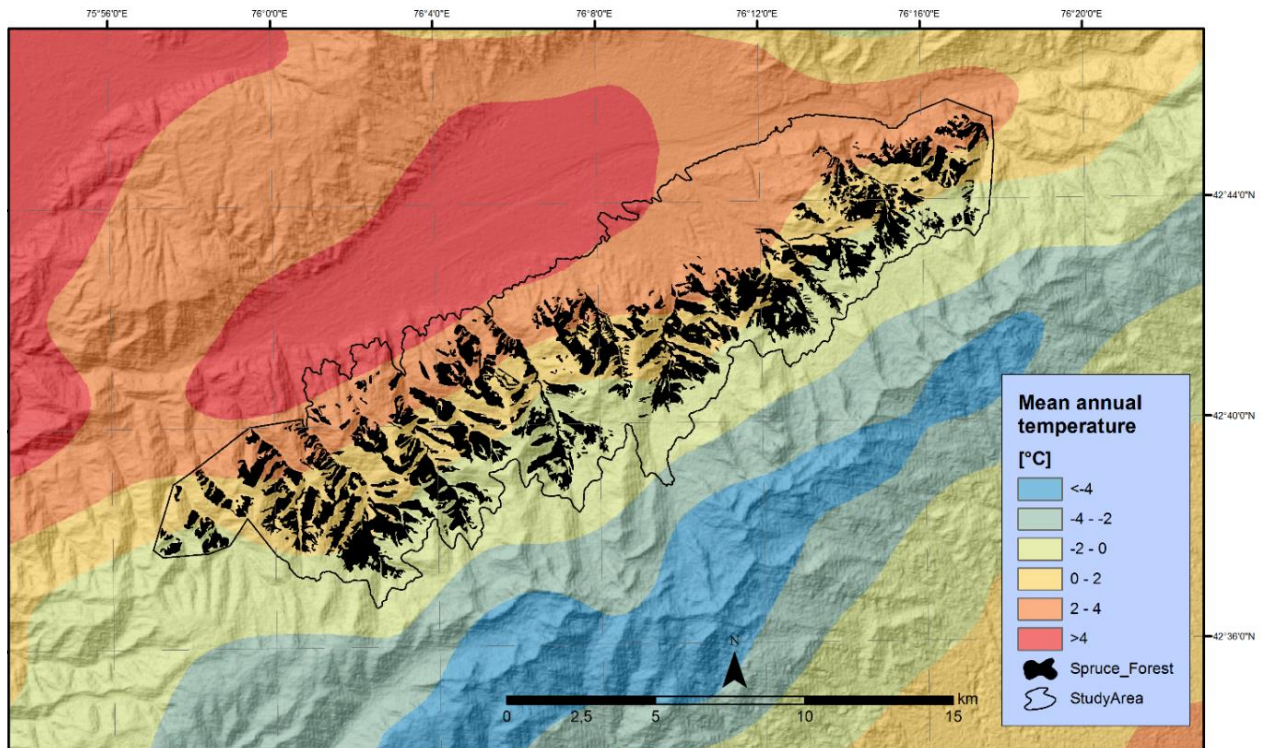


Figure 25: Mean annual temperature values (Geostatistical Kriging was applied on lower resolution Böhner (2006)-dataset), own figure.

Georeferencing and analyzing of forest maps of local authorities showed forest lines in Chong Kemin NP being situated at around 2,900 m.a.s.l., laying therefore in its entirety inside the High mountain zone (Figure 18). The 10°C monthly mean temperature of the warmest month (July) coincides with the actual forest line (Figure 26) as proposed by Klinge et al. (2015).

The temperature pattern for the warmest month of the year, i.e. July, is shown in Figure 27. The temperature difference between the Chong Kemin valley bottom and the upper treeline is more than 10°C.

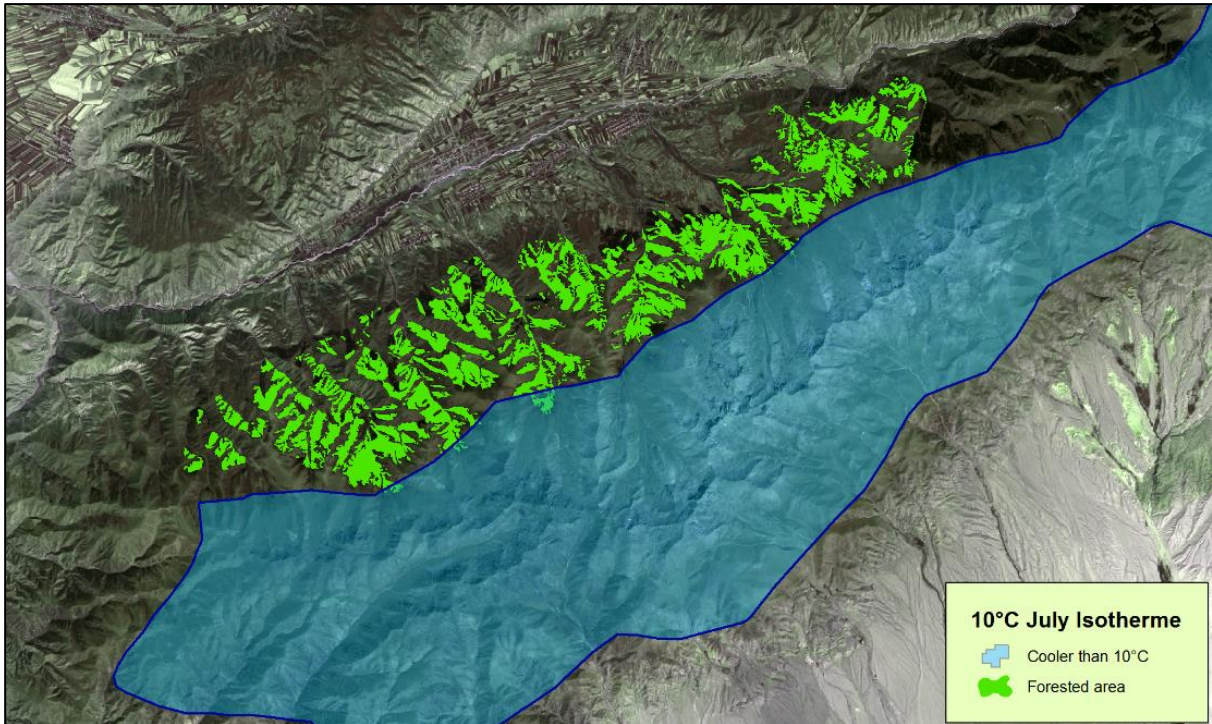


Figure 26: Coincidence of the 10°C July Isotherme with the upper treeline in the study area, own figure.

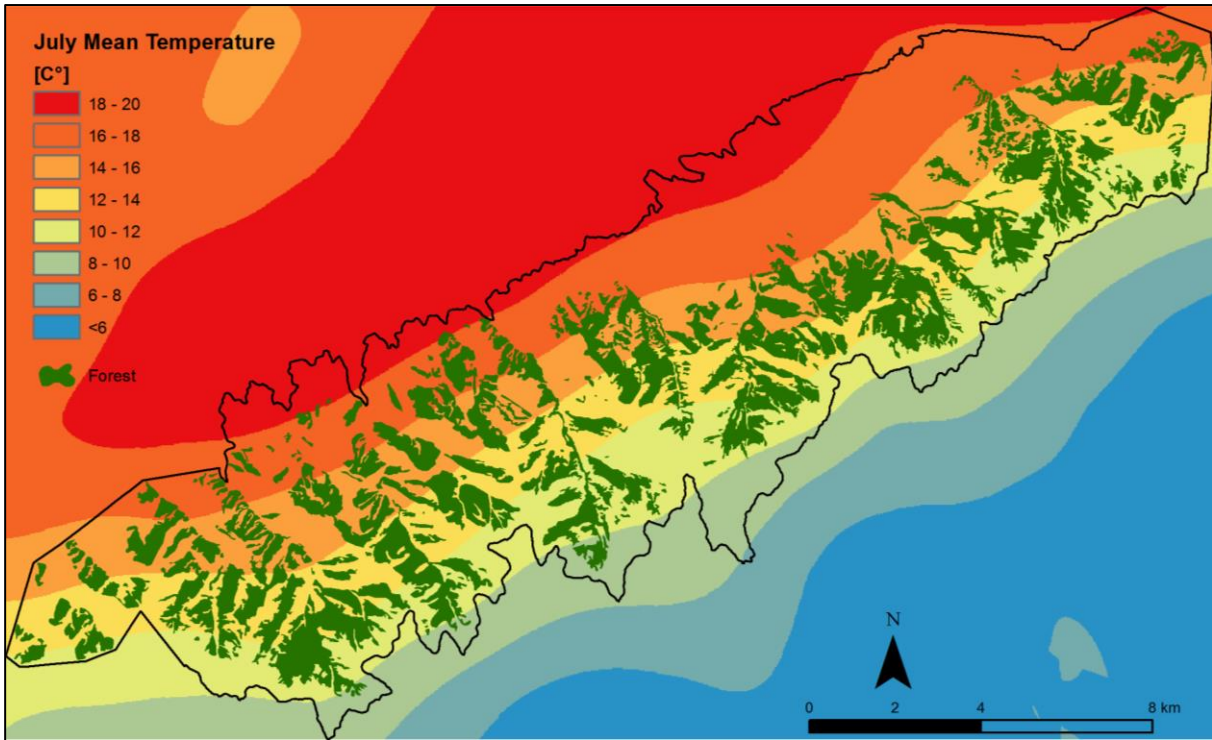


Figure 27: July mean temperature values of the study area, source: Böhner (2006), Kriging interpolation, own figure.

4.2.2 Precipitation

Regarding the annual precipitation, a range between 350 mm in the valley bottom and around 1100 mm at the upper forest borders is stable (Figure 28). The drier valley bottom gets therefore 750 mm less of precipitation per year than the upper forest border. The same is true for precipitation values for July (the hottest and driest month of the year). The values vary from around 25 mm at the lower forest borders to around 100 mm at higher elevations (Figure 29). The water vapor deficit is strongly negative during summer months (Table 6).

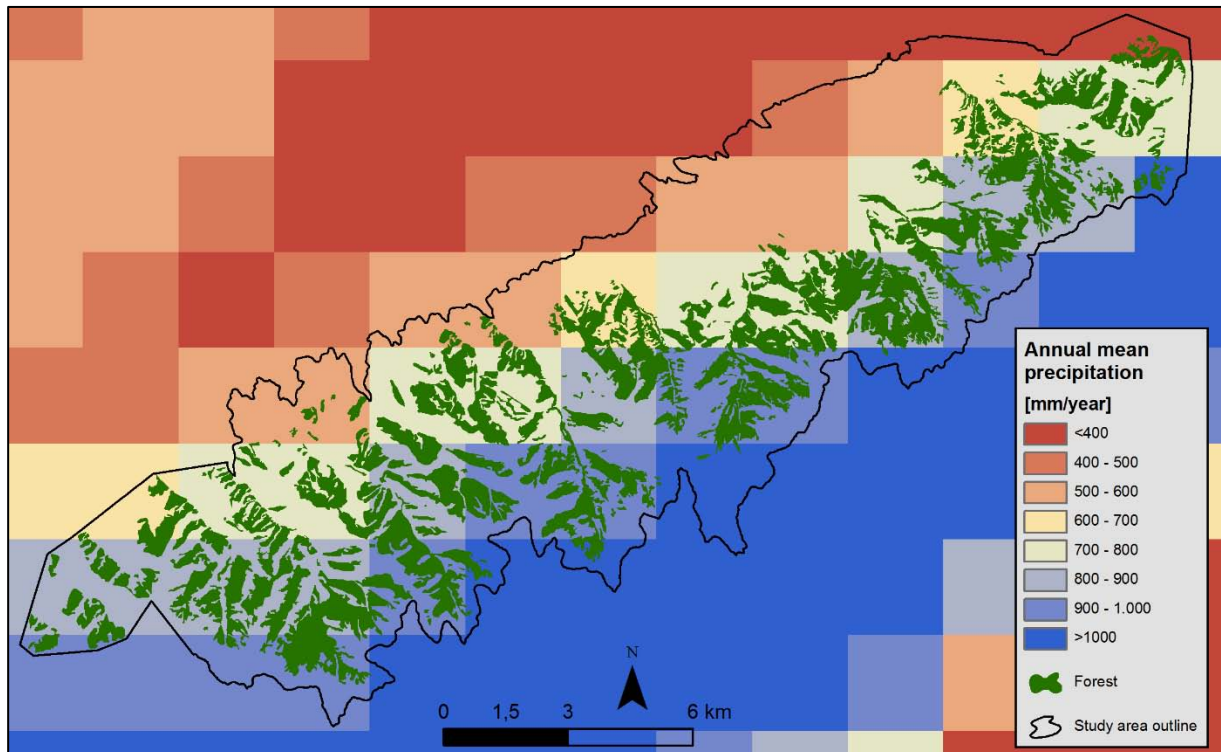


Figure 28: Annual mean precipitation values in the study area, source: (Böhner 2006), own figure.

The average annual rainfall measured at the only meteorological station in the area, Shabadan, is of 469 mm (DFHGI 2015). The station is situated at approx. 1,500 m.a.s.l. at 5 km distance from the lower border of the study area. It is not clear if the data records of it are part of the ample climate-dataset obtained by Prof. Dr. Böhner. All analysis in this study are solely done with this latter dataset.

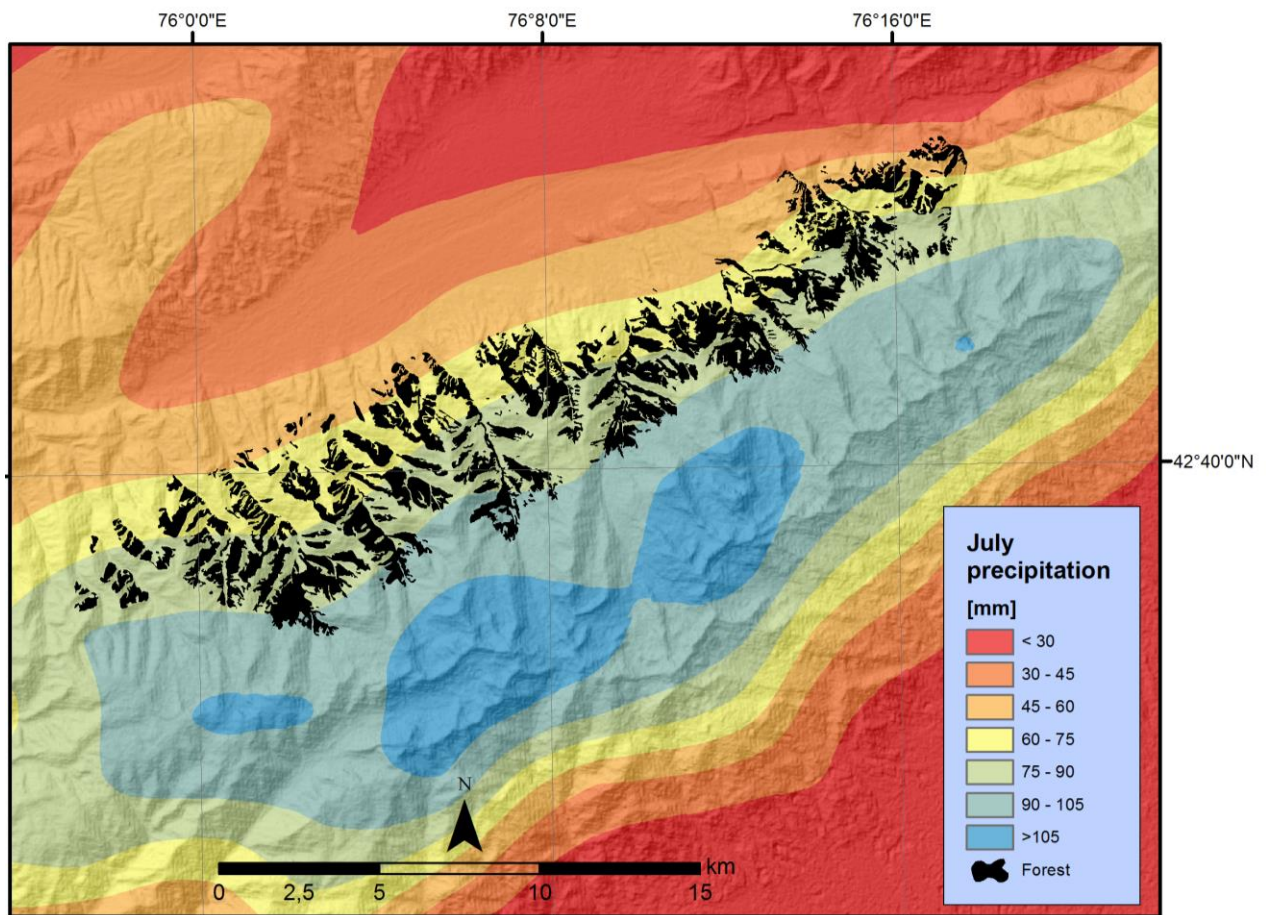


Figure 29: July mean precipitation of the study area and surroundings, own figure.

4.2.3 PET (Potential Evapotranspiration)

The Potential Evapotranspiration per year at the study site varies between ~350 mm at the upper treeline and ~530 mm in the valley bottom (see Table 6). Because of constant low temperature values during winter months, at the lower forest border there are at least 5 months with no Potential Evapotranspiration (values of zero). At the upper boundary this rises up to around 7 months of zero-PET values. There is a clearly negative ratio of PET/precipitation at the lower forest boundary and a strongly positive ratio at the upper forest boundary over the whole year. Here, precipitation exceeds the Potential Evapotranspiration for more than 700 mm. In July, the PET is much higher than rainfall at the lower areas. Only 45 mm of precipitation is confronted with more than 100 mm of PET. At the upper forest line things change: the PET values are slightly lower than the actual precipitation values.

Table 6: Exemplary annual Potential Evapotranspiration values for the study area at the lower (1,700 m.a.s.l.) and at the upper forest line (2,900 m.a.s.l.), values generated with the online available Thornthwaite's calculator tool (see Figure 16), nd = no data availability.

	Lower forest boundary		Upper forest boundary	
	PET [mm]	Precipitation [mm]	PET [mm]	Precipitation [mm]
January	0	26	0	42
February	0	nd	0	nd
March	0	nd	0	nd
April	42	nd	0	nd
May	70	nd	50	nd
June	101	nd	83	nd
July	117	45	95	110
August	102	nd	82	nd
September	66	nd	56	nd
October	25	nd	0	nd
November	0	nd	0	nd
December	0	nd	0	nd
Σ [mm/year]	523	350	366	1100

In Figure 30, the yearly Potential Evapotranspiration of the study area and its surroundings is plotted. The PET for the entire Kyrgyz National territory can be found in Appendix V.

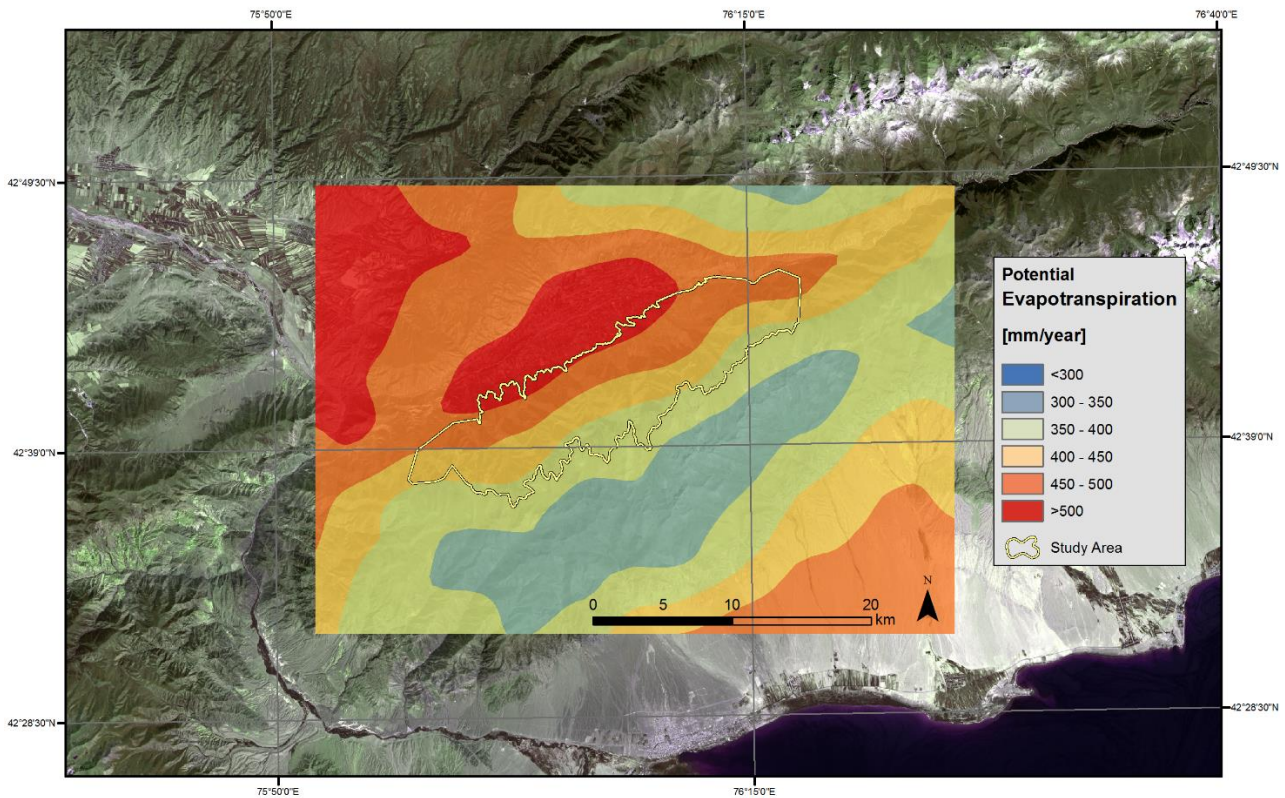


Figure 30: PET of the study area and surroundings derived with the Thornthwaite's method, input: Böhner (2006) monthly mean temperature data, ArcGis Kriging interpolation tool, data resolution: 28 x 28 m, own figure.

4.2.4 Radiation

During the vegetation period the incoming solar energy (radiation) is between 300 and 1300 kWh/m² at the study area. From Figure 31 can be noticed that forest occurs preferably on areas with lower insolation values (dark blue colored).

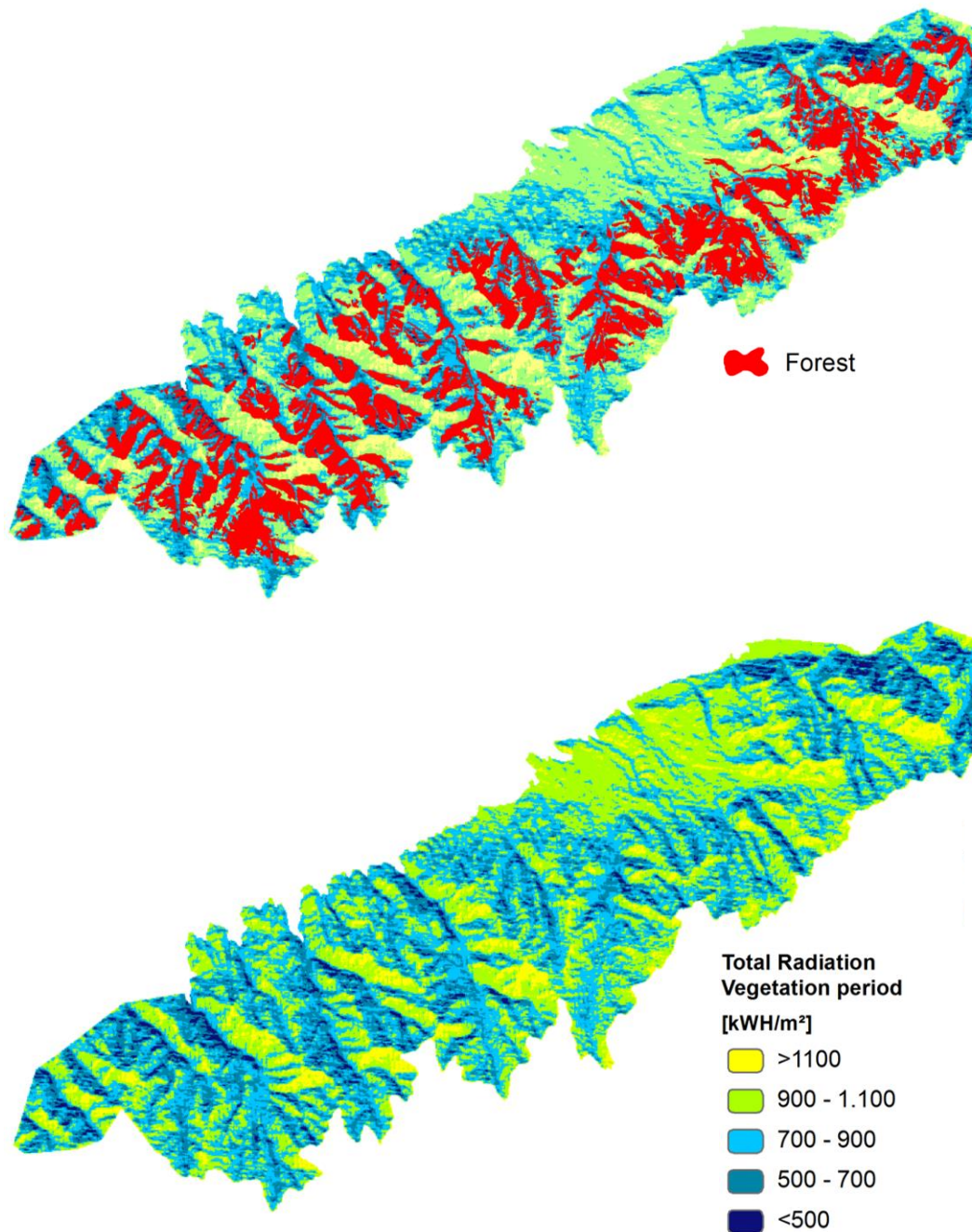


Figure 31: Relationship of forest occurrence (top) and radiation (bottom) to point out forest growth happening mostly on lower-radiation areas, source: Böhner (2006), own figure.

4.2.5 Forest occurrence

The Potential Evapotranspiration range of the study area is between 350 and 530 mm/year (Figure 32, left). Most of the areas of the study site have however PET values between 400 and 500 mm/year. Forest is growing between 370 and 510 mm of PET per year. The radiation sum during the vegetation period has shown to have a wide range reaching from around 300 up to 1350 kWh/m². Inside this range, forest does not grow everywhere. Only on areas with lower radiation values, forest seems to establish. It starts at the same point as the total radiation (300 kWh/m²) and ends with around 1,200 kWh/m² of incoming radiation during the vegetation period. Forest is avoiding therefore the spots with very high radiation inputs. The total amount of yearly precipitation is around 350 mm in the valley bottom and around 1,100 mm at the upper border of the study area. More forest grows on sites with a higher amount of precipitation. The forest-distribution graph shows a clear trend of forest to grow on areas with precipitation sums >600 mm/year. Below 600 mm/year, only a small percentage of the total forest can be found. A very similar behavior shows the forest distribution when it comes to July-precipitation pattern. At the lower edge of the study area there are around 25 mm of rain in July. On the upper border around 100 mm. Very few forest grows on areas with July-precipitation values below 50 mm. At areas between 50 – 90 mm, forest is establish best.

When analyzing the histograms here, it is important to always consider the possible different scaling of the Y-axis. This can lead to confusion when interpreting the graphs and has to be kept always in mind.

Juniper forest grows at sites with relatively low Potential Evapotranspiration values (about 400 mm/year, see Figure 32, right). Areas with PET values higher than 430 mm/year are not populated with Juniper. When it comes to the solar radiation input during the vegetation period, Juniper grows on spots with very low (400 kWh/m²) but also on spots with very high values (1,200 kWh/m²). There is, however a higher occurrence at areas with relatively high radiation values (between 800 and 1,000 kWh/m²). Juniper growth inside the study area is limited to yearly precipitation sums between 800 and 1,000 mm. A similar pattern shows Juniper growth and July-precipitation: growth is only happening between ~80 and 95 mm.

Spruce forest grows on areas with PET values between 370 and 510 mm/year with an agglomeration between around 400 and 470 mm/year (Figure 33, left). It does not grow on spots with radiation values higher than 1,100 kWh/m² during the vegetation period. A culmination of growth can be found on areas with radiation values between 600 and 800 kWh/m². The spruce forest distribution is limited to areas with precipitation values between 500 and around 1050 mm/year whereas below 600 mm/year, almost no forest occurs. July precipitation values show similar patterns: spruce forest growth happens between ~40 to 100 mm whereas below 60 mm only a negligible part of spruce forest is established.

The range where **planted forest** is growing, reaches from 400 to 510 mm of Potential Evapotranspiration per year (Figure 33, right). It grows on sites with a solar radiation input of between 300 and 1,100 kWh/m² during the vegetation period. This distribution is very similar with the one of spruce forest. Planted forest growth inside the study area is limited to a small range of yearly precipitation sums between 600 and 900 mm. A similar pattern shows Plantation growth and July-precipitation: it is only occurring between ~50 and 90 mm.

Birch forest occurs on areas with annual Potential Evapotranspiration sums between 430 and 510 mm/year (Figure 34, left). The range of insolation values where it occurs is 400 – 1,100 kWh/m². Birch forest distribution in the study area is on sites with annual precipitation sums from 450 and 850 mm. The range of July precipitation where it is growing is between 30 and 80 mm.

Bushes are growing at sites with a wide range of PET per year (Figure 34, right). It goes from 380 to 510 mm from a total annual range in the study area between 350 and 530 mm. Solar radiation input seems also to not influence bushes to grow. The range is the same as the total range of the study area. They also grow on areas with the lowest precipitation values. Only on sites with highest precipitation values (>1,000 mm/year), they cannot be found. A similar pattern shows the bushes distribution regarding the July precipitation. Here, a small gap with no bushes occurrence is observable between 40 and 50 mm whereas the range goes from 30 to 90 mm of precipitation in July.

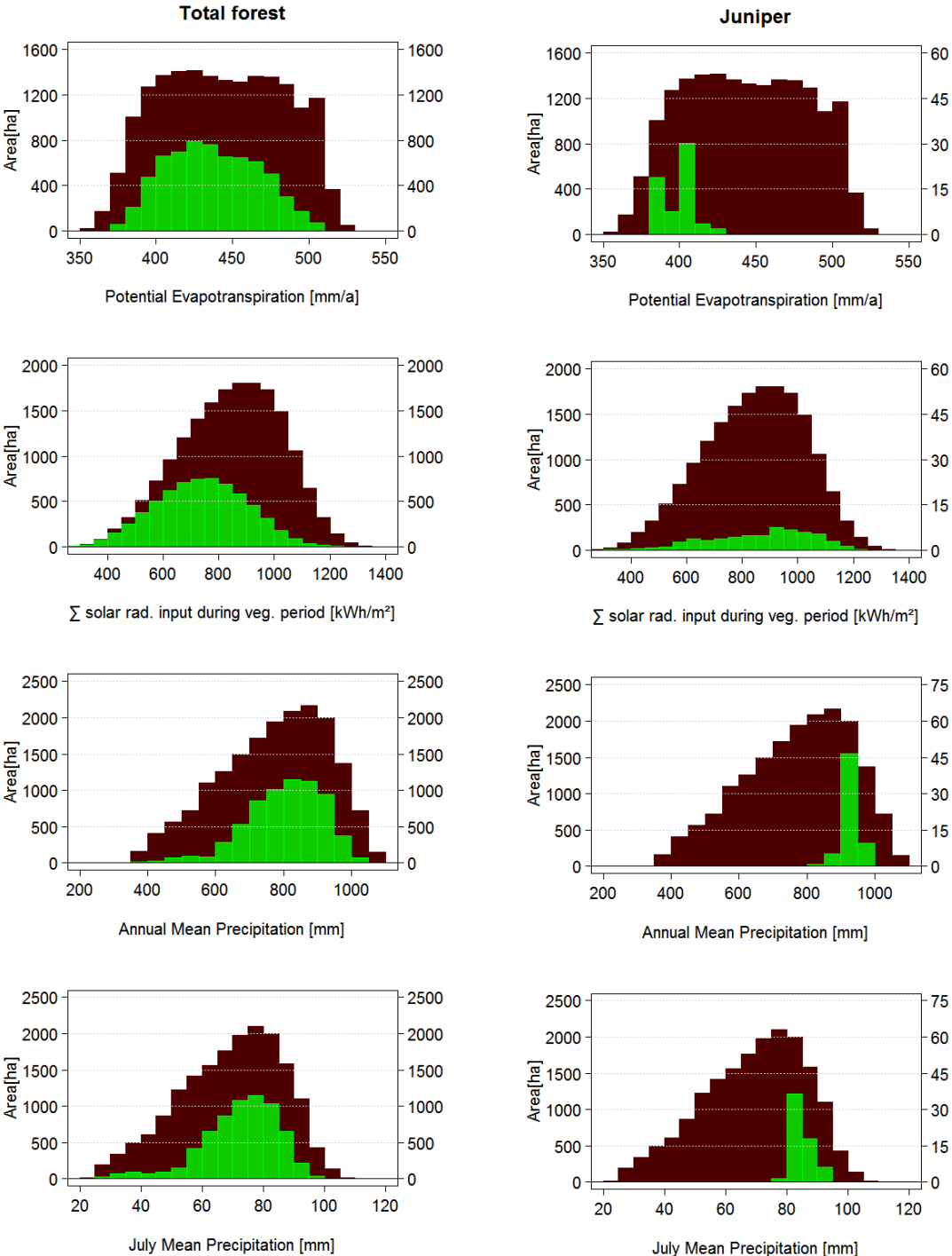


Figure 32: Frequency distribution (in ha) of climate parameters: total study area (brown, left Y-axis) in relation to spruce forest (left) and bushes (right). Mind the diverging Y-axis scaling.

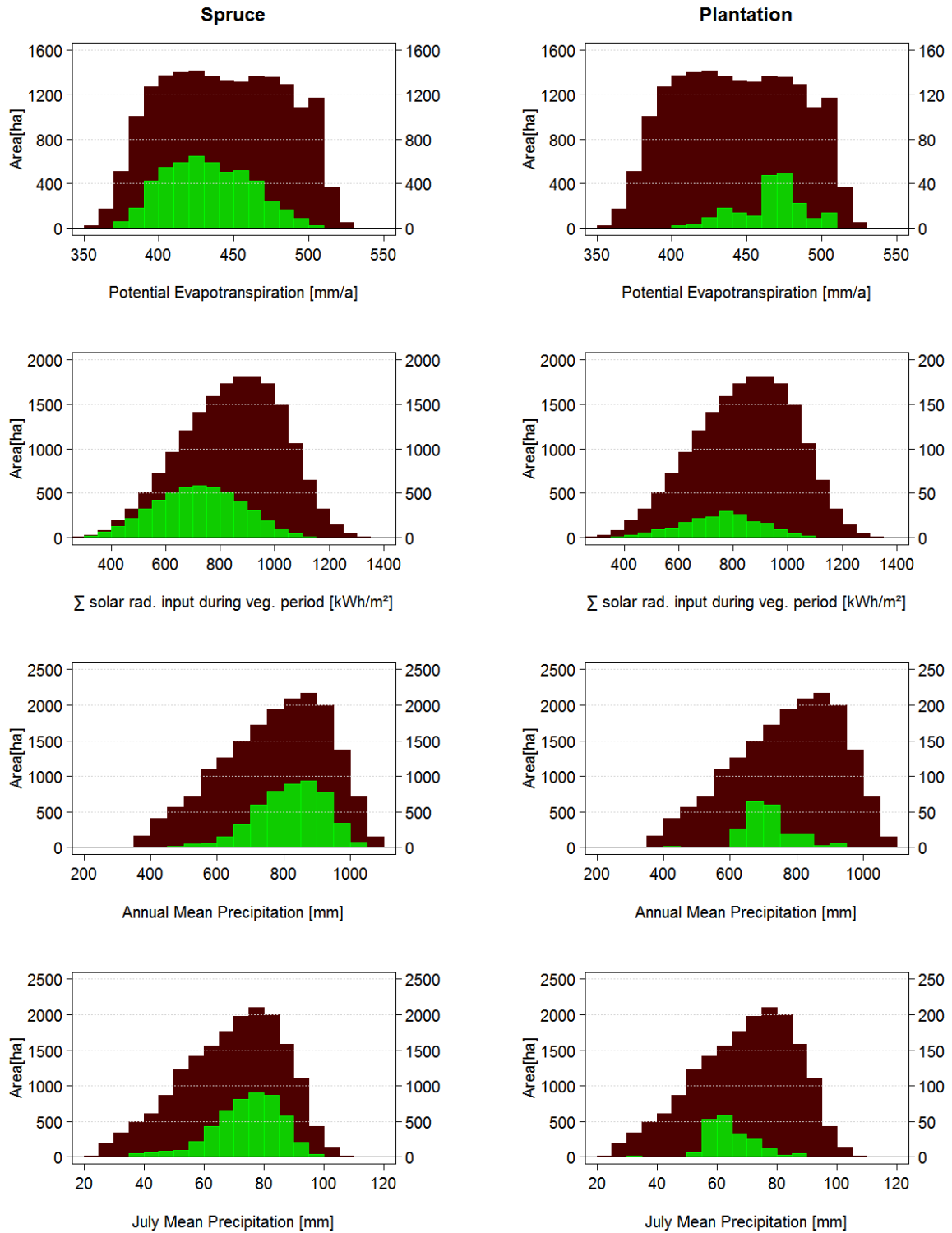


Figure 33: Frequency distribution (in ha) of climate parameters: total study area (brown, left Y-axis) in relation to spruce forest (left) and bushes (right). Mind the diverging Y-axis scaling.

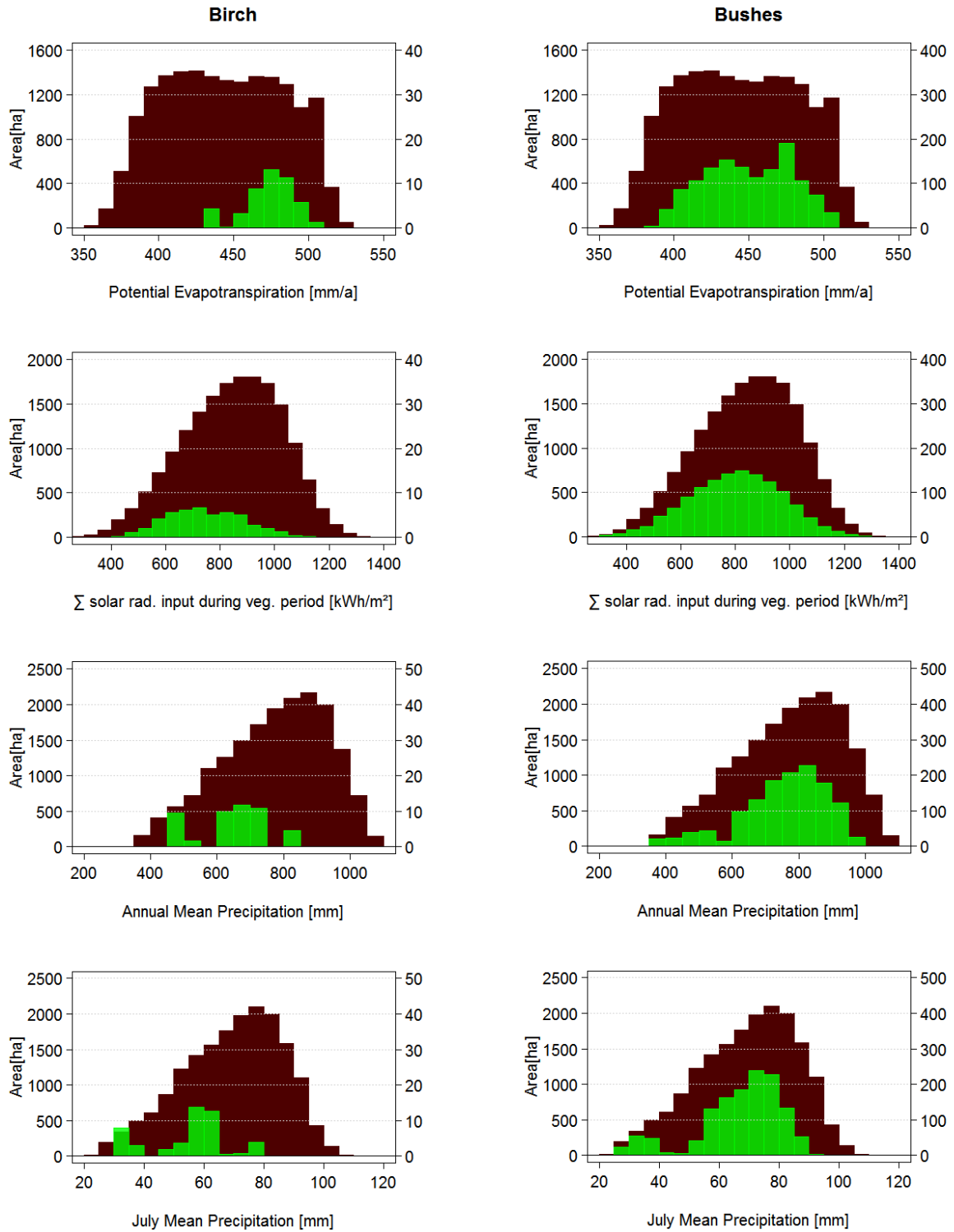


Figure 34: Frequency distribution (in ha) of climate parameters: total study area (brown, left Y-axis) in relation to spruce forest (left) and bushes (right). Mind the diverging Y-axis scaling.

4.3 Logistic Regression model

The four parameters which were selected to be used in the logistic regression model are: elevation, slope, aspect, radiation (see 3.3.3). The fact that they do not correlate with other morphological and climatological parameters (see Table 7 and Table 8), makes them suitable for being used to explain forest growth or no-forest growth.

The elevation variable was squared because there is an upper and a lower forest line. Forest is therefore growing between 1,700 and 2,900 m.a.s.l. (Figure 35). Regarding the aspect, it is evident that forest growth is very likely to occur on North facing slopes (315-0° and 0-45°) and rather unlikely to occur on South facing slopes (135-225°). This effect is stronger on spruce forest (Figure 36).

The probability of forest growth can be explained quite well with changing elevation values. This is true for the overall forest growth (Figure 35) and for spruce forest growth (Figure 36).

Slope does hardly not influence overall forest growth whereas it has an impact on spruce growth. The steeper the terrain is the more unlikely spruce forest occurs.

Radiation (solar energy input on a defined area) is influencing forest growth at the study site. Total forest and spruce forest are growing where the radiation is lower. Until a certain amount of radiation, the effect is not strong; growth probability is not changing with changing radiation intensity. After a certain threshold, however (at around 500 kWh/m² on total forest and around 600 kWh/m² on spruce forest) growth probability is decreasing almost linear with increasing radiation values.

The statistical power of the model (accuracy) is 0.76 the total forest model (Figure 35) and 0.80 for the spruce forest model (Figure 36). The coefficient of determination R_N^2 (Nagelkerke's R squared) is 0.44 for the total forest model and $R_N^2=0.54$ for the spruce forest model. This means the model is able to explain the total forest dataset well. The spruce dataset can be explained even better by the logistic regression model (for explanation see 3.3.1).

Table 7: Total forest, Table of coefficients

	Estimate	Std. Error	z value	Pr(> z)
(Intercept)	-5.074e+01	3.806e-01	-133.316	<0.0001 ***
elevation	4.814e-02	3.349e-04	143.746	<0.0001 ***
elevation2	-1.023e-05	7.212e-08	-141.779	<0.0001 ***
slope	-4.011e-03	7.143e-04	-5.615	<0.0001 ***
aspect	-1.528e-02	3.070e-04	-49.764	<0.0001 ***
aspect2	4.218e-05	8.428e-07	50.044	<0.0001 ***
radiation	-5.079e-03	4.951e-05	-102.596	<0.0001 ***

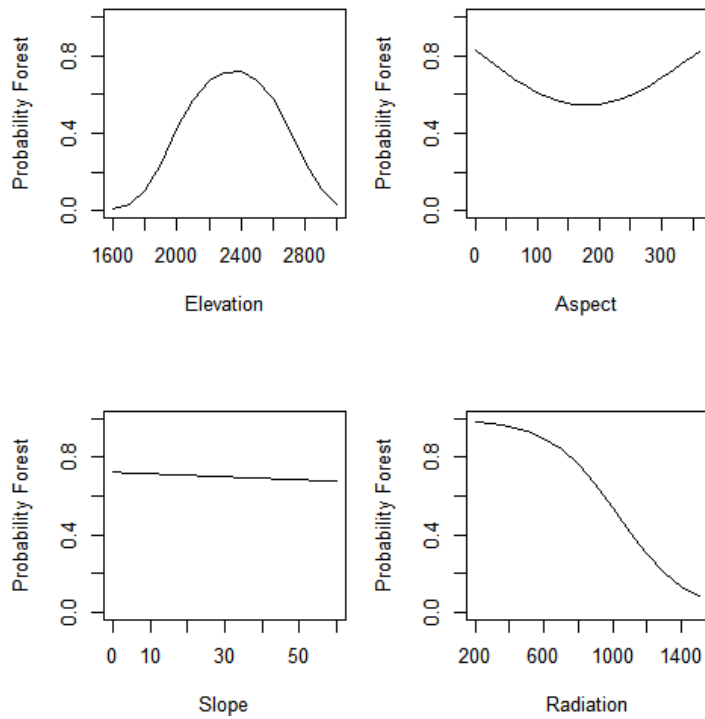


Figure 35: Total Forest area: Logistic regression probability plots which explain the probability forest growth according to the selected four variables, Elevation is in m.a.s.l, Aspect is in degree (N=315-0° and 0-45°, E=45-135°, S=135-225°, W=225-315°), Slope = inclination of the terrain in degree (°), Radiation is the solar insolation input in kWh/m² during the vegetation period.

Table 8: Spruce forest, Table of coefficients

	Estimate	Std. Error	z value	Pr(> z)
Intercept)	-6.769e+01	5.429e-01	-124.69	<0.0001 ***
Elevation	6.289e-02	4.729e-04	132.98	<0.0001 ***
Elevation2	-1.318e-05	1.006e-07	-131.08	<0.0001 ***
Slope	-1.369e-02	9.000e-04	-15.21	<0.0001 ***
Aspect	-2.063e-02	3.795e-04	-54.37	<0.0001 ***
Aspect2	5.894e-05	1.047e-06	56.31	<0.0001 ***
Radiation	-6.242e-03	6.258e-05	-99.75	<0.0001 ***

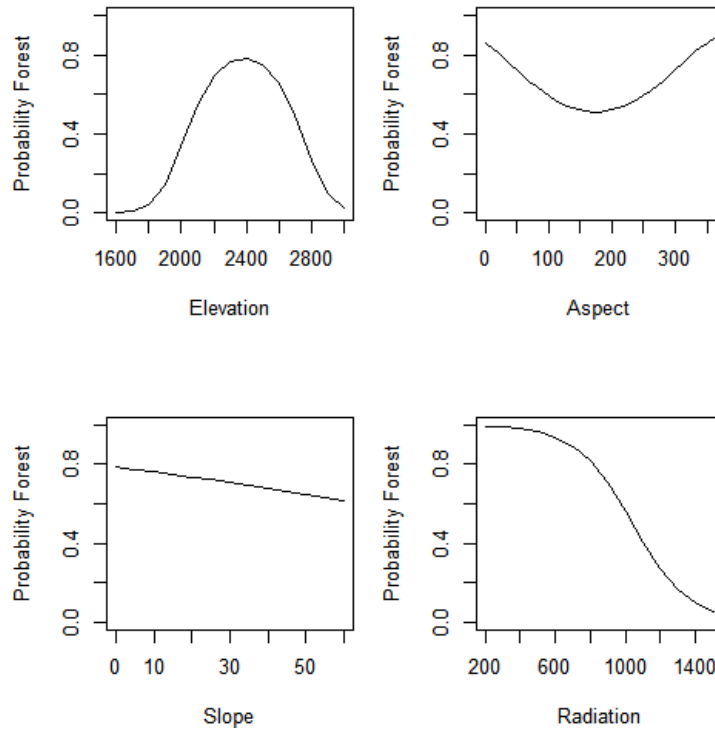


Figure 36: Spruce forest: Logistic regression probability plots that explain the probability spruce growth according to the selected four variables. Elevation is in m.a.s.l, Aspect is in degree (N=315-0° and 0-45°, E=45-135°, S=135-225°, W=225-315°), Slope = inclination of the terrain in degree (°), Radiation is the solar insolation input in kWh/m² during the vegetation period.

With a logistic regression model, forest occurrence was estimated and plotted. The predicted forest area is for the most part of the study site conform to the actual forest area (Figure 38). The model predicted 8,078 ha to be forested and 9,771 ha to be non-forested area (Figure 38). The actual (true) forest area though is around 6,618 ha and the non-forested area 11,231 ha. There are therefore parts which are classified as forest by the model, but no forest is growing on them (1,459 ha of mismatch).

The accuracy of the model is not the same for the entire study area (Figure 37). Some of the model-predicted forest areas match very good with the real forest occurrence, others don't.

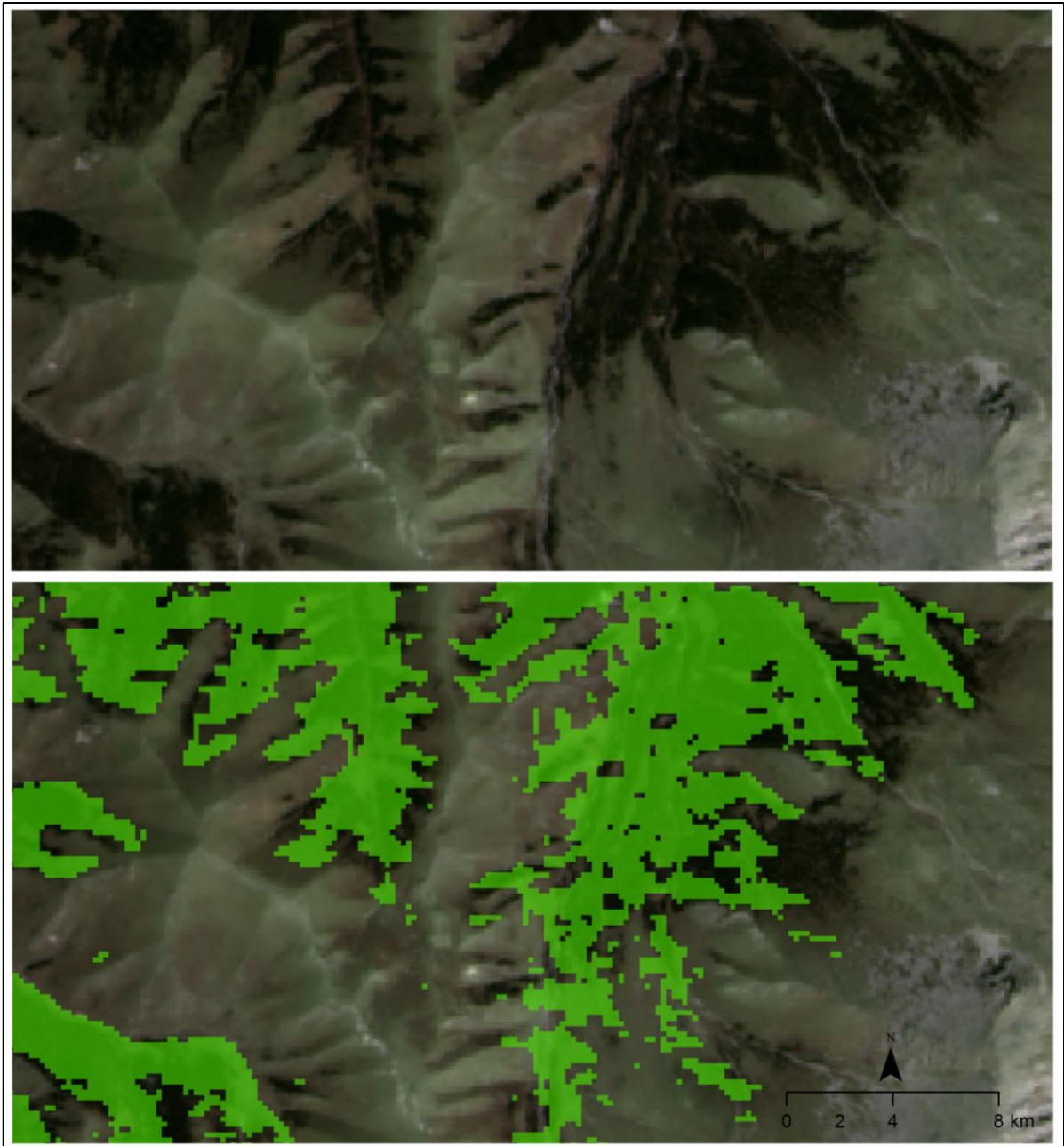


Figure 37: Detail of forested area at the upper forest boundary (upper image, darker areas=forest) and model-predicted forest areas (light green areas, lower image), own figure.

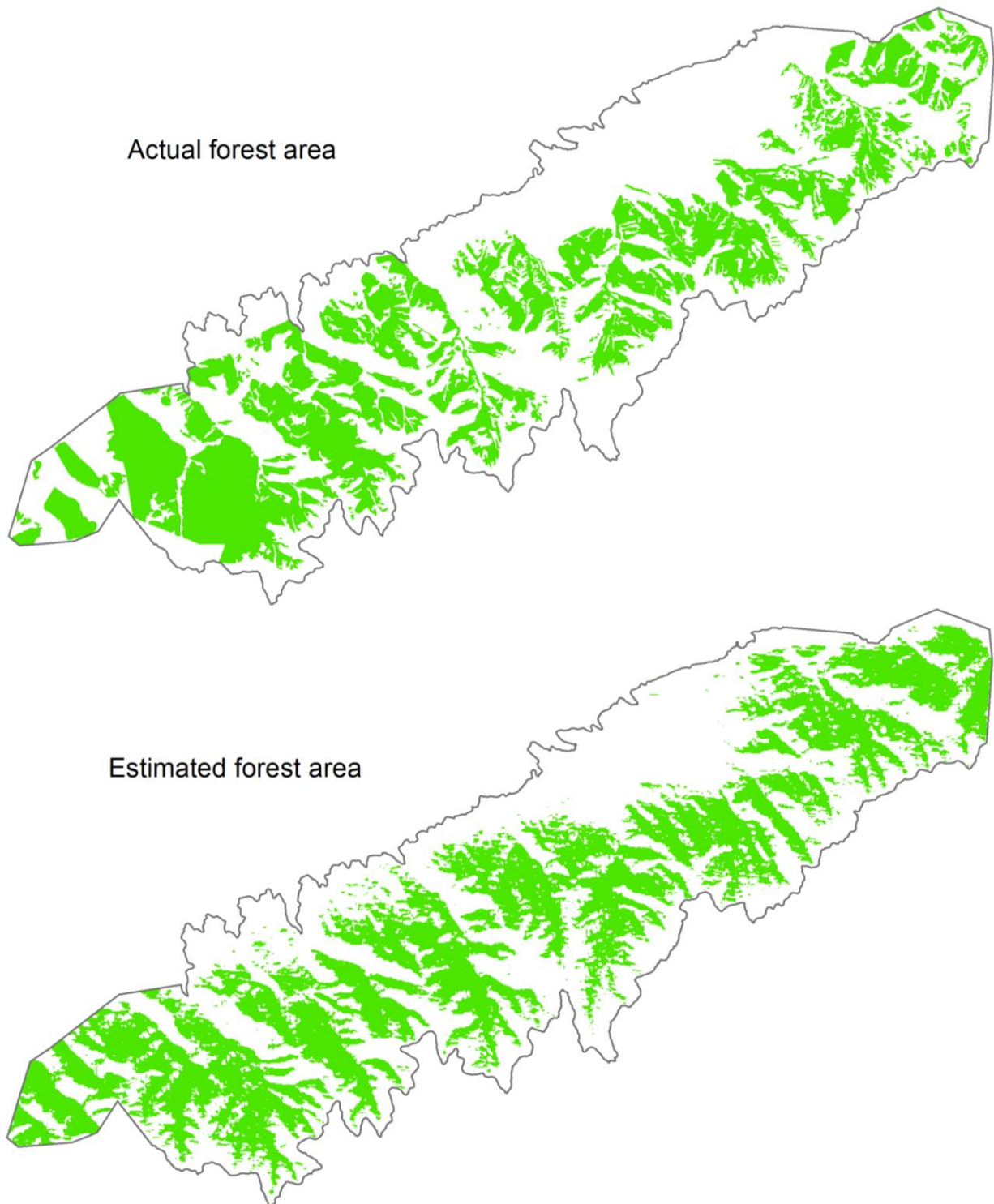


Figure 38: The actual forest area including all forest types (top) and the forest area estimated by the logistic regression model (bottom), own figure.

There are two types of “wrong” modelling: the model can overestimate the forest, i.e. predict forest where there is no forest actually and the model can underestimate, meaning to predict non-forest where there is actual forest occurring.

The overestimation of forested areas is shown in Figure 39. The red colored areas are the ones the model predicted to be forest but actually, there is none. These areas are distributed all over the study site with a higher occurrence at the westernmost and easternmost borders. The lower parts of the study site in the Northeast show almost no forested areas whereas the model would have expected forest to grow there. In addition, the model expected on some spots the treeline to be at higher elevations.

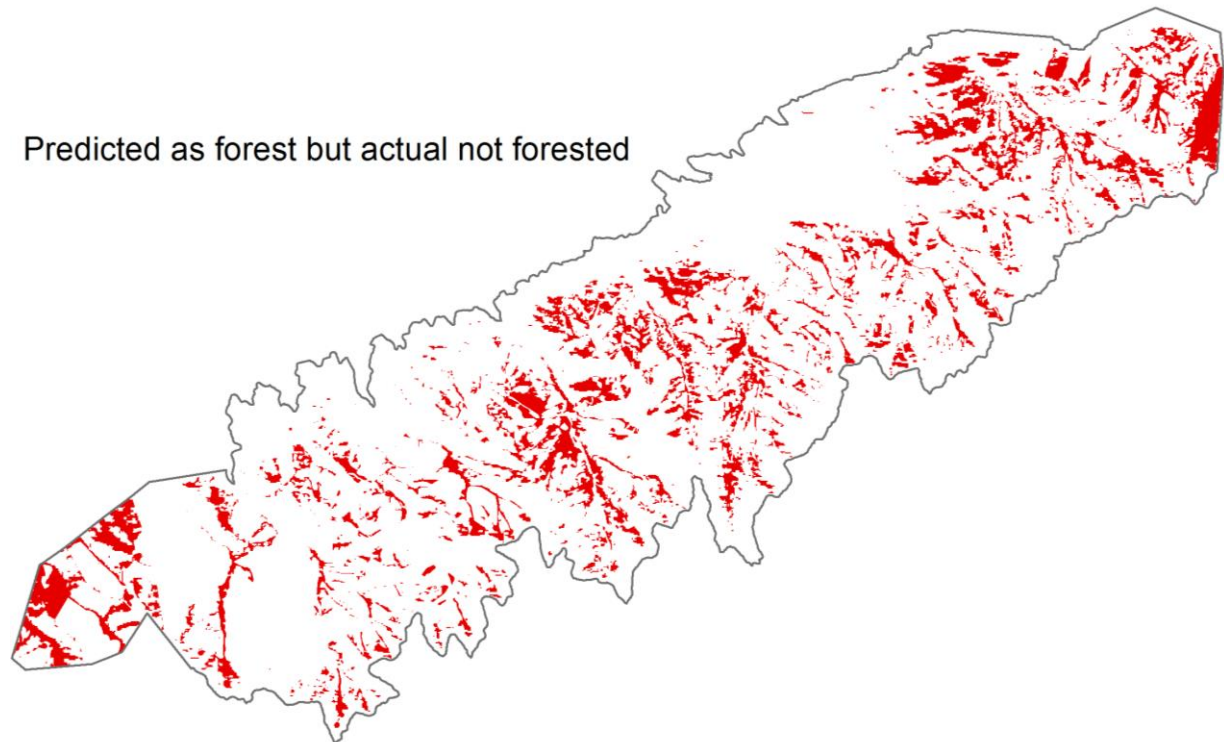


Figure 39: "Overestimated" forest areas by the model, own figure.

At some spots, the model predicted no forest to grow, but there is forest growing (Figure 40). Especially in the southern and southeastern parts, there is an accumulation of such areas. The amount of underestimated forest areas is smaller than the amount of overestimated areas. In the central part of the study area, there are a lot of overestimated but almost no underestimated areas.

Predicted as non-forest but actual forested

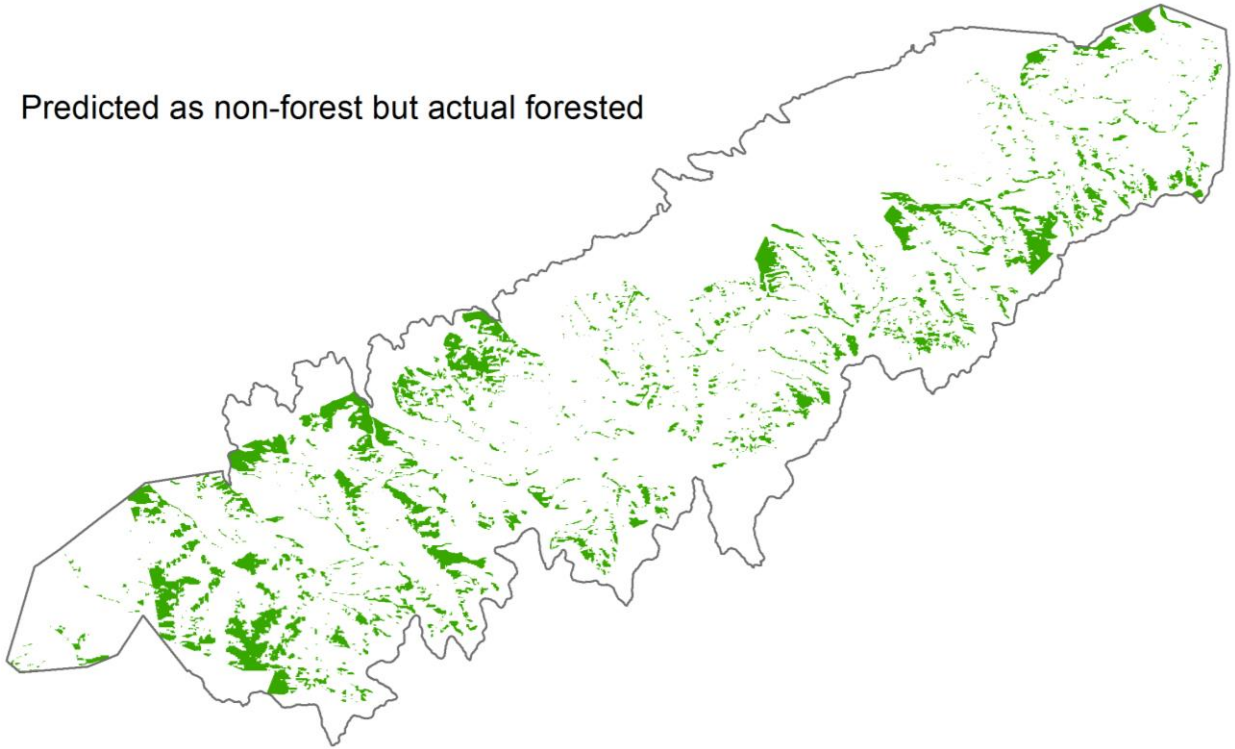


Figure 40: "Underestimated" forest areas, own figure.

5 Discussion

The forested share of Kyrgyzstan is relatively low (~5% of the country area) and shall be increased noticeable during the next decades (DFHGI 2015). This is due to the known benefits forest cover offers: protection against soil erosion, landslides and avalanches (Zeidler et al. 2016).

The aim of this study was to identify the forest cover of a study area inside the Chong Kemin National Park in Kyrgyzstan. After that, a computer-based logistic regression model was developed to predict forested areas according to morphological and climatological parameters. The model was “trained” on the real forest occurrence on site based on digitalized forest maps and satellite images.

This study was inspired and is in parts based on the work of Klinge et al. (2015), “*Modeling forest lines and forest distribution patterns with remote-sensing data in a mountainous region of semiarid central Asia*”. It was possible to estimate forest growth and non-forest-growth with a model-accuracy of around 80%. Klinge et al. (2015) obtained an accuracy of 89% for their forest- and treeline distribution model. While their study area covered a vast territory of around 800,000 ha, the study area used in this work has an extent of only around 18,000 ha. It can be assumed that with a bigger data input (bigger study area), accuracy of the model gets better. At the same time, the unknown factors which could influence forest growth get more with an increasing study area surface (Böhner 2005). Also, geologic and soil parameters were not considered in this study. They were assumed to be mostly similar over the study site (see: 3.1.1)(DFHGI 2015).

The treeline of the study area can be found at elevations of around 2,900 m.a.s.l. Körner (2012) found the treeline to be between 2,750 - 2,920 m.a.s.l. for the Kyrgyz Tien Shan. Trees are performing very poor at this elevations; they struggle to survive (Harsch & Bader 2011). The treeline-environment can therefore be considered as not suitable for afforestation purposes. When looking the elevational distribution of the present forest inside the study area it is evident that at elevations above 2,500 m.a.s.l., the forest cover decreases steadily (Figure 22). It is therefore not recommended to plant trees above this threshold in order to guarantee a higher planting success.

Treeline is often formed by *Juniper sp.* (see Figure 9). Heikkinen et al. (2002) found that the same is true generally for forests all over Central Asia. The habitus of *Juniper sp.* in the mountain environment is an upright, tree-like growth and its distribution can be stand-forming. They are able to grow on elevations where no other tree species occurs (Schickhoff et al. 2015).

Forest in the study area (and especially spruce forest), was found to grow mainly on North-facing (Northeast- North- and Northwest-facing) slopes (Figure 22). Klinge et al. (2015) came to the same result for Schrenk’s spruce (*Picea schrenkiana*) analyzing its geographical distribution in the mountainous regions of Central Asia. On the other hand it was found in this study, that on South-facing slopes, almost no forest occurs (see Figure 23). This is true for all forest types with the exception of bushes which do grow on some South-spots. Also on Southeast-facing and Southwest-facing slopes only very little forest is growing. There are therefore many slopes with a total lack of woody plant communities. Only different grass communities are growing here (3.1.1).

The aspect seems therefore to play a crucial role when it comes to forest growth at the study site. As noticed also in this study (see: 4.2.5), Zhao et al. (2005) found much higher solar radiation values on South-facing slopes than on the other cardinal directions.

In fact, the probability of forest occurrence was shown to decrease with higher radiation values reaching an almost zero-growth-probability at areas with maximum radiation input (Figure 35 & 36).

On the other hand, the calculated likelihood of forest growth was highest at areas with the lowest radiation values.

For the study area, radiation values were found varying from 300 to 1,300 kWh/m² during the vegetation period. Forests occurred on areas with radiation values not higher than 1,250 kWh/m². Klinge et al. (2015) found slightly higher values for Central Asia but with a vegetation period assumed to be longer than the one used in this study. Their calculated total solar radiation input was 650 – 1,550 kWh/m² whereas forest occurred on areas with values not higher than 1,450 kWh/m². Spruce forest cannot grow on slopes with high solar radiation due to a lack of moisture. Only if there is an additional source of water coming from the ground (permafrost, slope water, surface channel), Schrenk's spruce establishment is possible (Zeidler et al. 2016). This is not true for all species and for every environment. High solar radiation can also be a facilitating factor for tree growth. With sufficient precipitation during summer months, high radiation is not a limiting factor for forest growth (Weemstra et al. 2013).

Higher radiation values on South-facing slopes lead to higher soil temperatures and therefore higher evaporation values. This means South-facing slopes dry out much faster when they get direct solar radiation (Richardson et al. 2004). Seedling and growth of saplings was shown to correlate positive with higher soil moisture values. Soil moisture is, among others, directly correlated with precipitation patterns (Schickhoff et al. 2015). Moisture deficits during summer months lead to an inhibited root- and shoot growth (Burton et al. 1998) and are in dry environments leading to high seedling mortality (Persson 1981).

It can therefore be assumed that the combination of high temperatures during summer months (see Figure 27) combined with low precipitation (Figure 29) - and high insolation values (Figure 31) lead to a missing tree seedling establishment on exposed slopes. The seeds released by the surrounding vegetation may germinate in spring where temperatures are lower and soil moisture higher (DFHGI 2015), but fail to survive the dry and warm summer months.

Whether solar insolation becomes a limiting factor for plant growth or not is strongly related to the temperature regime of an area also. With higher summer temperatures, forest vegetation gets more prone to suffer water deficits (Way & Oren 2010). The radial increment as well as the height increment of Schrenk's spruce are low in areas with high summer temperatures and low precipitation values (Magnuszewski et al. 2015).

Large parts of the study area have rather high slope inclination values (Figure 21). Steep slopes can lead to a faster surface and belowground water runoff, which means faster drying of the soil. Magnuszewski et al. (2015) found that areas with slope values lower than 25 degrees of inclination can be effective in retaining water in the ground and keep it available for the plant. Only around one third of the study area shows slope values lower than 25 degrees. The rest of it is steeper with a maximum inclination of 46 degrees (Figure 21). The amount of water runoff generally depends on the type of precipitation. Short but intensive precipitation events can lead to high surface runoff whereas longer but modest events do not (Lal et al. 2007). There are short and intensive rain events during the summer period in the Chong Kemin valley (DFHGI 2015). This could mean that on spots with higher slope values, there is a higher (surface)-water runoff which again leads to a faster drying of the soil. In fact, this study showed that there is a slight probability-reduction of spruce growth with increasing slope values (Figure 36). The planted and established forest of the study area can be found on terrain up to 40-degree inclination (Figure 41). But, only on North-facing slopes where solar radiation values are again distinctly lower. For potential future afforestation it is therefore advisable to choose areas with inclination values lower than 40 degrees whenever possible.

Nevertheless, the species used so far for afforestation purposes in the study area (*Pine sp.* & *Picea shrenkiana*) can be considered well adapted to the harsh climatic conditions of the Kyrgyz Tien Shan mountains (3.1.1) (Körner 2012). A suggestion how to select potential future afforestation areas is therefore to avoid tree planting on Southeast-, South- and Southwest-facing slopes. Afforestation should be limited on East-, Northeast-, North-, Northwest- and West-facing slopes. Planting methods, planting time and the quality of planting material obviously play a crucial role and contribute to a successful establishment of forests (FAO 1989) but are not further discussed in this thesis.

The logistic regression model to predict forest growth was fed with the morphological parameters elevation, slope, aspect and radiation. Like in Zhao et al. (2005) and Klinge et al. (2015) these were the best fitting input variables to predict forest growth. Also, they did not show statistical correlation with all the other parameters what made them suitable to be used in the model.

The forest prediction model showed evident discrepancies of predicted forest and actual forest area (Figure 39 & Figure 40). Especially in some of the lower parts of the study area, in the North and in the South, the model predicted vast areas which have the morphological and climatic requirements which would allow forest growth. The reason why there is no forest growing could be the human impact in the study area. The vicinity to the villages and relatively low slope values makes the forest easier to access for timber use and at the same time suitable for agricultural purposes (compare FAO, 2007).

The spots before mentioned, where there is assumed that forests to grow but it is not, are prevalently occurring on North- and West-facing slopes (see also Figure 11). There are slopes where all forest types usually grow but do actually not grow on this spots. Beside the theory of a human-induced lack of forest, another plausible explanation could be unknown pedological factors. Also, a combination of these two factors seems possible. A former, inappropriate cut of a forested area and a later mismanagement could have led to a missing establishment of a new forest. Like most Kyrgyz forests, human influence reduced their distribution or led to treeline- and forest border shifts (Lioubimtseva et al. 2005). This is mostly due to animal (over)grazing, agricultural cultivation and illegal woodcutting with no reforestation. All of those factors often lead to a permanent deterioration of the former woodland (Dzunuzova 2008).

On the other hand, there is also an “underestimation” of forested land by the logistic regression model (Figure 40). The model predicts no forest growth for an area where actually forests are growing. There are much less of these spots than the “overestimated” ones but it is worth to have a closer look: these areas are mostly plantations-, birch- and bush-forest types. Again, they are occurring predominately on North- but also on East- and West-facing slopes. The fact, that on South-facing slope is almost no forest occurring and that a large share of slopes are North-facing, means that slope direction has probably no influence here. Spruce is by far the most dominant species in the study area (~76% of total forested area). The logistic regression model was therefore trained with mostly spruce-forest-pixel-types leading to an output strongly related to spruce growth pattern. This could explain the discrepancies for this “underestimated” spots dominated by birch and bushes.

Another factor which leads to wrong-modelling is the so called “summit-syndrome”. Due to the forces of wind and the loss of substrate, treeline gets depressed and forest border shifted near peaks and crests independent of the elevation. (Paulsen & Körner 2014; Körner 2012). This phenomenon can be observed well on the forest-prediction model output (Figure 39). Along several ridges, elongated areas with extensions of several hundreds of meters can be found. The areas which the model predicted as forest, are actually without any forest. An afforestation attempt should consider this phenomenon and

avoid planting directly on top of crests and ridges even if the other parameters of tree growth are guaranteed.

Many of the afforestation efforts made by the Kyrgyz authorities failed over the past decades (Orozumbekov et al. 2009). At the same time, a lot of experimenting and scientific research was carried out to find the best-adopted species and provenances and to find the right places and methods to plant and reestablish forests.

The question if the afforestation should be made with different, not indigenous species which can better cope with the above mentioned climatic and morphological conditions, was not part of this study. An investigation in this direction would however be worth, especially for areas where forest establishment is limited by the growth performance of species. It is entirely possible that allochthon species are able to grow on sites where indigenous species struggle (FAO 1989; Körner 2012).

Avoiding the errors of the past, being open to new scientific findings and developing effective and promising strategies for future interventions are the main goals set by the Kyrgyz Department of Forest, Hunting and Ground Inventory (DFHGI 2015). This study's aim was to point out limiting tree-growth factors for the Chong Kemin National Park. The logistic regression model was used to find sites where forest could be established, considering these tree-growth limiting factors.

6 References

- Backhaus, K. et al., 2007. *Multivariate Analysemethoden - Eine anwendungsorientierte Einführung* 9th ed., Heidelberg: Springer.
- Böhner, J., 2005. Advancements and new approaches in climate spatial prediction and environmental modelling. *Arbeitsberichte des Geographischen Instituts der HU ...*, (109), pp.49–90.
- Böhner, J., 2006. General climatic controls and topoclimatic variations in Central and High Asia. *Boreas*, 35(2), pp.279–295.
- Böhner, J., 2004. Regionalisierung bodenrelevanter Klimaparameter für das Niedersächsische Landesamt für Bodenforschung (NLFb) und die Bundesanstalt für Geowissenschaften und Rohstoffe (BGR) Inhaltsverzeichnis. *Arbeitshefte Boden*, pp.17–66.
- Böhner, J. & Antonic, O., 2009. Chapter 8 - Land-Surface Parameters Specific to Topo-Climatology. *GEOMORPHOMETRY*, 33.
- Burton, A.J., Pregitzer, K.S. & Zogg, G.P., 1998. Drought reduces root respiration in sugar maple forests. *Ecological Applications*, 8(3), pp.771–778.
- Cantarello, E. et al., 2014. Human Impacts on Forest Biodiversity in Protected Walnut-Fruit Forests in Kyrgyzstan. *Journal of Sustainable Forestry*, 33(5), pp.454–481.
- Chen, X. & Pan, W., 2002. Relationships among phenological growing season, time-integrated normalized difference vegetation index and climate forcing in the temperate region of eastern China. *International Journal of Climatology*, 22(14), pp.1781–1792.
- Chmielewski, F.M. & Rotzer, T., 2001. Response of tree phenology to climate change across Europe. *Agricultural and Forest Meteorology*, 108(2), pp.101–112.
- Cleland, E.E. et al., 2007. Shifting plant phenology in response to global change. *Trends in Ecology and Evolution*, 22(7), pp.357–365.
- Colak, A. & Rotherham, I.D., 2007. Classification of Turkish forests by altitudinal zones to improve silvicultural practice: a case-study of Turkish high mountain forests. *International Forestry Review*, 9(2), pp.641–652.
- DFHGI, 2015. *The Chong Kemin National Park - Report of the Department of Forest, Hunting and Ground Inventory*, Bishkek.
- Dzunuzova, M., 2008. *Country report on the state of plant genetic resources for food and agriculture*, Bishkek.
- Ellenberg, H., 1996. *Vegetation Mitteleuropas mit den Alpen in ökologischer, dynamischer und historischer Sicht.*, Stuttgart: Ulmer Verlag.
- ESRI, 2016. ArcGIS 10.3.1 for Desktop Spatial analyst tool.
- FAO, 1989. *Arid zone forestry: A guide for field technicians*, Rome
- FAO, 2004. *Carbon sequestration in dryland soils*, Rome
- FAO, 2014. *FAO Country Programming Framework in the Kyrgyz Republic 2015 - 2017.* , pp.1–33.
- FAO et al., 2007. *Mapping biophysical factors that influence agricultural production and rural vulnerability*

- FAO & UNESCO, 1978. *Soil map of the world - North and Central Asia*, Paris.
- Fet, G.N., 2007. *Satellite Image Processing for Biodiversity Conservation and Environmental Modeling in Kyrgyz Republic National Park*. Marshall University Graduate College of Huntington, West Virginia.
- Fu, P. & Rich, P., 2002. A geometric solar radiation model with applications in agriculture and forestry. *Computers and Electronics in Agriculture*, 37(1-3), pp.25–35.
- Fu, P. & Rich, P.M., 1999. *Design and Implementation of the Solar Analyst: an ArcView Extension for Modeling Solar Radiation at Landscape Scales*
- Fu, Y.H. et al., 2015. Increased heat requirement for leaf flushing in temperate woody species over 1980-2012: Effects of chilling, precipitation and insolation. *Global Change Biology*, 21(7), pp.2687–2697.
- Gehrig-Fasel, J., Guisan, A. & Zimmermann, N.E., 2007. Tree line shifts in the Swiss Alps: Climate change or land abandonment? *Journal of Vegetation Science*, 18(4), pp.571–582.
- Harsch, M.A. & Bader, M.Y., 2011. Treeline form - a potential key to understanding treeline dynamics. *Global Ecology and Biogeography*, 20(4), pp.582–596.
- Heikkinen, O., Tuovinen, M. & Autio, J., 2002. What determines the timberline? *Fennia*, 180(1-2), pp.67–74.
- Hoch, G. & Körner, C., 2009. Growth and carbon relations of tree forming conifers at constant vs. variable low temperatures. *The journal of ecology*, 97, pp.57–66.
- Klinge, M., Böhner, J. & Erasmi, S., 2015. Modeling forest lines and forest distribution patterns with remote-sensing data in a mountainous region of semiarid central Asia. *Biogeosciences*, 12(10), pp.2893–2905.
- Komatsu, H. et al., 2012. Simple modeling of the global variation in annual forest evapotranspiration. *Journal of Hydrology*, 420-421, pp.380–390.
- Körner, C., 1999. *Alpine Plant Life - Functional Plant Ecology of High Mountain Ecosystems*, Heidelberg: Springer.
- Körner, C., 2012. *Alpine Treelines - Functional Ecology of the Global High Elevation Tree Limits*, Basel: Springer.
- Kramer, K., 1994. A modeling analysis of the effects of climatic warming on the probability of spring frost damage to tree species in the Netherlands and Germany. *Plant Cell and Environment*, 17, pp.367–377.
- Kumar, K.K., Kumar, K.R. & Rakhecha, P.R., 1987. Comparison of Penman and Thornthwaite methods of estimating potential evapotranspiration for Indian conditions. *Theoretical and Applied Climatology*, 38, pp.140–146.
- Lal, R. et al., 2007. *Climate change and terrestrial carbon sequestration in central asia*,
- Lioubimtseva, E. et al., 2005. Impacts of climate and land-cover changes in arid lands of Central Asia. *Journal of Arid Environments*, 62(2), pp.285–308.
- Lioubimtseva, E. & Henebry, G.M., 2009. Climate and environmental change in arid Central Asia: Impacts, vulnerability, and adaptations. *Journal of Arid Environments*, 73(11), pp.963–977.
- Magnuszewski, M. et al., 2015. Different growth patterns of *Picea schrenkiana* subsp. *tianshanica*

- (Rupr.) Bykov and *Juglans regia* L. coexisting under the same ecological conditions in the Sary-Chelek Biosphere Reserve in Kyrgyzstan. *Dendrobiology*, 73(July), pp.11–20.
- Man, R.Z. & Lu, P.X., 2010. Effects of thermal model and base temperature on estimates of thermal time to bud break in white spruce seedlings. *Canadian Journal of Forest Research-Revue Canadienne De Recherche Forestiere*, 40(9), pp.1815–1820.
- Matsuda, Y. et al., 2006. Estimation of atmospheric transmissivity of solar radiation from precipitation in the Himalaya and the Tibetan Plateau. *Annals of Glaciology*, 43, pp.344–350.
- McMaster, G.S. & Wilhelm, W.W., 1997. *Growing degree-days: One equation, two interpretations*.
- Menzel, a & Fabian, P., 1999. Growing season extended in Europe. *Nature*, 397(6721), p.659.
- Murray, M.B., Cannell, M. & Smith, R., 1989. Date of budburst of 15 tree species in Britain following climatic warming. *Journal of Applied Ecology*.
- NASA & METI, 2016. ASTER Global Digital Elevation Model. *Advanced Spaceborne Thermal Emission and Reflection Radiometer*.
- Orozumbekov, A., Musuraliev, T. & Toktoraliev, B., 2009. Forest Rehabilitation in Kyrgyzstan. *IUFRO World Series 2009 Vol. 20 No. 4 pp. 131-182*, pp.131–182.
- Paulsen, J. & Korner, C., 2001. GIS-analysis of tree-line elevation in the Swiss Alps suggests no exposure effect. *Journal of Vegetation Science*, 12(6), pp.817–824.
- Paulsen, J. & Körner, C., 2014. A climate-based model to predict potential treeline position around the globe. *Alpine Botany*, pp.1–12.
- Persson, H., 1981. Fine root dynamics in a Scots pine stand with and without near-optimum nutrient and water regimes. *Acta Phytogeografica 68 - Studies in plant ecology*.
- Pidwirny, M. & Jones, S., 2009. physicalgeography.net. *University of British Columbia*.
- Pretzsch, H. et al., 2014. Forest stand growth dynamics in Central Europe have accelerated since 1870. *Nature communications*, 5, p.4967.
- R Development Core Team, 2010. R: A language and environment for statistical computing.
- Richardson, A.D., Lee, X. & Friedland, A.J., 2004. Microclimatology of treeline spruce-fir forests in mountains of the northeastern United States. *Agricultural and Forest Meteorology*, pp.53–66.
- Saha, K., 2008. *The Earth's Atmosphere: Its Physics and Dynamics*, Springer.
- Schickhoff, U. et al., 2015. Do Himalayan treelines respond to recent climate change? An evaluation of sensitivity indicators. *Earth System Dynamics*, 6(1), pp.245–265.
- Sultan, S. et al., 2014. Modeling of Diffuse Solar Radiation and Impact of Complex Terrain over Pakistan Using RS/GIS. *Journal of Geographic Information System*, 06(04), pp.404–413.
- Szerencsits, E., 2012. Swiss Tree Lines - a GIS-Based Approximation. *Landscape Online*, 28(1), pp.1–18.
- Thorntwaite, C.W., 1948. An Approach Toward a Rational Classification of Climate. *Geographical Review*, 38, pp.55–94.
- Undeland, A., 2012. *The development potential of forests in the kyrgyz republic (PROFOR)*, Washington: Program on Forests (PROFOR).
- Visualab, 2016. <http://visualab.sdsu.edu/>. Available at: <http://visualab.sdsu.edu/> [Accessed May 12,

2016].

- Way, D.A. & Oren, R., 2010. Differential responses to changes in growth temperature between trees from different functional groups and biomes: a review and synthesis of data. *Tree Physiology*, 30(6), pp.669–688.
- Weemstra, M. et al., 2013. Summer droughts limit tree growth across 10 temperate species on a productive forest site. *Forest Ecology and Management*, 306, pp.142–149.
- Will, J., 2011. Using high resolution DSMs to assess solar irradiation in urban environments.
- Xu, C.Y. & Singh, V.P., 2002. Cross comparison of empirical equations for calculating potential evapotranspiration with data from Switzerland. *Water Resources Management*, 16(3), pp.197–219.
- Zeidler, A., Perzl, F. & Maier, C., 2016. *Natural Hazard Risk Management for Transport Infrastructure in the Kyrgyz Republic - AwaProForest*,
- Zhao, C., Nan, Z. & Cheng, G., 2005. GIS-assisted modelling of the spatial distribution of Qinghai spruce (*Picea crassifolia*) in the Qilian Mountains, northwestern China. *International Geoscience and Remote Sensing Symposium (IGARSS)*, 1, pp.534–537.

6.1 List of tables

Table 1: Start and End of vegetation period from selected regions.....	6
Table 2: Defining vegetation period: temperature values to compare different scientific findings.....	8
Table 3: ASTER GDEM v2 Data Set Characteristics.....	20
Table 4: Example of solar incidence and percent of the total radiation intensity.....	25
Table 5: Constant K in Thornthwaite method.....	26
Table 6: Exemplary yearly Potential Evapotranspiration values for the study area.....	40
Table 7: Total forest, Table of coefficients.....	46
Table 8: Spruce forest, Table of coefficients.....	47

6.2 Tables of figures

Figure 1: Altitudinal zonation, Ellenberg (1996)	3
Figure 2: Accumulated yearly GDD above 0°C in Central Asia	4
Figure 3: Length of the vegetation period in Central Asia	7
Figure 4: The three energy sources on a slope	9
Figure 5: Proportion of direct, diffuse and global insolation during the year.....	9
Figure 6: Monthly values of potential insolation [W/m ²] at different latitudes	10
Figure 7: Overview and detail of the study area	13
Figure 8: <i>Picea shrenkiana</i> forests growing on North-facing slopes, alpine meadow or steppe on all other slopes, Chong Kemin NP	15
Figure 9: Sequence of vegetation types, examples of the Tien-Shan mountain chain	16
Figure 10: Forest- and treeline behavior at the upper forest border	16
Figure 11: Treeline-ecotone at the study area.....	17
Figure 12: Original Forest map obtained by the Department of Forest, Hunting and Ground Inventory in November 2015.....	18
Figure 13: Digitalization process of the forest areas.....	19
Figure 14: Comparison of data resolution before (left) and after (right) geostatistical Kriging	23
Figure 15: Workflow to extract climate data from Böhner (2006), ArcGis Model builder	24
Figure 16: Interface of online PET-Thornthwaite-method-calculator, (Visualab 2016).....	27

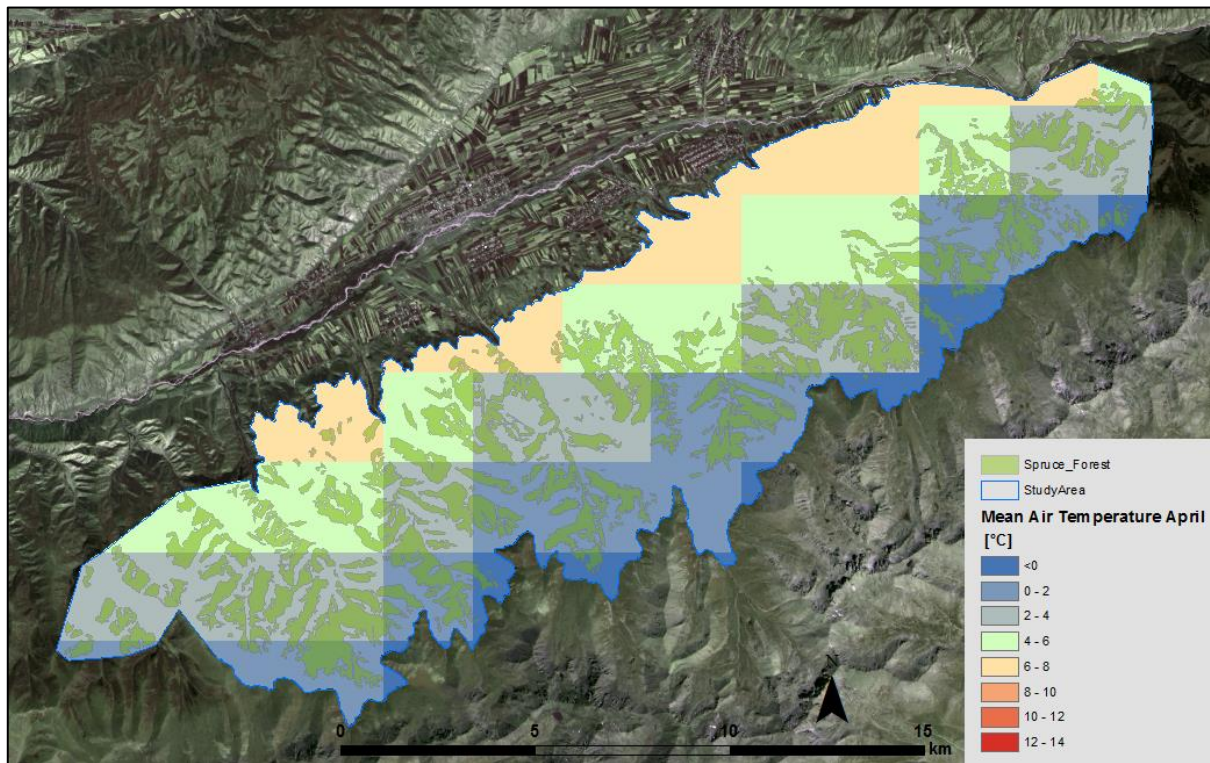
Figure 17: Altitudinal zonation of Kyrgyz National territory	28
Figure 18: Altitudinal zonation of the study area according to Orozumbekov et al. (2009).....	29
Figure 19: Forest edge image and forest types distribution in the study area	31
Figure 20: Aspect classes (cardinal direction) of the study area.....	30
Figure 21: Slope values at the study area	30
Figure 22: Frequency distribution of morphological parameters of the study area (Total forest and Juniper).....	33
Figure 23: Frequency distribution of morphological parameters of the study area (Spruce and Bushes)	34
Figure 24: Frequency distribution of morphological parameters of the study area (Birch and Plantations)	35
Figure 25: Mean annual temperature values.....	36
Figure 26: Coincidence of the 10°C July Isotherme with the upper treeline in the study area	37
Figure 27: July mean precipitation of the study area and surroundings.	39
Figure 28: PET of the study area and surroundings derived with the Thornthwaite's method.....	40
Figure 30: Relationship aspect-incoming radiation.....	41
Figure 31: Frequency distribution (in ha) of climate parameters (Total forest and Juniper)	43
Figure 32: Frequency distribution (in ha) of climate parameters (Spruce and Bushes).	44
Figure 33: Frequency distribution (in ha) of climate parameters (Birch and Plantations).	45
Figure 34: Total Forest area: Logistic regression probability plots which explain the probability forest growth according to the selected four variables.	47
Figure 35: Spruce forest: Logistic regression probability plots that explain the probability spruce growth according to the selected four variables.....	48
Figure 36: The actual forest area (green), the forest area estimated by the logistic regression model (black) and the "overestimated" by the model forest areas.....	51
Figure 37: Detail of forested area at the upper forest boundary	49

7 Appendix

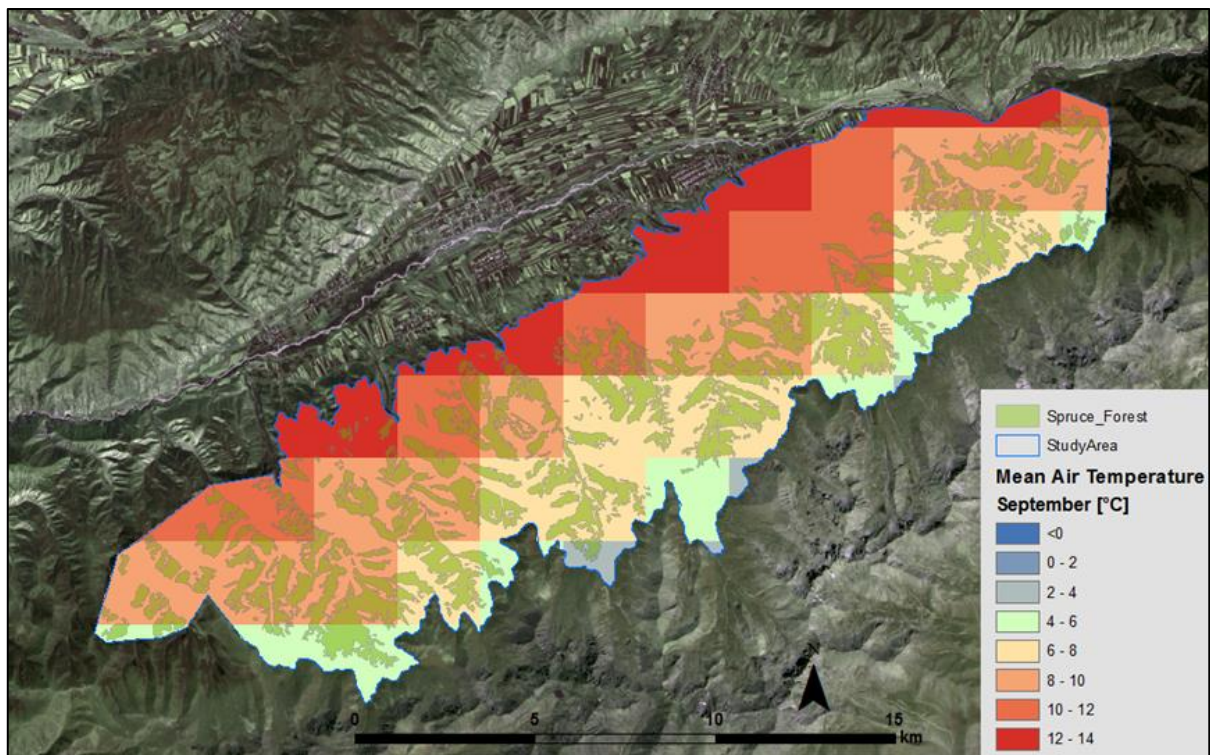
Appendix I: Correlation matrix between climatological and morphological parameters, green=no correlation ($R^2 \leq \pm 0.5$), red=correlation higher than ± 0.5 , n13=annual mean precipitation, n07=mean precipitation July, t13=annual mean temperature, t11=mean temperature November, t10=mean temperature October, t09=mean temperature September, pet=Potential Evapotranspiration, tveg=mean temperature during vegetation period (April-September)

	elevation	slope	aspect	n13	n07	t13	t11	t10	t09	t08	t07	t06	t05	t04	t03	radiation	pet	tveg
elevation	1	0,21	-0,01	0,90	0,86	-0,91	-0,93	-0,94	-0,94	-0,94	-0,94	-0,94	-0,94	-0,39	-0,94	0,04	-0,94	-0,95
slope	0,21	1	-0,08	0,23	0,20	-0,21	-0,19	-0,20	-0,20	-0,19	-0,20	-0,20	-0,19	-0,11	-0,19	-0,41	-0,20	-0,20
aspect	-0,01	-0,08	1	-0,05	-0,04	0,03	0,02	0,03	0,03	0,03	0,03	0,03	0,03	0,02	0,02	0,20	0,03	0,03
n13	0,90	0,23	-0,05	1	0,99	-0,92	-0,90	-0,90	-0,93	-0,93	-0,94	-0,94	-0,93	-0,38	-0,91	-0,03	-0,93	-0,94
n07	0,86	0,20	-0,04	0,99	1	-0,89	-0,86	-0,87	-0,90	-0,90	-0,91	-0,91	-0,90	-0,36	-0,88	-0,01	-0,90	-0,91
t13	-0,91	-0,21	0,03	-0,92	-0,89	1	0,94	0,96	0,95	0,95	0,96	0,96	0,95	0,39	0,95	0,01	0,96	0,96
t11	-0,93	-0,19	0,02	-0,90	-0,86	0,94	1	0,97	0,98	0,98	0,97	0,97	0,97	0,40	0,99	0,01	0,98	0,98
t10	-0,94	-0,20	0,03	-0,90	-0,87	0,96	0,97	1	0,98	0,97	0,97	0,97	0,97	0,40	0,96	0,01	0,98	0,98
t09	-0,94	-0,20	0,03	-0,93	-0,90	0,95	0,98	0,98	1	0,98	0,98	0,98	0,98	0,40	0,98	0,01	0,98	0,99
t08	-0,94	-0,19	0,03	-0,93	-0,90	0,95	0,98	0,97	0,98	1	0,99	0,99	0,98	0,40	0,98	0,01	0,98	1,00
t07	-0,94	-0,20	0,03	-0,94	-0,91	0,96	0,97	0,97	0,98	0,99	1	0,99	0,99	0,40	0,98	0,01	0,98	1,00
t06	-0,94	-0,20	0,03	-0,94	-0,91	0,96	0,97	0,97	0,98	0,99	0,99	1	0,99	0,40	0,98	0,01	0,98	1,00
t05	-0,94	-0,19	0,03	-0,93	-0,90	0,95	0,97	0,97	0,98	0,98	0,99	0,99	1	0,40	0,98	0,01	0,98	0,99
t04	-0,39	-0,11	0,02	-0,38	-0,36	0,39	0,40	0,40	0,40	0,40	0,40	0,40	0,40	1	0,40	0,03	0,41	0,41
t03	-0,94	-0,19	0,02	-0,91	-0,88	0,95	0,99	0,96	0,98	0,98	0,98	0,98	0,98	0,40	1	0,01	0,98	0,99
radiation	0,04	-0,41	0,20	-0,03	-0,01	0,01	0,01	0,01	0,01	0,01	0,01	0,01	0,01	0,03	0,01	1	0,01	0,01
pet	-0,94	-0,20	0,03	-0,93	-0,90	0,96	0,98	0,98	0,98	0,98	0,98	0,98	0,98	0,41	0,98	0,01	1	0,99
tveg	-0,95	-0,20	0,03	-0,94	-0,91	0,96	0,98	0,98	0,99	1,00	1,00	1,00	0,99	0,41	0,99	0,01	0,99	1

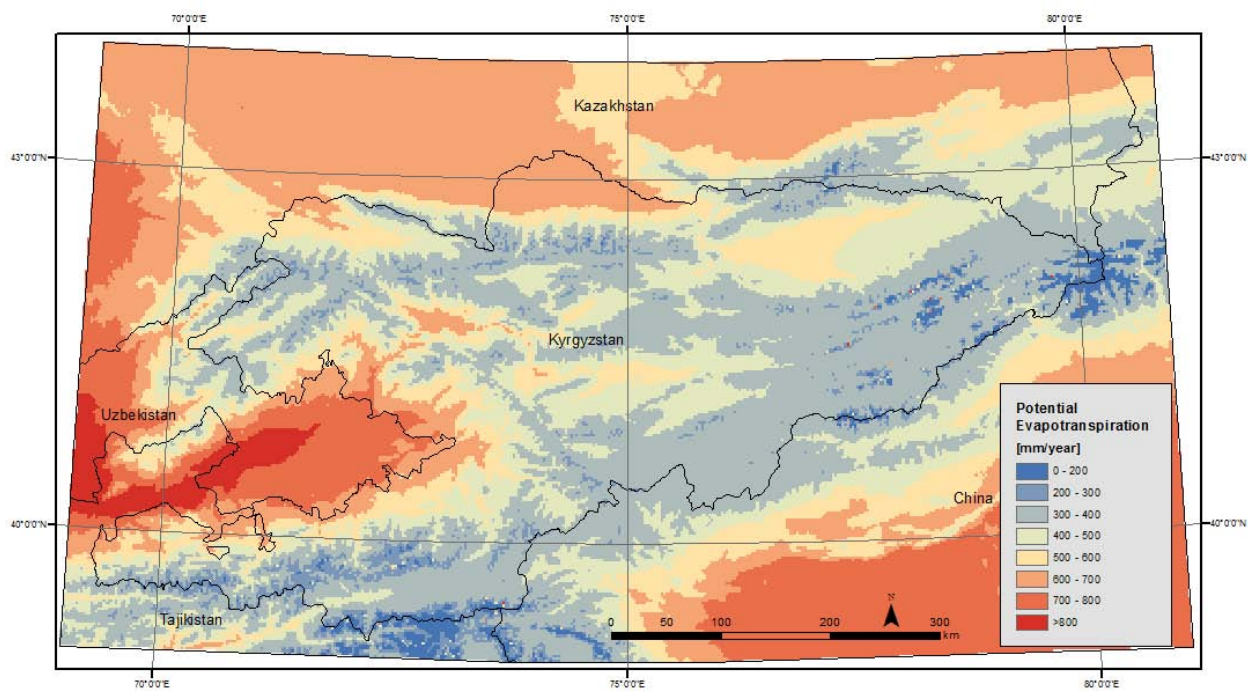
Appendix III: Study area long term monthly temperature means for April, source: (Böhner 2006), own figure.



Appendix IV: Study area long term monthly temperature means for September, source: (Böhner 2006), own figure.



Appendix V: Potential Evapotranspiration in mm/year, resolution: 2,300 x 2,300 m, generated with the Thornthwaite's method, data source: Böhner (2006), own figure



Appendix VI: Visualization of radiation data provided by Prof. Dr. Jürgen Böhner, own figure.

